UU-77-7-E

DEPARTMENT OF GEOLOGY AND GEOPHYSICS

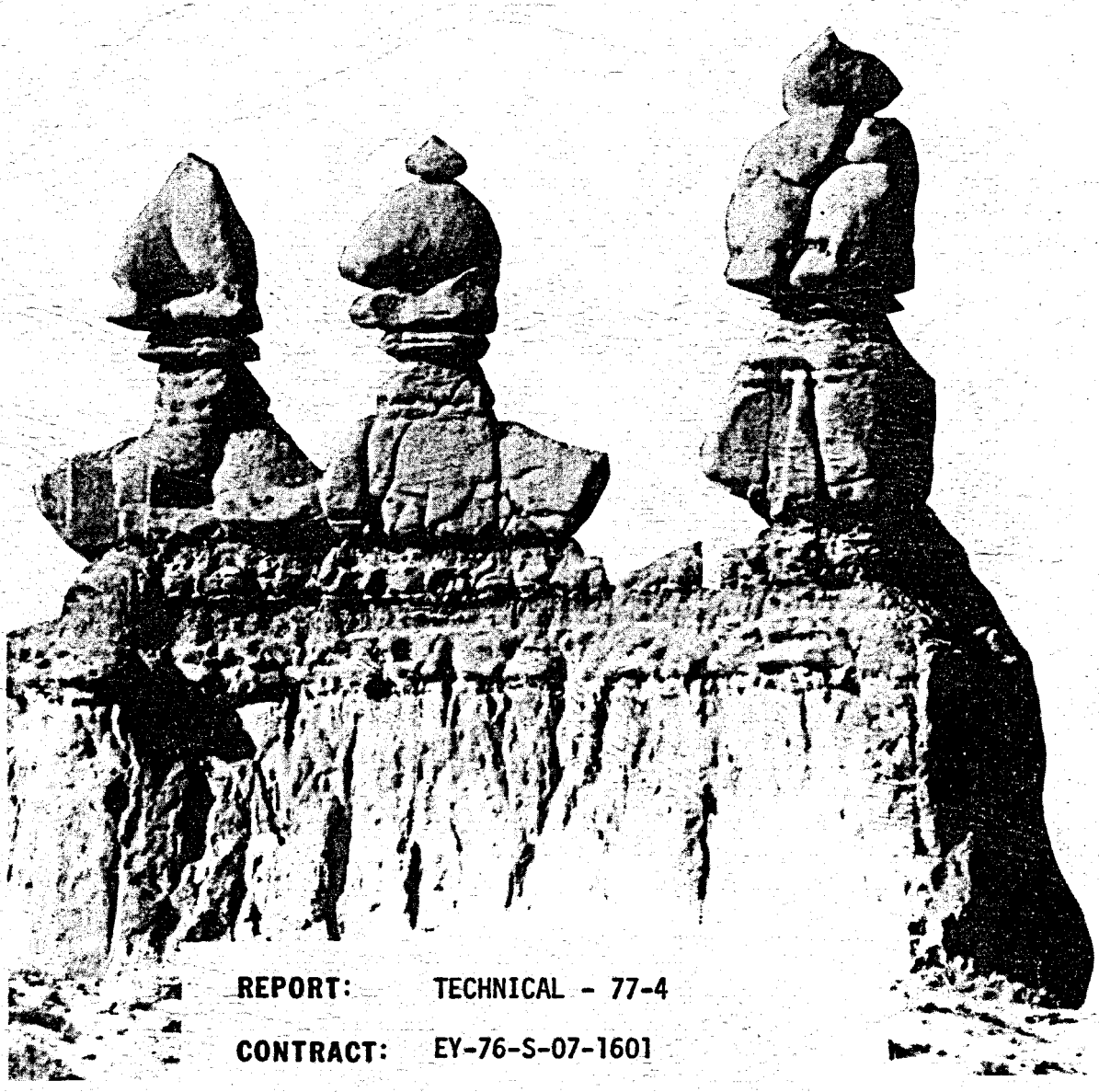

REPORT: TECHNICAL - 77-4

CONTRACT: EY-76-S-07-1601

AGENCY: ERDA

TITLE: GRAVITY SURVEY OF THE COVE FORT - SULPHURDALE KGRA AND THE NORTH MINERAL MOUNTAINS AREA, MILLARD AND BEAVER COUNTIES, UTAH

AUTHORS: WILLIAM D. BRUMBAUGH AND KENNETH L. COOK

DATE: AUGUST 1, 1977

UNIVERSITY OF UTAH SALT LAKE CITY, UTAH 84112

DISCLAIMER

GRAVITY SURVEY OF THE COVE FORT - SULPHURDALE KGRA AND THE NORTH MINERAL MOUNTAINS AREA, MILLARD AND BEAVER COUNTIES, UTAH

By

William D. Brumbaugh and Kenneth L. Cook

PREFACE

The attached report was submitted by William D. Brumbaugh in partial fulfillment of the requirements for the degree of Master of Science in Geophysics, Department of Geology and Geophysics at the University of Utah. The work was performed under the direction of Dr. Kenneth L. Cook.

CONTENTS

CONTENTS (Continued)

ABSTRACT

During the summers of 1975 and 1976, a gravity survey was conducted in the Cove Fort - Sulphurdale KGRA and north Mineral Mountains area, Millard and Beaver counties, Utah. The survey consisted of 671 gravity stations covering an area of about 1300 km^2, and included two orthogonal gravity profiles traversing the area. The gravity data are presented as a terrain-corrected Bouguer gravity anomaly map with a contour interval of 1 mgal and as an isometric three-dimensional gravity anomaly surface. Selected anomaly separation techniques were applied to the hand-digitized gravity data (at 1-km intervals on the Universal Transverse Mercator grid) in both the frequency and space domains, including Fourier decomposition, second vertical derivative, strike-filter, and polynomial fitting analysis, respectively.

Residual gravity gradients of 0.5 to 8.0 mgal/km across north-trending gravity contours observed through the Cove Fort area, the Sulphurdale area, and the areas east of the East Mineral Mountains, along the west flanks of the Tushar Mountains, and on both the east and west flanks of the north Mineral Mountains, were attributed to north-trending Basin and Range high-angle faults. Gravity highs exist over the community of Black Rock area, the north Mineral Mountains, the Paleozoic outcrops in the east Cove Creek-Dog Valley-

White Sage Flats areas, the sedimentary thrust zone of the southern Pavant Range, and the East Mineral Mountains. The gravity lows over north Milford Valley, southern Black Rock Desert, Cunningham Wash, and northern Beaver Valley are separated from the above gravity highs by steep gravity gradients attributed to a combination of crustal warping and faulting. A gravity low with a closure of 2 mgal corresponds with Sulphur Cove, a circular topographic feature containing sulphur deposits.

An extension of the Laramide overthrust sheet observed in the southern Pavant Range is indicated as extending westward under alluvial and volcanic cover by a southwest-trending gravity saddle that lies over the Paleozoic sedimentary exposures in the east Cove Creek area and the Pinnacle Pass igneous-sedimentary contact zone, and that separates the gravity low over north Milford Valley into northern and southern closures with a right-lateral offset. The possible buried, upwarped edge of this thrust sheet is indicated by a steep gravity gradient on the north-south gravity profile; Basin and Range high-angle faulting is indicated on the east-west gravity profile.

The gravity saddle over the Pinnacle Pass Contact zone overlies a possible east-west strike-slip fault zone between the Mineral Mountains pluton on the south and the Laramide overthrust on the north. The gravity highs lying north and south of Pinnacle Pass indicate a right-lateral offset along and east-west zone that continues eastward along an east-west geomorphic and structural feature to Clear Creek Canyon (which includes Sulphur Cove) in the Tushar Mountains outlining

an inferred east-west strike-slip fault zone (supported also by aeromagnetic data).

The principal occurrences of hydrothermal alteration, hot spring deposits, and flowing hot springs and hot-water wells in the survey area apparently coincide with the inferred intersections of: 1) east-west, and 2) north-south and/or north-northeastward trending fault zones. These occurrences include Sulphurdale Hot Springs, Sulphur Cove, and the Dog Valley area.

LIST OF ILLUSTRATIONS

Figures

LIST OF ILLUSTRATIONS (Continued)

LIST OF ILLUSTRATIONS (Continued)

Table

ACKNOWLEDGMENTS

The author wishes to thank Dr. K. L. Cook, Dr. J. A. Whelan, and Dr. W. R. Sill, members of his Supervisory Committee, for their encouragement and numerous consultations and for their critical reviews of this manuscript.

T. J. Crebs, Ittichai Thangsuphanich, and L. S. Yurich gave invaluable assistance during the field work and data reduction phases of the study. J. H. Snow and R. F. Sawyer materially contributed to the implementation of several of the computer programs used in the later phases of interpretation and modeling.

Dr. J. R Montgomery of ASARCO generously provided his time and the polynomial fitting gravity programs used in the processing of the gravity data.

Financial support for this study was provided by the Energy Research and Development Administration (ERDA) under contract number EY-76-S-07-1601.

INTRODUCTION

Location of Survey

During June through September 1975 and June 1976, a gravity survey was made in the Cove Fort - Sulphurdale KGRA and north Mineral Mountains area in Millard and Beaver counties, Utah (Fig. 1). The purpose of the study was to help evaluate the geothermal potential of this region. The survey forms part of a larger study that has been in progress since 1974 by the Geothermal Team of faculty and students of the Department of Geology and Geophysics, University of Utah to evaluate the geothermal potential of the broader geothermal region in southwestern Utah.

Topography

The survey area, which lies about 200 miles south-southwest of Salt Lake City, extends east of the Union Pacific Railroad in the Escalante Desert, through the Black Rock Desert, to the western flanks of the Tushar Mountains and south from the community of Black Rock to the Millard-Beaver county line with a small area east of the Mineral Mountains (Figs. 1 and 2).

The centralmost feature of the survey area is the Mineral Mountains, which rise to over 8000 ft above sea level, which is at least 2000 ft above the desert floor found on three sides. To the west of these mountains lies Milford Valley, forming a northern arm of the Escalante Desert; to the east lies Beaver Valley; and to the north

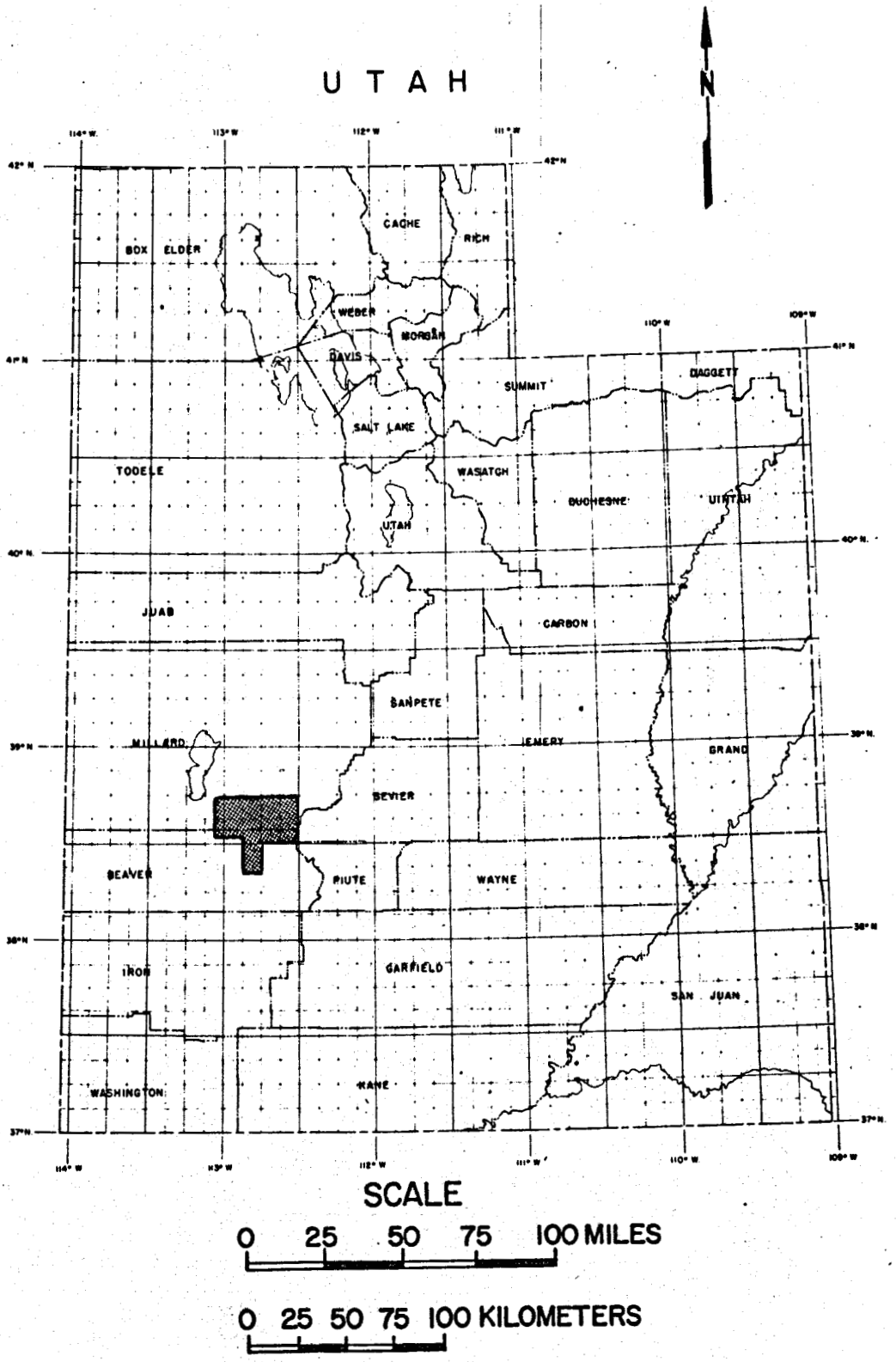

Figure 1 Map of Utah showing the survey area

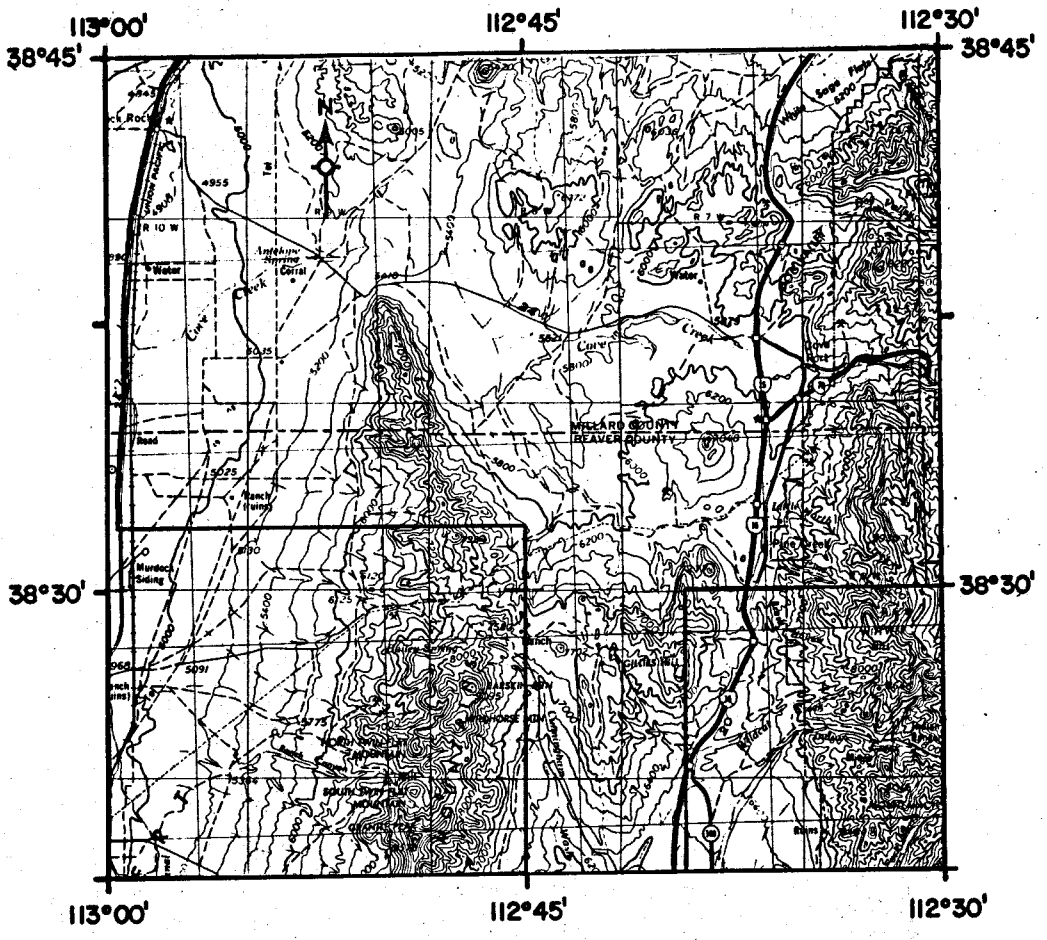

Figure 2 Index map of the survey area

lies the Black Rock Desert. The general topographic relief increases overall by about 1200 ft southward and by about 4000 ft eastward. A second central feature is the Cove Fort Cinder Cone, which lies between the Mineral Range on the west and the Pavant and Tushar Ranges on the east and which rises to an elevation of 7000 ft.

The southern part of the survey area, lying east of the Mineral Mountains, is a topographic high. This region includes Gillies Hill and Four-Mile Ridge and is separated from the Mineral Mountains by Cunningham Wash. In this study this elevated region will be referred to as the "East Mineral Mountains".

Access to the general area is best made by Utah highways 257 and 21 that service Milford from the north and south, and west, respectively. Beaver and Cove Fort are serviced principally by U.S. Interstate Highway 15 extending north-south. Black Rock Road, extending generally east-west from Cove Fort to the community of Black Rock on Utah highway 257 is the only all-weather road (gravel) suitable for passenber vehicles traversing the area. Limited access by air may be made to either Milford or Beaver by light plane (both have 5000 ft all-weather landing strips). Jeep trails lace the entire area and are negotiable by any two-wheel-drive, high-ground-clearance vehicle in dry weather. Wet weather demands a four-wheel-drive vehicle, however, as the roads and bare basalt trails become slick and mucky.

Climate and Vegetation

The area is considered dry temperate, semi-arid. Summer temperatures range from 100°F (37.8°C) in the daytime to 80°F (26.7°C)

at night (due to the altitude); however, in winter the temperature drops to below -10°F (-23.3°C). The mean annual temperature is 49°F (9.4°C). Normal annual precipitation varies from less than 7 in. (17.78 cm) in the Black Rock Desert in the north to 11 in. (27.94 cm) in Beaver Valley in the south, and from 10 in. (25.40 cm) to 25 in. (63.50 cm) in the mountains. More than half of this is due to spring and summer rains. The average annual snowfall is 35 in. (88.90 cm) occurring from November to March.

Sagebrush, cacti, cheat and june grass abound on the valley floors not disturbed by cultivation or irrigation. The less rugged mountain flanks grade from sagebrush into juniper and pinion pine at relatively low elevations and scrub oak and quaking aspen at higher elevations, especially on northern exposures. Sheltered canyons containing perennial streams host a lush growth of cottonwoods, boxelders, maples, and bunch grass.

Prior Investigations

Geologic studies of the survey area probably first appeared in a work by Dutton (1880) in which he described the Pavant and Tushar Mountains as the transition zone between the Basin and Range province and the Colorado plateau. Lee (1908) wrote about the water resources of the region. Butler et al. (1920) and Crawford and Buranek (1945) investigated the various geologic conditions in relation to the mining districts found here.

Callaghan (1939, 1962, 1973), Maxey (1946), Crosby (1959), Rodrigues (1960), and Caskey and Shuey (1975) have all investigated

various aspects of the geology of the Pavant and Tushar Mountains, and Condie and Barsky (1972) and Zimmerman (1961) were interested in the Black Rock Desert and Cove Creek geology, respectively. Mapping of the Mineral Mountains began with Liese (1957), Earll (1957), and Condie (1960), and is being continued at the present time by the faculty and students of the University of Utah.

The following surveys have been made over portions of the area: regional gravity surveys by Mugdett (1963), Sontag (1965), Peterson (1972), and Carter (1977); a microearthquake survey by Olson (1976); and two regional aeromagnetic surveys, one assembled by R. T. Shuey (1974) into a statewide aeromagnetic map (Zietz et al., 1976), and one made for the University of Utah Geothermal Project in 1975.

Currently, detailed geology mapping, heat flow measurements, geochemistry, and additional geophysical surveys are being conducted in the area by an investigating team from the University of Utah and several other teams from private industry to determine the geothermal potential of the region.

Purpose and Scope

The present survey augments those of Crebs (1976) and Thangsuphanich (1976) to the north and east, giving a more complete regional picture of the gravity variations surrounding the Mineral Range. It should be noted that the gravity method can indicate normal faulting, and in a geothermal system such faults may serve as conduits to any rising hot waters, or they may serve to increase reservoir permeability (Rinehart, 1975). Normal faulting may also be a control in determining the boundaries of the geothermal system.

The gravity survey conducted at the Cove Fort - Sulphurdale KGRA and the north Mineral Mountains area was performed to try to indicate a possible heat source (i.e., a magma chamber), any effects of sediment alteration (densification), and geologic structure. Appendix 1 contains a summary of past applications of gravity surveys in developing geothermal explorations.

GENERAL GEOLOGY

The geology of the survey area encompasses two physiographic provinces and a 5-fold regional deformation pattern. The Pavant and Tushar Mountains--separated by Clear Creek Canyon--is recognized as the transition zone between the Basin and Range to the west, and the Colorado plateau to the east. Here too, is a portion of the Intermountain Seismic Belt lying within an east-west lineament of Tertiary and Quaternary volcanism, and gravity and magnetic disparities.

Mineral Mountains.--The most striking feature of this entire region is the Mineral Mountains. This mountain range is primarily a north-south-trending granitic pluton, about 12 miles in length. At the north end of the pluton lies a sedimentary section of the range probably originating in the early compressional phase of the Laramide orogeny. This orogeny brought a period of thrusting in western Utah which can be seen from the Wah Wah Range to the west, to the Pavant Mountains on the east side of the survey area. In the north Mineral Mountains this is manifest as lower and middle Cambrian quartzites over middle and upper Cambrian limestones. This sedimentary thrust sheet was then domed up by a quartz monzonite intrusion, bringing it to roughly the same altitude as the crest of the pluton forming the balance of the range (J. A. Whelan, 1976, personal communication). Pinnacle Pass marks the contact zone between

the granitic pluton to the south and the domed-up sedimentary thrust sheet to the north; here also, on the eastern side of Pinnacle Pass, is an anomalous basalt cone that is the postulated source of olivine basalts found in the area, on both sides of the pass. The reader is referred to the works of Leise (1957), Earll (1957), Condie (1960), Petersen (1974), Crebs (1976), Thangsuphanich (1976), Evans (1977), and Bowers (1977) for detailed discussions of the geology of the Mineral Mountains.

East Mineral Mountains.--To the east of the Mineral Mountains is found an elevated area termed the "East Mineral Mountains" in this study. It extends for several miles east from the flanks of the central pluton into Beaver Valley (south of Negro Mag Wash and the Pole-line road) and rises to an elevation of 7800 ft. This portion of the survey area, encompassing also the western portion of northern Beaver Valley, has had the least geologic mapping of any region in the survey area, and this summary of the geology of this area is based largely on the knowledge and preliminary mapping of J. A. Whelan (1975-77, personal communication) to supplement the regional geology of Hintze (1963).

The East Mineral Mountains is principally composed, west to east, of a granitic pediment from the Mineral Mountains pluton overlain by a finger of Quaternary Cove Fort basalts in northern Cunningham Wash. Considerable amounts of the Tertiary Sevier River formation composed of partly consolidated fanglomerate, conglomerate, sand and silt are found in the washes. In the southern Cunningham Wash area the Sevier River formation contains numerous basalt flows

and ash deposits of varying thicknesses and depths of burial. These presumably are related to the Mineral Mountains and Cove Fort volcanic activity, the latest of which is the post-Bonneville Cove Fort cinder cone. Also in Cunningham Wash, near the Tom Harris mine, are Paleozoic outliers that butt against Tertiary, silicic, volcanic flows originating in the Tushar Mountains to the east. These flows form a convex crescent-shape and are composed of Bullion Canyon andesites, the oldest (Miocene), which unconformably lie on the upper Cretaceous and lower Tertiary series, and Mount Belknap rhyolites (overlaying the Bullion Canyon formation). On some ridges, Dry Hollow latities form "caps" over the Bullion Canyon volcanics below. The Bullion Canyon volcanics are not only the oldest volcanics of the region, but also the thickest, being 5000 ft thick in some places.

The Cove Fort-Sulphurdale KGRA.--The silicious, Tertiary, Dry Hollow latites, Mount Belknap rhyolites and Bullion Canyon andesites of the Tushar Mountains east of Beaver Valley extend north and east to Clear Creek Canyon (gravity downwarp, Sontag, 1965) where they meet the folded and weathered Paleozoic and Mesozoic sediments of the Pavant Mountains (Crosby, 1959). Here, too, are found the rhyolites of the Tushar Mountains interbedded with flows of latite and Joe Lott tuffs). At this intersection, evidence of hydrothermal alteration, sulphur deposits, flourspar, and base metals are found. Sulphur deposits at Sulphurdale and in Sulphur Cove, east of Cove Fort, are associated with a zone of intense faulting: 1) range front faults evidenced at the mouth of Clear Creek Canyon, 2) east-

west faulting found at the volcanic-sediment contact (dolomites and limestones) east of Cove Fort, and 3) northeastward-trending faults characteristic of this portion of the physiographic transition zone, (Lee, 1908; Rodrigues, 1960; Hintze, 1963; Sontag, 1965; Olson, 1976). Acid hot springs and a 91°C water well in eastern Dog Valley (Olson, 1976; Crosby, 1959) are also associated with a similar zone of faulting, some 8 miles north of Sulphurdale.

The Pavant Mountains form a drainage divide between the Great Basin to the west and the Clear Creek downwarp to the south and southeast (Callaghan and Parker, 1962b). The majority of sedimentary rocks in the survey area are found in the Pavant Mountains. Cambrian, Ordovician, Permian, Triassic, Jurassic, and Cretaceous strata dip generally west-northwestward beneath a cover of Tertiary and Quaternary sediments and volcanics (Hintze, 1963). Callaghan and Parker (1962b) described thrust faults and folds in rocks older than the Cretaceous and Tertiary that are of much different character than the later normal faults and broad flexures. Some of these can be seen in the leading edge of an eastward thrusting sheet of Paleozoic rocks of Cambrian and Ordovician age that appear to be thrust eastward over Mesozoic sandstones, shales, siltstones and conglomerates (Butler and Gale, 1912; Maxey, 1946).

Cove Creek and Black Rock Desert area.--Zimmerman (1961) found a variety of Cenozoic and Paleozoic sedimentary rocks with about 25 percent of the surface rocks consisting of Tertiary rhyolites and andesites, as well as Quaternary basalts and vitrophyre exposures. Most of the basalts in this area originated with the post-Bonneville

Cove Fort cinder cone. The basalt flows radiate circularly from this cone east to Cove Fort, west to the Mineral Mountains, north to Cove Creek, and south to Four-mile Ridge as well as south in a narrow finger down Cunningham Wash. Many normal faults displace the Tertiary Sevier River formation and all older sediments in the area. More recent normal faulting can be found in the radial flows themselves that must be post-Bonneville, as is the volcano itself. Most of these faults trend northeastward and cut older north-trending Basin and Range structures and east-west faults.

Strata of Permian and Pennsylvanian rocks seem to be less deformed in the Cove Creek area than in the Pavant Mountains. This, and Paleozoic and Mesozoic sedimentary thickening to the west lends to the possibility of an anticlinal nose plunging west-southwest.

Crosby (1973) described the north Mineral Mountains--Black Rock Desert boundary, and associated volcanics, from the southern Pavant Mountains west to the Beaver Lake Mountains (including the Cove Creek area) as the "Black Rock Offset" because of major features he observed in the sedimentary thrust sheets in the two ranges.

Slemmons (1967) noted strong east-west trends in a zone of Tertiary volcanism laced with Quaternary deformation, extrusion, intrusion and seismic activity extending from the Tushar Mountains west, possibly to the Garlock fault in California.

GENERAL GEOPHYSICS

Gravity and Magnetics.--The northern part of Milford Valley appears to be a Basin and Range graben; and according to Crebs (1976), the maximum thickness of the alluvial valley fill is about 1.8 km along its axis. It is bounded by the Rocky and Beaver Lake Mountain Ranges on the west, and the Mineral Range on the east. Gravity surveys (Peterson, 1872; Crebs, 1976; and Thangsuphanich, 1976) place high-angle Basin and Range faults along the southwest and southeast flanks of the Mineral Mountains with total throws of over 1000 m and a stepped series of smaller range front faults on the western flanks of the central part of the Mineral Mountains.

East-west gravity lineaments (Cook et al., 1975), the aeromagnetic map of Utah (Zietz et al., 1976; Shuey et al., 1974) and steep local gravity gradients show features coincident with Crosby's (1973) "Black Rock Offset". In his regional gravity evaluation, Sontag (1965) also detected east-west gravity lineaments that aligned with an east-west zone through Cove Fort and Clear Creek Canyon.

Seismic.--Olson (1976) observed contemporary microseismic activity in "swarms" along northeast-trending fault zones in Dog Valley and Sulphur Cove, east of Cove Fort. He also detected considerable east-west strike-slip components in the fault-plane solutions for these swarms (Olson, 1976, personal communication).

From the microearthquake survey conducted over the entire region by Olson (1976), several patterns are apparent:

1. There is a consistent trend for microseismic occurrences to follow the Basin and Range faults along the west flank of the Mineral Range.

2. There is an absence of seismicity along the northeast boundary and the entire southern part of the range.

3. Rather than following what seems to be Basin and Range structure in Cunningham Wash, along the east side of the Mineral Range, the seismic pattern follows a northeastern curve away from the Mineral Range.

4. A line drawn through these microseismic epicenters roughly follows a line connecting the volcanic cones of Crater Knoll, Red Knoll, Cinder Pit, and Cove Fort cinder cone.

5. Microearthquake swarms were observed 3.5 km east of Cove Fort in a zone of extreme alteration and in the sedimentary thrusts of Dog Valley.

6. The Black Rock Offset seems to be accompanied by deep-seated bending of the Basin and Range grain to the northeast, east of the Mineral Mountains with microearthquakes along the zones of greatest curature.

The high-density microearthquake clusters around Cove Fort and Dog Valley were interpreted by Olson to be along a north-northeast-trending fault dipping about 70°W just west of Sulphur Peak. Dog Valley seismicity indicated a diffusion of this fault pattern with east-west as well as north-south slippage components and focal depths indication that the seismic epicenters deepen from Cove Fort northward. Baker Canyon, north of Dog Valley on U. S. Interstate Highway 15 displays east-west faulting evidence with signs of slippage not only in the rocks but also in en echélon cracks, downwarps, and even some minor offsets (right lateral) in the pavement of the road surface itself

which is only 7 years old at this writing.

From P-wave delays and S-wave attenuations between sources in the Cove Fort, Dog Valley area and Ranch Canyon stations in the Mineral Mountains, a low velocity "soft" zone of partially molten rock was postulated by Olson (1976) to occur between longitude 112° 40'W and Ranch Canyon. Crebs (1976) cited this as a possible zone of partial melt beneath the central Mineral Mountains that may be responsible for the heat source of the Roosevelt Hot Springs area.

DATA ACQUISITION

Instrumentation

The gravity field data were collected with the Worden Geodesist model 127 gravimeter, number 735, and a LaCoste and Romberg gravity meter model G number 264. The Worden has a linear sensitivity of 0.1247(3) milligal (mgal) per dial division and was read to the nearest 0.1 dial division on a vernier scale, thus affording an accuracy of 0.01 mgal and a precision of about 0.2 dial division. The gravimeter was always read by approaching the null point from the left to avoid errors caused by reversing the direction of the driving screw. Only 87 stations were established with this instrument and 10 percent of those were repeated with the LaCoste and Romberg with a disagreement no larger than 0.18 mgal and averaging 0.11 mgal. The balance of 584 stations was established with the LaCoste and Romberg gravity meter alone, which has a scale constant ranging from 1.05609 to 1.05865 mgal per dial division, giving an accuracy of 0.001 mgal and a reading precision of about 0.003 dial division. This gravimeter was always read by approaching the null point (2.7 on the internal scale) from the right to avoid errors caused by reversing the direction of the mechanical drive. This gravimeter was temperature compensated to operate internally at 58^{o}C. The Worden mechanism was encased entirely in a Dewar flask but had no other temperature compensation.

For elevations of a few stations, two Wallace and Tiernan barometric altimeters, model 185 were read to the nearest foot.

Field Procedures

Before either gravimeter was taken to the field, the approximate calibration of each instrument was checked by reoccupying the Salt Lake City calibration loop established by Dr. K. L. Cook between the University of Utah and the Liberty Park base. This was also done during and subsequent to the survey. The calibration difference noted was 18.90 mgal using the above instrument sensitivities. All individual field gravity measurements were made as members of closed "loop" sequences beginning in the morning and ending at night at either the Milford or Beaver gravity base. These two bases are part of the Utah Gravity Base Station Network (Cook et al., 1971). Complete descriptions and exact locations of these bases can be obtained from this reference. Two field base stations were established centrally in the survey area and tied to this base station network in Beaver and Milford by the oscillation technique where 3 pairs of readings are taken alternately at a network gravity base and the chosen field base (Dobrin, 1960, p. 222). Complete descriptions of these bases are given in Appendix 3. Tidal variations and instrument drift effects were minimized by making short (about 3 hr) observation loops with respect to a field base, tying the field base to one of the network base stations in the early morning and late evening, taking care to relocate several prior data stations in each new loop run. Where good location control and accessibility were apparent,

the Wallace and Tiernan altimeters were used in place of surveyed elevations. This was done by the "ABA" looping technique where a reference reading is made at a point of unknown elevation and then a final reference reading made at the starting point, "A", of known elevation. The change in elevation was calculated from the average of all four (two with each altimeter) elevation increments measured. This minimizes the effects of any instrument drift; no measurements were accepted where the total drift around the "ABA" loop of any one altimeter exceeded 2 ft. The altimeters were only used for indicated incremental changes in elevation between station "A" and station "B" of 250 ft or less. From experience, it was found that altimeters used between full dawn and 11:00 A.M. on clear days usually drifted less than 2 ft if loop times did not exceed about 20 min.

All the maps used in this survey were U.S.G.S. advance prints (blue lines) 7.5 minute series topographic quadrangles dated from 1958 to 1962 with 40-ft contour intervals (except Black Rock 3 NE, 3 NW, and 3 SW, which had 20-ft contour control). In all cases the bench marks are accurate to 1 ft and the spot and summit elevations are accurate to one-half a contour interval. Horizontal control of geographic features is within 0.01 min of arc giving a location accuracy of approximately 50 ft.

Fresh surface samples were taken at any outcrop close by a station and assigned the station number.

Data Reduction

The observed raw field readings were transferred to computer IBM cards in chronologically looped sequences, which were processed

on the University of Utah UNIVAC 1108 computer. The reduction routine computed the simple Bouguer gravity anomaly values at the various station locations referenced to absolute gravity values at the Salt Lake City airport (Cook, et al., 1971) with drift corrections included (assumed linear) made between the first and last readings in a survey loop. The routine uses the International Gravity Formula (Swick, 1942) to obtain the theoretical gravity on the geoid from which a station's latitude correction is derived, using a datum of mean sea level. A free-air correction of 0.09406 mgal/ft in conjunction with a Bouguer correction for an infinite slab of density 2.67 gm/cc between the station elevation and mean sea level, results in the total elevation correction of 0.5999 mgal/ft used by the routine.

Terrain corrections were carried out on all data stations through 20 km. This was accomplished in two parts; the first was by hand, including zones B through E of the U. S. Coast and Geodetic Survey terrain correction templates (again assuming an average crustal rock density of 2.67 gm/cc) (Stewart, 1958; Cook et al., 1964; Hardman, 1964); the second phase, from zone F of these templates out to 20 km (which includes the template area out through 40 percent of zone L), was accomplished on the UNIVAC 1108 computer using a terrain correction algorithm (Kane, 1962) adapted from a computer routine written by Hardman (1964). All 671 stations were terrain corrected with a minimum total correction of 0.25 mgal in the flat valleys to a maximum of 22.51 mgal on a mountain peak in the north Mineral

Mountains. The final result of all reductions applied to the data was Bouguer gravity anomaly values that were terrain-corrected to 20 km.

DATA ERROR ANALYSIS

Collection

Although the LaCoste and Romberg gravimeter has a precision of 0.003 dial divisions (equivalent to about 0.003 mgal), the Worden gravimeter only has a precision of 0.2 dial divisions (approximately 0.025 mgal). Linear drift corrections are of limited value (Nettleton, 1940, p. 59) when applied to earth tidal variations which have a maximum sinusoidal amplitude of 0.3 mgal in 6 hours during the new and full moon phases. Differences in reduced gravity values at reoccupied stations at varying times of day never exceeded 0.30 mgal and averaged 0.21 mgal. Vertical control was accurate to 1 ft at bench marks and to half a contour interval or better for spot and altimeter elevations. Since the contour interval is at most 40 ft the maximum error from this source is 1.2 mgal. Because of the unchanging nature of the area and the choice of station positioning, it is estimated that a probable maximum error of 5 ft is more likely than 20 ft, giving a corresponding error of 0.3 mgal. Horizontal inaccuracies in station placement (primarily in a north-south direction) will result in errors in the latitude correction during data reduction. This correction is about 1.4 mgal/mile (north-south) at the latitudes of the survey, resulting in an error of 0.01 mgal for every 50 ft of north-south displacement from an assumed position. It is doubtful that this source of error contributes more than 0.05

mgal anywhere.

Data Reduction

Because the raw gravity data were not corrected for earth tides, errors from this source could conceivably be as large as 0.30 mgal. As for the Bouguer and terrain corrections, errors could be introduced if the vertical column of material between the reference datum and the station in question deviated far from 2.67 gm/cc. No attempt has been made to calculate these possible errors since they are considered small by comparison to the anomalies being sought (Hardman, 1964). The terrain correction is subject to two inherent sources of error. The first is the propagation of error in the average elevation of a terrain zone from which the correction is calculated. The second is the error introduced into the total terrain correction by the combination of the inner zone terrain correction derived from zones B through E of the U.S.C. & G.S. zone templates with the outer zone terrain correction calculated from M. Kane's (1962) computer algorithm; this error, however, was shown to be about 0.04 mgal (Kane, 1962).

Total terrain correction accuracy is judged here to be within 10 percent of a stated value; that is, within 2.25 mgal in the mountains and about 0.05 mgal in the valleys in the worst cases. This gives a total estimated accumulative possible error of about 3 mgal in the mountains grading down to approximately 0.4 mgal in the valleys.

DATA CONTROLS

Surface material densities of the surveyed area were divided into three classifications: (1) Paleozoic and Mesozoic sedimentary rocks, including dolomites, massive limestones, shales, sandstones, and conglomerates, (2) intrusive rocks of Tertiary age, mainly quartz monzonites, and (3) volcanic and clastic rocks of Tertiary and/or Quaternary age, including rhyolite, basalt, and andesitic flows. These broad classifications of rock types were used as a guide in compiling the general geology map shown in Figure 3. Because of limited access to outcrops, samples were primarily collected for density measurements at gravity stations associated with rock outcrops.

Laboratory wet bulk, mean density measurements were made on all samples collected. These are summarized in Table 1 along with other characteristic samples of the area for comparison. Although the samples showed some weathering, the densities within a rock type did not vary greatly (Nettleton, 1940, p. 101); however, composition, texture and culpability did vary to a high degree. Individual sample densities and the locations from which the samples were taken are given in Appendix 2.

On the basis of the average densities observed in the above general rock types, the average density contrast between the Tertiary and Quaternary clastic deposits and volcanic rocks which constitute

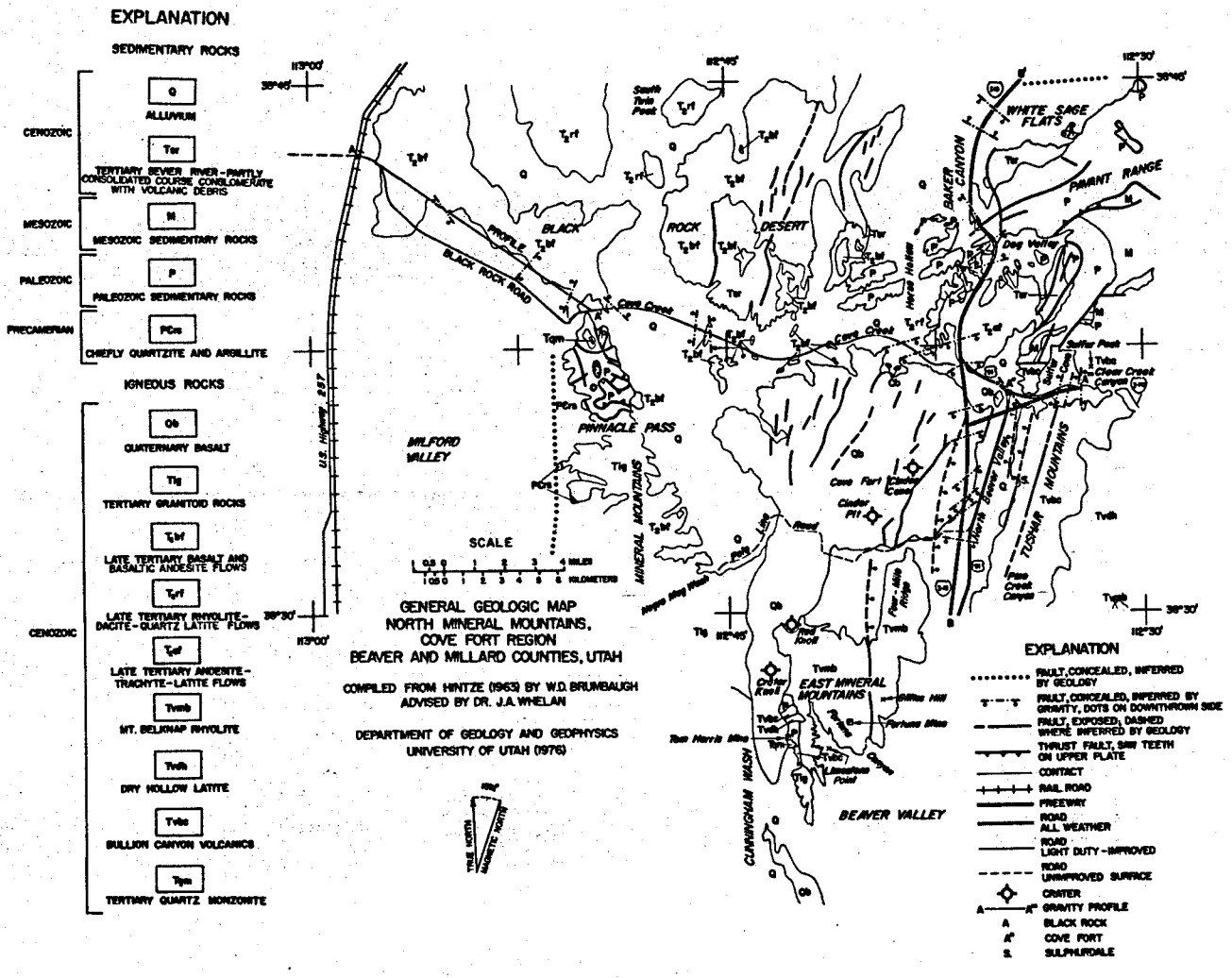

Figure 3 General geologic map, north Mineral Mountains, Cove Fort region, Beaver and Millard counties, Utah

Table 1. Wet Bulk Sample Densities[1]

Rock Types	No. of Samples	Density Range (gm/cm)	Mean Density (gm/cm)
Lamprophyre Dike[2]	2	2.69-3.44	3.12
Gneiss and Schist[2]	8	2.63-2.74	2.69
Limestone (fossiliferous and dolomitic)	13	2.29-2.79	2.64
Granite[2]	11	2.54-2.69	2.60
Quartzite	8	2.41-2.63	2.58
Sandstone	1	2.57-2.57	2.57
Basalt	6	2.20-2.68	2.44
Rhyolite	21	1.92-2.62	2.38
Obsidian[2,3]	3	2.34-2.35	2.34
Latite	3	1.92-2.55	2.15
Alluvium[2]	--	2.0 $\pm$ 0.1	2.00

[1]Density measurements taken by the author unless otherwise indicated.

[2]At least one sample density measurement taken from Crebs (1976).

[3]At least one sample density measurement taken from Thangsuphanich (1976).

the valley fill, and the pre-Tertiary sediments, Tertiary intrusives, and gneiss/schists that constitutes the bedrock of the mountain ranges, is estimated to lie between 0.35 gm/cc and 0.5 gm/cc, depending upon the volcanics (intrusive and extrusive)/unconsolidated alluvium ratio. The mean density of alluvium was taken to be 2.0 $\pm$ 0.1 gm/cc from a study made by Crebs (1976).

Slim-hole drilling has been widely used by private industry in this area principally for heat flow measurements, but most of the results are proprietary at this time.

Of the well logs available, the deepest is for a dry oil well drilled in 1950 by the Beaver Valley Oil Company about 1 km south of the community of Black Rock near the axis of Milford Valley. Drilling was stopped at 3,682 ft when salt water was encountered in a sand-shale sequence (Heylum, 1963). A water well, now plugged and abandoned, was drilled in 1938 about 8 miles west of the present Interstate Highway 15 and 100 ft south of Black Rock Road in section 21, T25S, R8W. The well passed through 188 ft of basalt before entering white marls at a depth of 320 ft (Utah State Engineer's office, Dept. of Water and Water Rights, 1976, oral communication).

PRESENTATION OF DATA

The reduced gravity data set is presented here in three different ways, along with a generalized geologic map and a regional aeromagnetic map of the survey area for comparison. Figures 4 and 5 show hand-contoured, terrain-corrected Bouguer gravity anomaly maps with a 1-mgal contour interval. These maps represent all of the data taken during the survey and are the most detailed. Figure 6 illustrates these same data, at the same contour interval, after they had been hand-digitized on the 1-km Universal Transverse Mercator grid system and then contoured on the UNIVAC 1108. Lastly, Figure 7 displays these data in a three-dimensional, 45^{o} isometric projection, which is also computer drawn from the digitized data.

The regional aeromagnetic map (Fig. 15) was reduced from the aeromagnetic map of Utah (Zietz et al., 1976) which has a contour interval of 20 and 100 gammas and which has the earth's main field removed; but no attempt at any reduction to the pole has been made. Thus anomalies and gradients are shifted slightly to the south-southwest due to the inclination (66^{o}) and the declination (N 15^{o} 30' E) of the main magnetic field of the earth.

The generalized geology map (Fig. 3) was compiled to show the spacial relationships of the basic and acidic volcanics, alluvial fill in the valleys, and the Paleozoic and Mesozoic sedimentary outcrops. It was hoped that this breakdown, together with indications

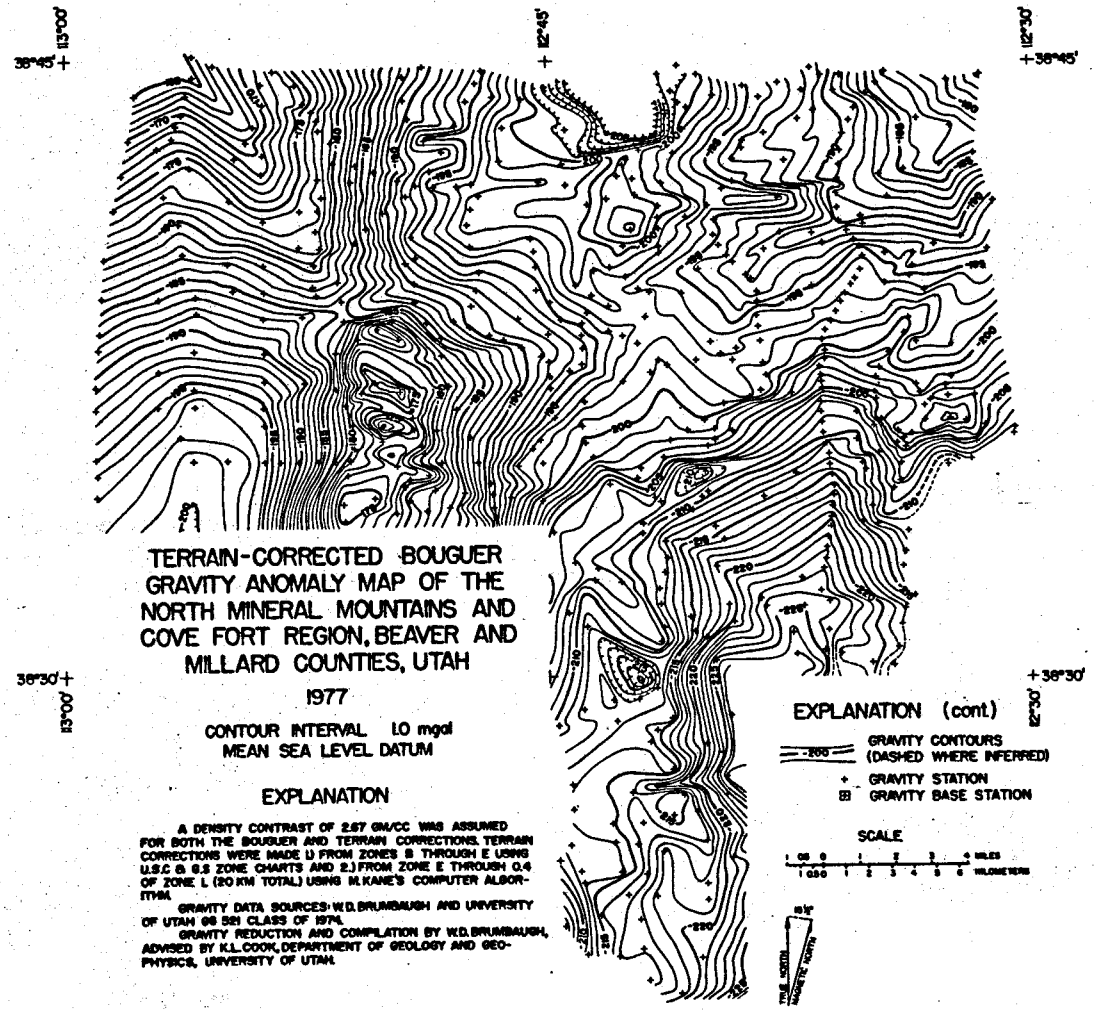

Figure 4 Terrain-corrected Bouguer gravity anomaly map of the north Mineral Mountains and Cove Fort region, Beaver and Millard counties, Utah; hand-contoured, contour interval = 1 mgal

TERRAIN-CORRECTED BOUGUER GRAVITY
ANOMALY MAP OF THE
COVE FORT-SULPHURDALE REGION
BEAVER AND MILLARD COUNTIES, UTAH
1977

CONTOUR INTERVAL 1.0 mgal
MEAN SEA LEVEL DATUM

EXPLANATION

- GRAVITY CONTOURS DASHED WHERE INFERRED
- GRAVITY STATION
- GRAVITY BASE STATION
- WATER WELL
- HOT SPRINGS
- PROSPECT
- FREEWAY
- TWO LANE, HARD SURFACED ROAD
- DIRT ROAD

A DENSITY CONTRAST OF 2.67 GM/CC WAS ASSUMED FOR BOTH THE BOUGUER AND TERRAIN CORRECTIONS. TERRAIN CORRECTIONS WERE MADE 1) FROM ZONES B THROUGH E USING U.S.C. & G.S. ZONE CHARTS AND 2) FROM ZONE E THROUGH 0.4 OF ZONE L (20 KM TOTAL) USING M. KANE'S COMPUTER ALGORITHM.

GRAVITY DATA SOURCES: W.D. BRUMBAUGH
GRAVITY REDUCTION AND COMPILATION BY W.D. BRUMBAUGH, ADVISED BY K.L. COOK, DEPARTMENT OF GEOLOGY AND GEOPHYSICS, UNIVERSITY OF UTAH.

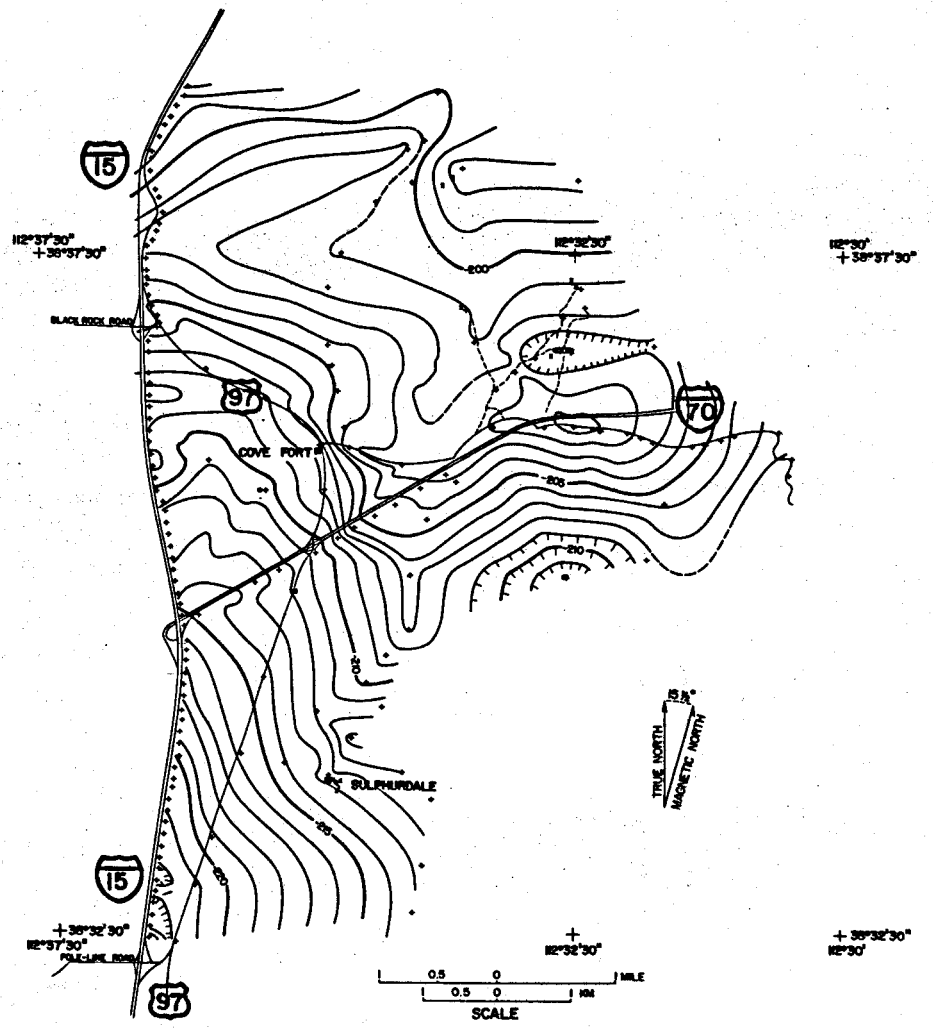

Figure 5 Terrain-corrected Bouguer gravity anomaly map of the Cove Fort - Sulphurdale region, Beaver and Millard counties, Utah; contour interval = 1 mgal

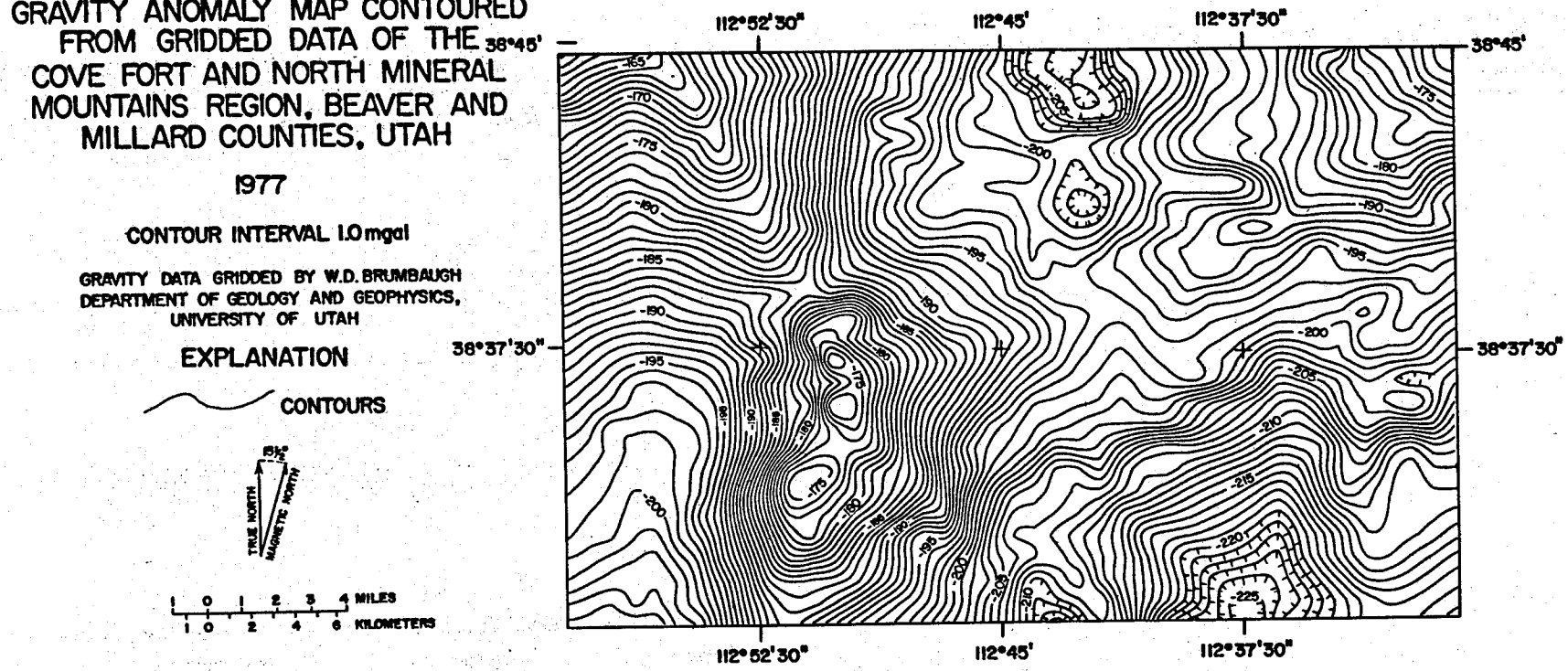

Figure 6 Terrain-corrected Bouguer gravity anomaly map of the north Mineral Mountains and Cove Fort region, Beaver and Millard counties, Utah; hand-digitized at 1-km intervals, machine-contoured; contour interval = 1 mgal

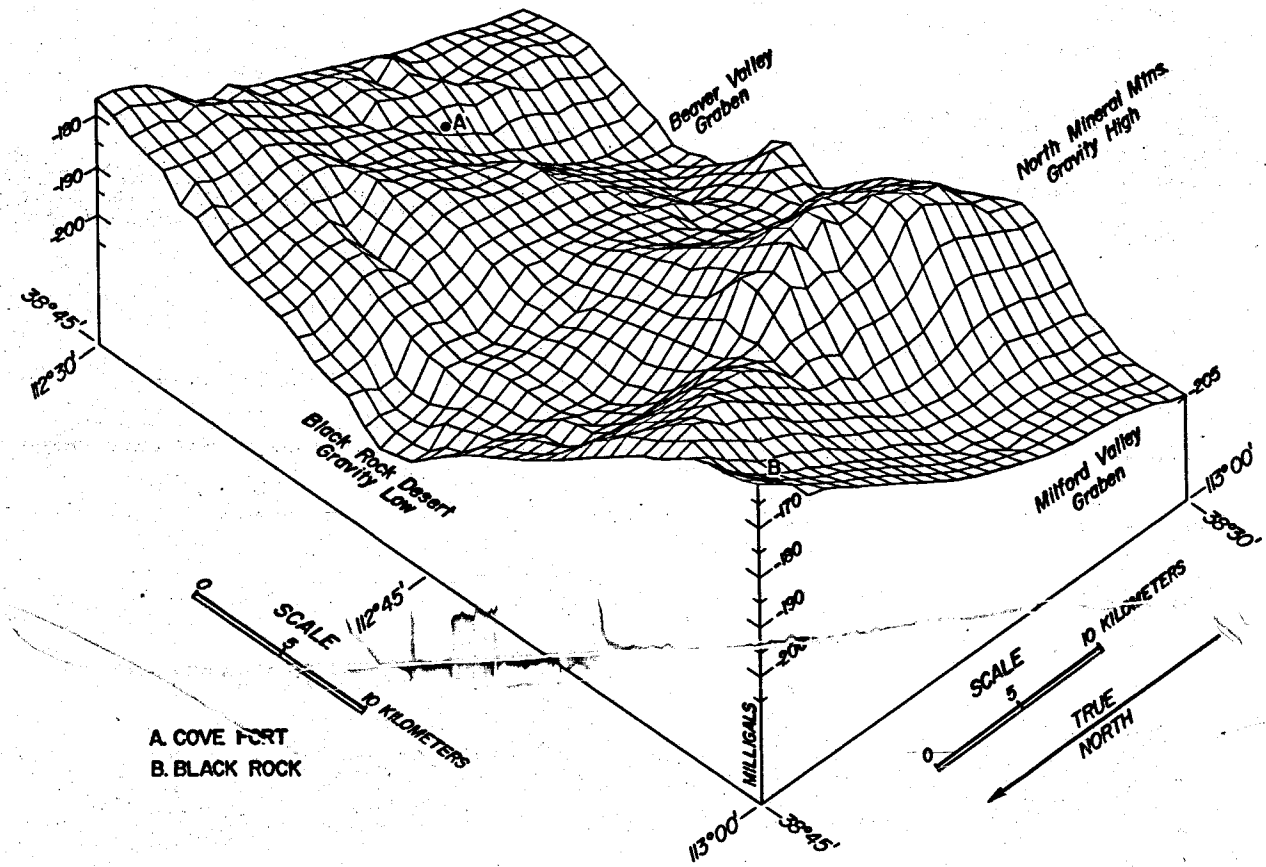

Figure 7 TERRAIN-CORRECTED BOUGUER GRAVITY ANOMALY MAP OF THE NORTH MINERAL MOUNTAINS AND COVE FORT REGION, BEAVER AND MILLARD COUNTIES, UTAH: THREE DIMENSIONAL, 45° ISOMETRIC VIEW FROM THE NORTHWEST CORNER OF THE SURVEY AREA.

of the known major faults, would serve as a guide to subsurface structure interpretation of the gravity data.

In addition, Figures 8, 9, and 10 show the high-pass filtered, second-order polynomial residual, the second vertical derivative Bouguer gravity anomaly maps, respectively. Strike-filtered Bouguer gravity anomaly maps in the four directions of an eight-point mariner's compass (Figs. 11-14) were produced in an effort to further separate meaningful trends from the background data.

Lastly, the Talwani two-dimensional modeling method (Talwani et al., 1959) was used to calculate the expected anomaly across two roughly orthogonal gravity profile models: 1) one along Black Rock Road (Fig. 16), which traverses the survey area west-northwest to east-southeast with a station density of about one per km, and 2) the other on Interstate Highway 15 (Fig. 17) traversing the area north to south with a station density of about one per two-tenths of a mile. These profiles are presented with observed, assumed regional, and residual values.

These profiles are meant to show the relationships between regional gravity patterns and interpretive geologic cross sections.

ANALYSIS OF THE GRAVITY DATA

Gravity Patterns

The terrain-corrected Bouguer gravity anomaly data (Figs. 4 and 6) show the complex nature and high relief of the gravity field in the geologic province transition zone that constitutes the area of study (Fig. 3). The Basin and Range orogeny signature in the gravity field dominates the western half of the study area. Here are found large gravity gradients indicated by contours trending primarily north and south on: 1) both sides of the Mineral Mountains; and 2) the gradient on the east side of the Mineral Mountains extends northward along the eastern margin of the Black Rock volcanic flows. These strong gradients are obvious on the observed gravity contour maps, but become striking on the polynomial residual, high-pass filtered, and north-south strike-filtered anomaly maps. This is misleading however, in at least the instance of the west flanks of the central Mineral Mountains, as will be discussed in a later section.

East of the Mineral Mountains the gravity signature changes sharply as the Colorado plateau is approached. Approximately half of the gravity gradient that forms the north-south Basin and Range fault zone on the southeastern side of the Mineral Mountains (Thangsuphanich, 1976) diverges to the east in the vicinity of the Pole-line road and passes through the Clear Creek Canyon area at right angles to its

original trend. This interruption of the north-south gravity trend manifests itself as a gravity saddle (first reported by Sontag, 1965 as the Black Point gravity high) separating the Black Rock Desert gravity low from the Beaver Valley graben gravity low. On the surface, this gives the appearance of connecting the east-west trending gravity gradient found in Clear Creek Canyon with the east-west gravity gradient forming the northern end of the Escalante Desert (Milford Valley graben); this connection (if interpreted as such) gives the impression of an east-west lineation extending from the Cricket Mountains, west of Black Rock, east through Clear Creek Canyon toward Monroe. Crosby (1973) has discussed the possibility of such a lineation which he terms the "Black Rock Offset".

The form of the observed gravity anomaly field then, can be viewed initially as a sheet draped over a 2-layer bedrock, alluvium and/or volcanics model comprised of two zones of elevated bedrock, one at each northern corner of the survey area, and an elevated parallelepiped of high density material forming the Mineral Mountains north of Negro Mag Wash (Fig. 7). It is this basic model and the subsequent draped gravity field that is to be assigned geologic significance and continuity in the following sections.

Terrain-corrected Bouguer Gravity Anomaly Map

Overall trends.--On the terrain-corrected Bouguer gravity anomaly map (Fig. 4), the highest observed gravity value was -164.4 mgal north-northwest of Black Rock and the lowest value was -233.0 mgal east of Gillies Hill on U.S. Highway 91 (Fig. 2). This represents a total difference of 68.6 mgal over a distance of about 42 km (approx. 26 mi)

and an average gradient of -1.63 mgal/km (-2.64 mgal/mi) northwest to southeast. Most of this gravity relief is in the north-south direction as is demonstrated by the overall gravity change along northward-trending Interstate Highway 15. The gravity values range from -182.4 mgal on the north to -233.0 mgal on the south (a total change of 50.6 mgal) over a distance of about 31 km; thus there is a gradient of -1.65 mgal/km (-2.65 mgal/mi). Along U.S. Highway 257, north to south, the maximum gravity value was -164.4 mgal and the minimum was -205.0 mgal. This gives a relief of 40.6 mgal in 26 km (16 mi) or a gradient of -1.56 mgal/km (-2.50 mgal/mi). Along the northern boundary of the survey in a west to east direction, there is a decrease of 20 mgal over a distance of 48 km (30 mi) or a gradient of -0.41 mgal/km (-0.67 mgal/mi). Along the southern boundary in a west to east direction, there is a decrease of 28 mgal in the same distance, giving a gradient -0.58 mgal/km (-0.63 mgal/mi).

Gravity Highs.--A gravity high occurs in the northwest corner of the survey area north of the community of Black Rock. Although the high shows no closure, it does exhibit right-angle contours with the gravity values decreasing almost uniformly over 40 mgal to the south into the Milford Valley graben and east into the Black Rock Desert gravity low. This area is covered by thick basalt flows (several scores of meters are exposed as cliffs) and gives no direct evidence as to what may lie below. The basalt here is vesicular, as it is further east toward Cove Fort, and is about 0.3 - 0.45 gm/cc less dense than the assumed 2.67 gm/cc of bedrock (Appendix 2). This

gravity high is ascribed to near-surface Paleozoic bedrock that crops out in the Cricket Mountains about 4 km west-northwest of Black Rock (R. W. Case and J. A. Carter, 1977, personal communication). Evidence for this interpretation is indicated in the strike (east) and dip (26^{o} ESE) of the Paleozoic strata exposed in the Cricket Mountains that, if continuous to the east, could account for its presence under the Black Rock area at a shallow depth resulting in the observed gravity high.

The northern portion of the Mineral Mountains that lies within the survey area (north of the Pole-line road) is also represented by a gravity high with a closure of about 11 mgal. Within this high are several subordinate highs that can be divided into two categories: 1) those associated with the Mineral Range pluton, and 2) those north of the pluton associated with the Paleozoic sedimentary rocks.

The group (2) local gravity highs center over the domed-up Paleozoic rocks, whereas the gravity highs associated with the Mineral Range pluton are centered about 2.5 km to the west of the mountain range's main north-south ridge line. Crebs (1976) also found this to be true of a gravity high south of Negro Mag Wash in the Corral Canyon area. He ascribed this westerly offset from the pluton due to a series of Precambrian exposures of higher density than the Mineral Range pluton. Although contact metamorphism exposures of Precambrian gneiss/schist exist on the northwest edge, edge, marbleized limestone is also found here. The role of sedimentary rocks buried beneath alluvium cannot be discounted as a partial cause to the offsetting of the gravity high south of Pinnacle Pass and

west of the range. Between these groups of gravity highs there is a striking gravity saddle with at least 6 mgal relief and 3/4 km wide in the gravity surface corresponding to the "Pinnacle Pass Contact zone" (K. L. Cook, 1977, personal communication) that marks the northern boundary of the Mineral Range pluton. Several facts at this point are noteworthy:

1. Quartz monzonite and the granitic pluton have about the same mean density of 2.57 gm/cc.

2. The Paleozoic rocks draped over the monzonite intrusion have a mean density of 2.68 gm/cc.

3. The Pinnacle Pass Contact Zone occurs at a cleft in the Mineral Mountains 1 km wide in line with the range and 2 km deep transverse to the range. There is only a narrow ridge (Pinnacle Pass) joining the mountains together across this cleft.

4. The mean values of the local gravity highs on both sides of this contact zone differ by less than 1.0 mgal and have a total mean value of -176.0 mgal.

5. There is a Quaternary basalt cone on the east flanks of Pinnacle Pass with average vesicular basalt densities of 2.50 gm/cc.

6. On the Mineral Mountains geology map of Evans and Nash (1977, personal communication) a fault cutting transverse to the range is shown that corresponds with the gravity low.

7. The east-west-trending contact zone shows extreme contact metamorphism, particularly in marbleized limestone outcrops found near mining prospects and the grading of the granitic pluton material toward the gneiss/schist composition found on its western flanks.

8. Quartz latite dikes, sometimes in places 2 m thick, cut the pluton striking north-northwest to south-southeast. Latites have an average density of 2.58 gm/cc in this region (J. A. Carter, 1977, personal communication).

This gravity saddle is probably caused by a near-surface mass deficiency. Its narrow breadth and 6-mgal relief indicates that this

mass deficiency cannot be more than about 1/3 km in depth assuming a density contrast of less than 0.45 gm/cc (the approximate difference between the quartz latite and the pluton/quartz monzonite aggregate densities). The overall northern Mineral Mountains gravity high, of which the Pinnacle Pass Contact zone is superimposed, is 9.5 km long north to south and 4.5 km wide and can be attributed to the granitic pluton that comprise the range (Crebs, 1976).

A third gravity high is found in the northeastern corner of the survey area. Its maximum gravity values are comparable with those found over the Paleozoic rocks of the north Mineral Mountains and about 8 mgal less than those found north-northeast of Black Rock. This gravity high is directly attributable to the Paleozoic bedrock that crops out at the leading edge of a Laramide overthrust sheet found there (see General Geology and Data Control sections). Here again there is no gravity closure, only non-uniform contours expressing gravity relief to the west of about 25 mgal and to the south of about 45 mgal. This gravity high appears to be the southwestern end of a larger gravity feature north and west of the Pavant Mountains.

The East Mineral Mountains shows a gravity high between Cunningham Wash (Fig. 2) and Beaver Valley centered over Fortuna Canyon between the Fortuna mine (gold in quartz veins) and Limestone Point, the high which extends about 3 km in a north-south direction and 4 km in a northwest-southeast direction, has a closure of 2 mgal and marks the position of Paleozoic quartzite outliers north of the Tom Harris mine. These Paleozoic rocks are the probable source of the gravity high

since they are surrounded on three sides by the comparatively low-density rhyolites and latites of the Tushar Mountains volcanic sequence and on the fourth side by the vesicular Cove Fort basalts. There is an outcrop of quartz monzonite within the sedimentary outliers with a density of about 2.62 gm/cc that may be associated with a sub-surface intrusive. Although there is a small (about 1 mgal of closure) gravity anomaly over this area, it is not known whether this anomaly is connected with the Paleozoic rocks or the possible intrusion.

Gravity Saddles.--The three major gravity highs found in the survey area are connected by two gravity saddles, one between the Black Rock gravity high and the north Mineral Mountains and one following the outcrops of Paleozoic rocks from the thrust faults of Dog Valley to the Pinnacle Pass Contact zone of the north Mineral Mountains. A third gravity saddle occurs between the north Mineral Mountains gravity high and the central Mineral Mountains gravity high. This saddle was first observed and described by Crebs (1976); it is centered at about the Pole-line road traversing the Mineral Mountain range at Negro Mag Wash with only the northern limb lying within this survey area. There are several factors the above gravity saddles have in common:

1) The following springs are found on the indicated saddle:

   a) Roosevelt Hot Springs and Bailey Springs on the central Mineral Mountains gravity saddle

   b) Antelope Springs on the north Mineral Mountains-Black Rock saddle

   c) Horse Hollow Springs lie on the gravity saddle between the gravity highs over the southern Pavant

Range and the north Mineral Mountains that was originally reported by Sontag (1965) as the "Black Point Gravity High".

2) An interruption, in each case, of the smooth slope of gravity contours:

   a) In the area where the eastward-trending Negro Mag Wash intersects the northern limb of the central Mineral Mountains gravity saddle (Crebs, 1976)

   b) At the north end of the Mineral Mountains where Black Rock Road circumvents the northern end of the range on the southern limb of the Black Rock - north Mineral Range gravity saddle

   c) North and west of Horse Hollow on the Black Point gravity saddle

Of the points listed above the interruptions of smooth contours are probably the most important as the implied increase in gravity gradient of these areas may indicate the presence of major faulting transverse to the saddle.

Gravity gradients.--The principal gravity gradient observed in the survey area lies between the north Mineral Mountains and the Beaver Valley graben. In a distance of 24 km, there is a gravity change of about 60 mgal representing a gradient of -2.50 mgal/km (-4.00 mgal/mi over 15 miles). At the approximate latitude of the Pinnacle Pass Contact zone (about 38° 36.5'N) the contours representing this gradient split, with 40 mgal of contours turning east and passing through the Clear Creek Canyon area, and 20 mgal of contours extending northward to form half of the Black Rock gravity high relief. An interesting observation here is the nearly perfect alignment of Crater Knoll, Red Knoll, Cinder Pit, and the Cove Fort cinder cone (Fig. 3) with the center of the northeast-southwest

trending segment of the gravity contours that pass through Clear Creek Canyon. This portion of the east-swinging set of gravity contours may be due to a zone of faulting and therefore a zone of crustal weakness where basaltic lava could easily extrude. Along the southeastern end of the Mineral Mountains, Thangsuphanich (1976) has interpreted a gravity profile along the Pass Road, and obtained a total displacement of about 6,200 ft (1.9 km) along a series of faults located within this steep slope of gravity contours, using a bedrock-to-alluvium density contrast of 0.5 gm/cc. Along the same profile on the west side of the Mineral Mountains, Thangsuphanich (1976) modeled a series of step faults resulting in a total alluvium depth of 4,500 ft (1.4 km).

At the north end of the Mineral Mountains, a Basin and Range fault has been modeled (see the section on gravity profiles) with a throw of 1800 ft (0.55 km).

Of the steep slope of gravity contours east of Cunningham Wash, approximately 15 mgal within 3 km of the edge of the Beaver Valley graben correlates well with a north-south trending fault mapped in 1975 by J. A. Whelan (1976, personal communication). This fault shows many tens of meters of vertical displacement exposed above ground level and cuts the Tertiary Mt. Belknap rhyolites that crop out south of the Cove Fort cinder cone.

Pronounced gravity gradients are also evident flanking the east and west sides of the Black Rock Desert gravity low that dominates the north-central portion of Figure 4. It is not clear at this time whether these slopes across the gravity contours represent Basin and

Range faulting or a depression of the Paleozoic bedrock, or both.

The steep gravity gradient that marks the eastern margin of the Milford Valley graben are still somewhat enigmatic. Crebs (1976) and Thangsuphanich (1976) have shown that although Basin and Range faulting dominates the southern end of the Mineral Mountains in relation to the Milford Valley graben, the floor of the Milford Valley graben ascends at a shallow angle toward the western flanks of the central Mineral Mountains with only small step-like Basin and Range faulting indicated. This rise in the valley floor toward the western mountain flanks continues toward the north end of the Milford Valley graben at least as far as Pinnacle Pass, where a profile was modeled by the Gravity and Magnetics class (GG-521), University of Utah, of 1974. The Black Rock Road profile modeled in this study, however, indicated the presence of a Basin and Range fault zone on the northwest end of the Mineral Mountains with a total throw of about 2100 ft (0.63 km). The structure of the Milford Valley graben floor is not yet fully understood. The slope of the gravity contours south of the community of Black Rock clearly forms the northern boundary of the Milford Valley graben. But again, at what point or extent the sloping Paleozoic rocks give way to faulting is unknown at this time. The only well log available (see Data Control section) is indeterminate since the hole bottomed in unidentified strata.

Gravity Lows.--The principle gravity lows of the survey area are those over the Milford Valley graben, the Beaver Valley graben and the Black Rock Desert gravity low. Both the Milford and Beaver

valleys are intermountain basins, whereas the Black Rock Desert displays only the minor Cove Creek drainage depression with Little topographic relief that would indicate a gravity low of the observed magnitude or extent. The Black Rock Desert gravity low is divided into north and south components, which are separated by a minor gravity saddle. Although the northern portion of the low appears to be the main feature, it has no closure within the limits of the survey area. The southern extension, however, has a closure of 3 mgal over a roughly circular area of radius 1.5 km with narrow, low gravity zones extending about 5 km east and west of the closure. The eastern zone has a closure of 1 mgal.

The Black Rock Desert gravity low is probably caused partly by a Basin and Range graben and partly by a depression of the Paleozoic bedrock beneath the overlying volcanics. This is inferred from the angle and direction of dip of the plunging Paleozoic bedrock strata exposed in the Cricket Mountains to the west and the Pavant Mountains to the east, and the large lateral distance covered by gravity contours with uniform slope on both the east and west sides of the gravity low.

A long, narrow, northward-trending gravity low of about 8 km in length and 5 km in width but showing no closure within the survey area is centered over the northern end of Beaver Valley. This anomaly is probably caused by thick alluvial fill in the basin between the Tushar Mountains and the East Mineral Mountain rise. The thickness of alluvium is about 2200 ft (0.67 km) using a bedrock-to-alluvium contrast of 0.5 gm/cc (see section on interpretive profiles,

Interstate Highway 15).

On the west side of the north Mineral Range and south of Black Rock, there is a broad northward-trending gravity low that coincides with the north end of Milford Valley. The size of the gravity low extends to the west and south off the map. Crebs (1976) reported this low to be about 20 km in length and 8 im in maximum width with a closure of at least 5 mgal. He arrived at a depth of alluvium in the center of this gravity low (due west of Bearskin Mountain) of 1.8 km, using a density contrast of 0.5 gm/cc between alluvial fill and bedrock (granite). In this study the extreme northern end of the Milford Valley gravity low shows a depth of alluvial fill of 2100 ft (0.65 km) at a point 2 km southeast of Black Rock along the Black Rock Road profile. A density contrast between alluvial fill and bedrock of 0.5 gm/cc was used here also for comparative purposes. It is clear that the Milford Valley graben terminates with Basin and Range faulting on the northeast at the north end of the Mineral Mountains, although the termination of the structure at the north end of the valley is still uncertain.

Two small gravity lows are observed in Figure 4 within the gravity contours that bend east from the Mineral Mountains and pass through Clear Creek Canyon. One, which is based on the gravity value of a single station northwest of the Cove Fort cinder cone, measures about 1 km in width (north-south), 2 km in length (east-west), and has a closure of 3 mgal. Although the principal facts of the station were checked, the anomaly may be caused by a reading error. Moreover, the anomaly cannot be accounted for geologically. The

second small gravity low is also centered about a single station north and west of Red Knoll but it is supported in part by several other data points. Trending northwest-southeast (orthogonal to the surrounding contours), the anomaly is about 4 km long and 3 km wide with a closure of 5 mgal. Even though it also is suspect, the anomaly may be of some geologic significance since it also lies along an east-west geomorphic feature extending from Negro Mag Wash in Milford Valley to Pine Creek Canyon south of Sulphurdale. Moreover, the anomaly also lies along the striking northeastward-trending alignment of four cinder cones designated from south to north as Crater Knoll, Red Knoll, Cinder Pit and Cove Fort cinder cones (Fig. 3). Irrespective of the validity of this gravity low, it is considered significant that in this general area of the belt of cinder cones, there is a pronounced interruption of the northeastward-trending gravity contours, for example the gravity nose lying north of Red Knoll cinder cone.

Gravity Patterns of the Cove Fort-Sulphurdale KGRA

The Cove Fort-Sulphurdale KGRA lies within the gravity contours bordering the northern Tushar Mountains gravity low on the north and northwest respectively (Fig. 5). To the north is the gravity high observed over the surface exposures of Paleozoic and Mesozoic rocks discussed earlier. To the south the gravity values decrease as the surface rock type changes at Clear Creek Canyon from the more dense Paleozoic and Mesozoic sedimentary rocks of the southern Pavant Mountains to the Tertiary volcanic flows of rhyolite and latite that

comprise the northern Tushar Mountains.

Cove Fort.--In the area east of Cove Fort there is a sharp increase in the slope of the gravity contours east of Cove Fort indicating a local gradient of about 17 mgal/km (40 mgal/mi), which probably indicates a northward-trending Basin and Range fault across the mouth of Clear Creek Canyon. All of the water wells drilled on the west side of this fault (in the area of Cove Fort) are cold. The geothermal activity associated with Cove Fort is actually 3.5 km east-northeast of Cove Fort in Sulphur Cove. Here are found several sulphur prospects in an area approximately 2 km square where the alteration of alluvium and the presence of free sulphur is extensive.

The primary sulphur prospect is an open pit in the center of this cove coincident with a gravity low about 2 km long (east-west) and 1 km wide (north-south) centered about 1 km north of U.S. Interstate Highway 70, and with a closure of about 3 mgal.

A gravity high 2 km long (east-west) and less than 1 km wide (north-south) with a closure of 2 mgal is centered 1 km south of the Sulphur Cove gravity low. The author observed no outcrops over this gravity high but noticed that the primary Clear Creek Canyon drainage was about 0.2 km south of its center (on Utah highway 13 about 3.5 km east of Cove Fort). This gravity high lies between two major fault zones inferred (Hintze, 1963; Sontag, 1965) to trend northeast and located west of Sulphur Peak and along the east margin of Sulphur Cove.

The gravity low surrounding the sulphur prospects is probably caused by leaching and alteration of the alluvium and underlying sedimentary rocks. Even though there are no freely flowing hot springs

in Sulphur Cove at this time, several areas of hot spring deposits, "hollow ground" (areas that resound with a kettle drum-like boom when hit with a heavy object), are evidence that the area was geothermally active in the past.

The gravity high centered on Utah highway 13 is probably a tilted fault block of relatively unaltered sedimentary bedrock. The evidence for this interpretation is threefold. First, the density contrast used to model this feature on the interpretive two-dimensional model for the Black Rock Road gravity profile was 0.35 gm/cc, the approximate difference between the mean limestone density of 2.64 gm/cc and the mean rhyolite/latite density of 2.30 gm/cc. Secondly, the eastward trend of Clear Creek Canyon fault (Caskey and Shuey, 1975) could provide a mechanism for terminating a fault block on the north, and two known fault zones exist on each side of the hypothetical block; and consequently the block could dip south, in a direction compatible with the Clear Creek downwarp (Sontag, 1965). Lastly, the aeromagnetic map of Utah (Zietz et al., 1976) shows this portion of the Clear Creek downwarp as a magnetic low of about 360 gamma closure (Fig. 15) which is unlikely if an intrusive were the cause of the gravity high. It should be noted that the area east of Cove Fort including Sulphur Cove is apparently on an upthrown fault block that is indicated by the gravity high just discussed (see interpretive two-dimensional model for the Black Rock Road gravity profile).

Sulphurdale.--Sulphurdale Hot Springs exist along north-south and north-northeast-trending fault zones. The trend of the gravity contours

surrounding Sulphurdale is south-southeast with the nose of a local gravity high interrupting this primary gravity contour trend from the east. The smooth slope of the gravity contours is disrupted on the end of this gravity nose, however, and probably signifies the continuation of the range-front faulting detected across Clear Creek Canyon east of Cove Fort. Although the gravity data east of Sulphurdale are sparse, they are sufficient to show 1) a gravity gradient with a total relief of about 5 mgal that indicates a northward-trending Basin and Range fault zone through the Sulphurdale Hot Springs and 2) a small gravity nose over the Sulphur Hot Springs extending from a gravity high to the east exhibiting no closure.

Anomaly Separation Techniques

As an aid to interpretation, several anomaly separation techniques were employed (Appendix 5). Comparison of Figures 4 and 6 show that the aliasing introduced by digitizing the hand-contoured map is reflected back into anomalies of frequencies lower than the Nyquist frequency of 0.5 cycles/km--dictated by the 1-km digitization interval employed.

Figure 7 shows an isometric view of the terrain-corrected gravity field and the extreme relief observed. After removing the "logical" regional gravity (Appendix 4), residual maps were generated to show several different classes of anomalies.

Anomaly Separations Used

High-pass filtered data.--The high-pass filtered Bouguer

gravity anomaly data (Fig. 8) is composed of gravity anomalies whose spacial frequencies are higher than 0.05 cycles/km and lower than 0.5 cycles/km. These are represented on a contour map at a contour interval of 1.0 mgal representing gravity anomalies larger than 2 km but smaller than 20 km. An integral part of the filtered representation is an established zero-mean approximately midway between the highest and the lowest gravity anomaly value extremes.

Figure 8 shows several gravity features not readily apparent on the terrain-corrected Bouguer gravity anomaly map of Figure 6. The ones of significance here are listed below:

1) A closure of 2 mgal indicates that the Black Rock gravity high must be caused by near-surface density contrasts.

2) The Milford Valley gravity low is shown as a southern closure stretching off of the map and a northern closure of at least 2 mgal.

3) The southern closure shows the same westerly shift as does the gravity high over the north end of the Mineral Mountains granitic pluton.

4) The gravity saddle separating the northern and southern closures of the Milford Valley gravity low lies along a line connecting the Paleozoic rocks exposed in the southern Pavant Mountains and Cove Creek areas with the Pinnacle Pass Contact zone in the north Mineral Mountains.

5) The Black Rock Desert gravity low is shown as several gravity low closures whose connecting saddles trend east-west demonstrating a possible "rippling" in the underlying bedrock.

6) A gravity low of 4-mgal closure is shown in the northeast corner of the survey area. This is most likely due to edge effects generated during the filtering process as data in this region was sparse.

7) The absence of the large gravity gradient seen in Figure 6 through Clear Creek Canyon is evidence

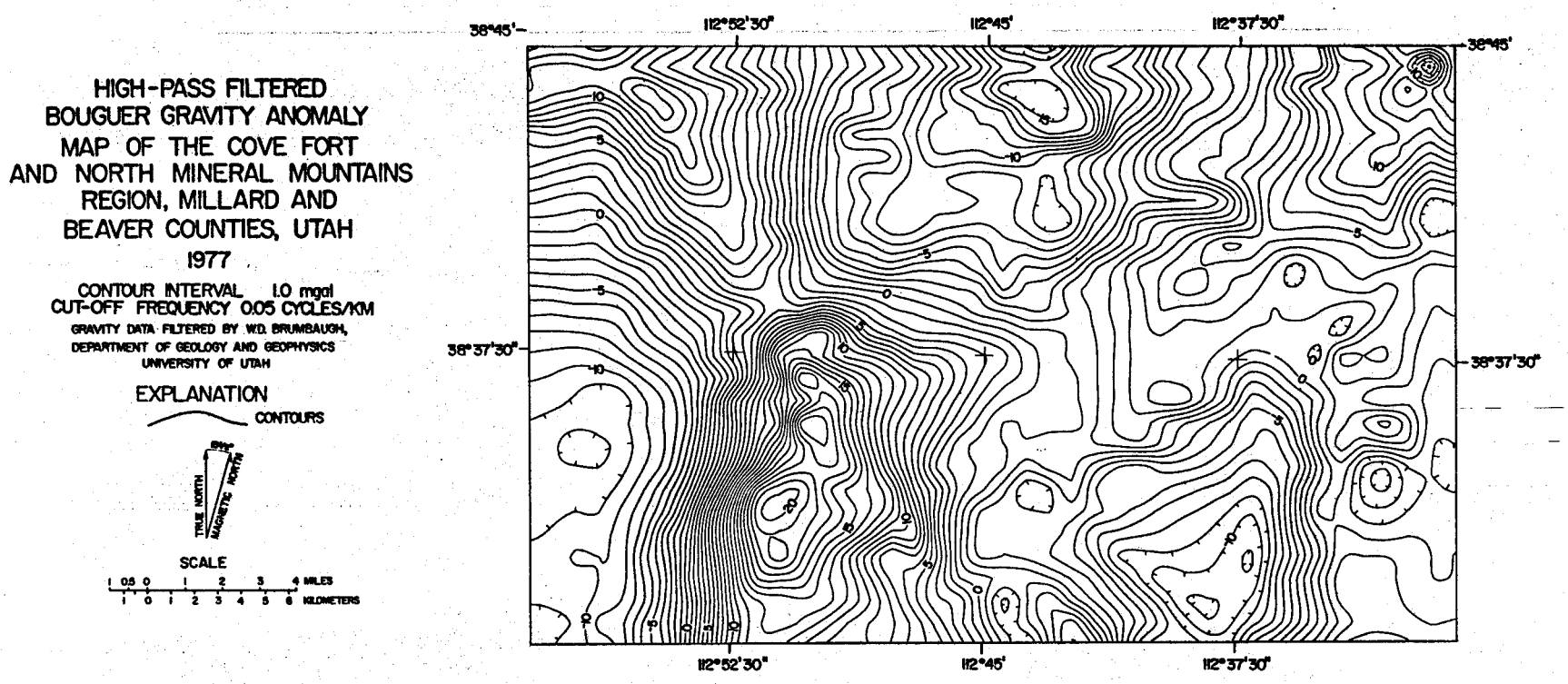

Figure 8 High-pass filtered Bouguer gravity anomaly map of the north Mineral Mountains and Cove Fort region, Beaver and Millard counties, Utah; contour interval = 1 mgal

that it is probably due to deep crustal density variations.

8) The north-south-trending contours east of Cove Fort are enhanced, and probably represent a range-front fault forming the eastern boundary of north Beaver Valley.

9) The gravity contours now border north Beaver Valley in an inverted and lop-sided "V" and suggest closure to the south of the survey area.

10) Sulphurdale is seen to lie on a gravity saddle transverse to the north-south trend of the major contours in the area. The gravity saddle is flanked on the north and south by gravity high spurs, on the west by the north Beaver Valley gravity low and on the east by a gravity low over the Dead Cow Springs area (cold) of 3-mgal closure.

The relative gravity anomaly magnitudes range from the +20 mgal local gravity high associated with the northwestern edge of the Mineral Mountains granitic pluton to the -15 mgal gravity low closure of the Black Rock Desert gravity low.

Polynomial fitting.--Polynomial surfaces of orders zero through 10 were compared with the terrain-corrected Bouguer gravity anomaly data. A surface of each order was calculated that best represented the gravity data (point-wise least-mean-square-error). The "zeroth" order polynomial surface represented a Bouguer gravity anomaly mean value of about -183 mgal while the first-order polynomial surface displayed an average Bouguer gravity anomaly trend of -24 mgal north to south, and -22 mgal west to east.

A second-order polynomial residual gravity anomaly map (Appendix 4, Fig. 9) was produced at a contour interval of 1.0 mgal for comparison with the high-pass filtered gravity anomaly map. It was not surprising to find both maps so similar, as both residual methods eliminate the long wave-length, and retain the short wave-

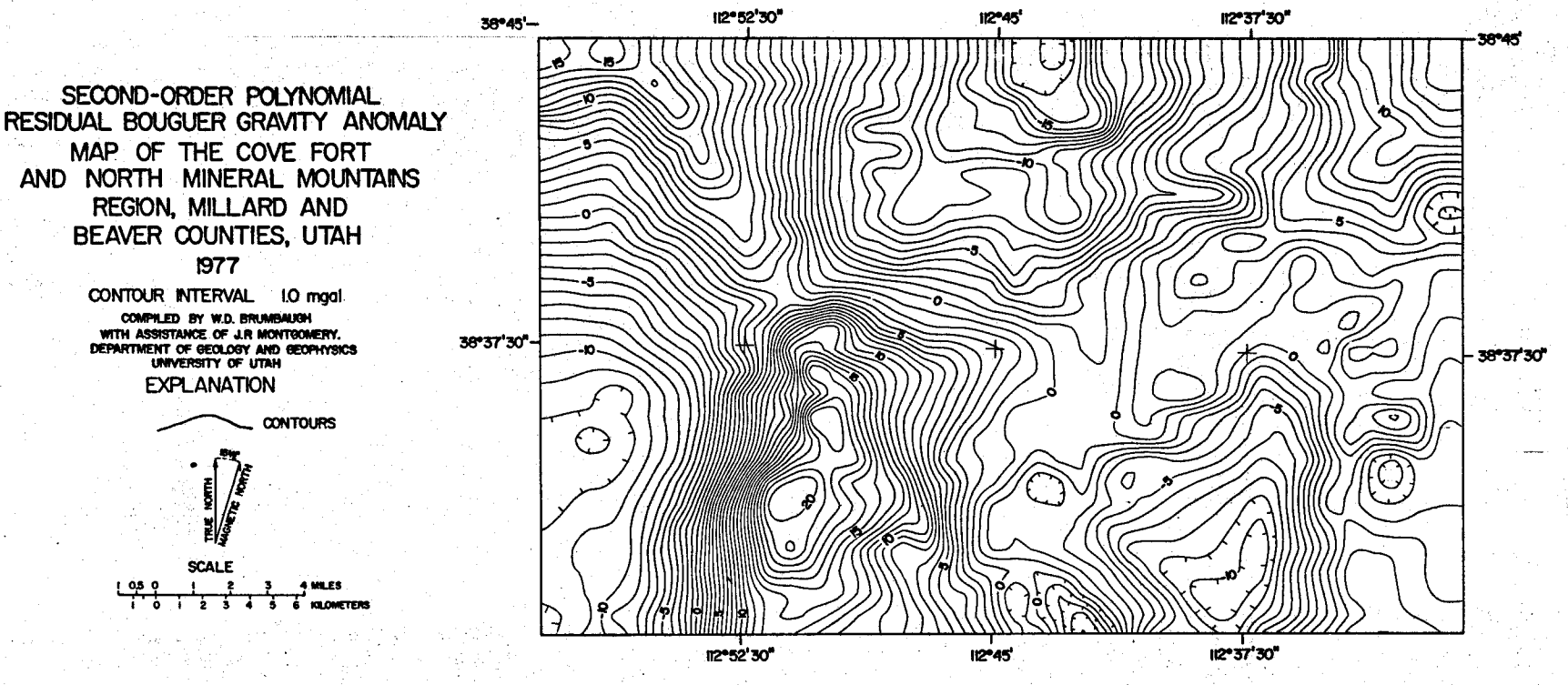

Figure 9 Second-order polynomial residual gravity anomaly map of the north Mineral Mountains and Cove Fort region, Beaver and Millard counties, Utah; contour interval = 1 mgal

length anomalies. The ability to adjust high-and-low frequency cut-offs utilizing Fourier decomposition allowed greater flexibility than filtering the gravity data by a polynomial order. Edge effects were noticeably less on the second-order polynomial residual gravity anomaly map while more high-frequency components were retained in the high-pass filtered Bouguer gravity anomaly map.

Second vertical derivative technique.--A low-pass filtered second vertical derivative anomaly map was produced at a contour interval of 1.0 mgal (replacing calculated units of mgal/km^2 with mgal). A low-pass cut-off frequency of 0.33 cycles/km was employed to eliminate anomalies smaller than 3 km so that the output would not be dominated by noise generated from the magnification of the highest frequency components in the gravity data (Fig. 10).

Several anomaly closures were shown by this technique (Fig. 10) that were not shown by the other anomaly separation techniques:

1) A gravity reentrant south of the Black Rock gravity high shows up as a gravity low with a closure of 5 mgal.

2) A series of gravity lows of 1 to 5 mgal closures are seen to flank the Black Rock and north Mineral Mountains gravity highs (as well as the gravity saddle that joins them) on the west. Topographically, this corresponds to a narrow north-south-trending valley containing South Twin Peaks in the north and alluvial washes to the south.

3) A definite lineation is seen between small gravity closures extending from the north end of the Milford Valley gravity low, across the northern end of the Mineral Mountains, through Cove Creek, and into the Clear Creek Canyon area.

4) An alternating pattern of high and low gravity closures flank the lineation of (3) on the south, east of the Mineral Mountains. It is not clear whether these are Gibb's phenomena in the output

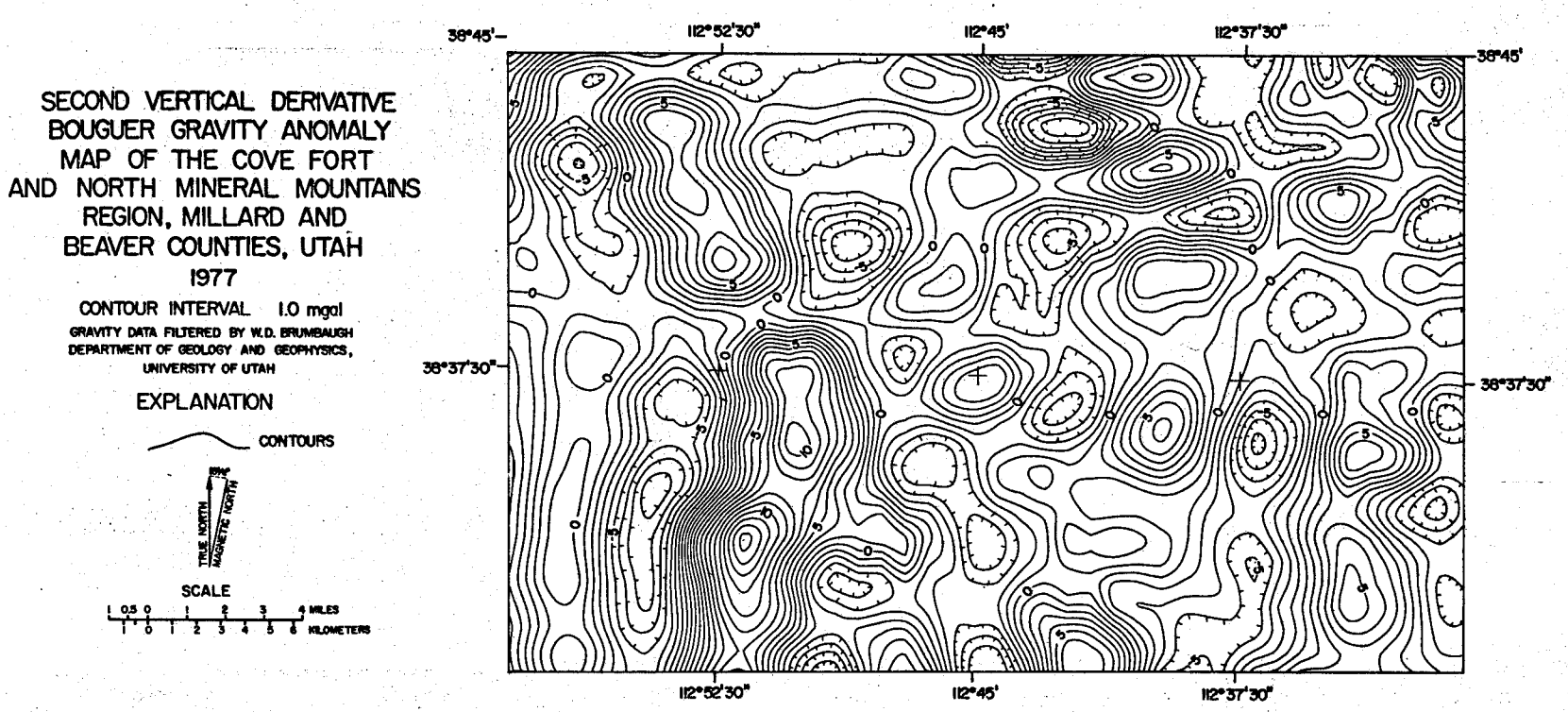

Figure 10 Second vertical derivative gravity anomaly map of the north Mineral Mountains and Cove Fort region, Beaver and Millard counties, Utah; contour interval = 1 mgal

or may possibly have a geologic significance. This line of gravity highs and lows correlates well however, with the aeromagnetic lineation seen in Figure 15 (discussed below).

5) The flat topographic valley that includes Cove Fort is seen as a gravity low with 4-mgal closure.

An elongated magnetic intensity low separates relative magnetic intensity highs over the Black Rock Desert (gravity low) and the southern Pavant Range (gravity high) from magnetic intensity highs over the Mineral Mountains (gravity high), Beaver Valley (gravity low), and the Tushar Mountains (gravity high relative to Beaver Valley, but a gravity low with respect to the Pavant Range). The observation of (4) above applies to the almost perfect superposition of this elongated magnetic intensity low (Fig. 15) with the line of alternating positive and negative gravity anomalies observed on the second vertical derivative map (Fig. 10). This superposition of gravity and magnetic intensity features also lies along a geomorphic lineament in the topography. This coincidence of anomalies occurs along an east-southeast-trending zone connecting the north Mineral Mountains north of Pinnacle Pass with the Clear Creek Canyon area, and is centered over the Cove Fort - Sulphurdale KGRA. This magnetic intensity feature also coincides with the apparent right-lateral offset in gravity contours observed in the southeast-northwest strike-filtered gravity anomaly map (Fig. 14).

The overall form of the second vertical derivative anomaly map is similar to the previously discussed residual maps and shows many of the same anomalies. The large gravity gradient through Clear Creek Canyon observed on the terrain-corrected Bouguer gravity anomaly map

(Fig. 6) is again absent, adding further evidence of a deep crustal cause.

Strike-filtering techniques.--Four strike-filters were applied to the terrain-corrected Bouguer gravity anomaly data: They were designed to enhance anomalous trends striking in the north-south (Fig. 11), east-west (Fig. 12), northeast-southwest (Fig. 13), and northwest-southeast (Fig. 14) directions and suppress all others. This was accomplished by using an azmithal filter of frequency band width 0.05 cycles/km to 0.5 cycles/km. The filters enhanced anomalies trending within a 60^{o} "pie-slice" of the central strike direction, thus covering all 360^{o} of the compass (Appendix 5).

The central strike-directions were chosen by evaluating the terrain-corrected Bouguer gravity anomaly map and the 3 residual maps discussed above. Several dominant trend directions were apparent:

1) The north-south trend of gravity contours that probably represents Basin and Range faulting,

2) The near east-west alignment of the north end of the Milford Valley gravity low and the Mineral Mountains gravity high with the north-south gradient passing through Clear Creek Canyon. Also there appears to be series of gravity lows associated with the geomorphic lineament from Negro Mag Wash, west of the Mineral Mountains, east, across northern Beaver Valley and into the Pine Creek Canyon area of the Tushar Mountains.

3) The east-northeast-west-southwest trend of the gravity highs found over the Paleozoic exposures (appearing to be the upturned leading edge of an overthrust sheet).

4) The Black Rock - north Mineral Mountains gravity saddle aligns with a spur from the Black Rock gravity high.

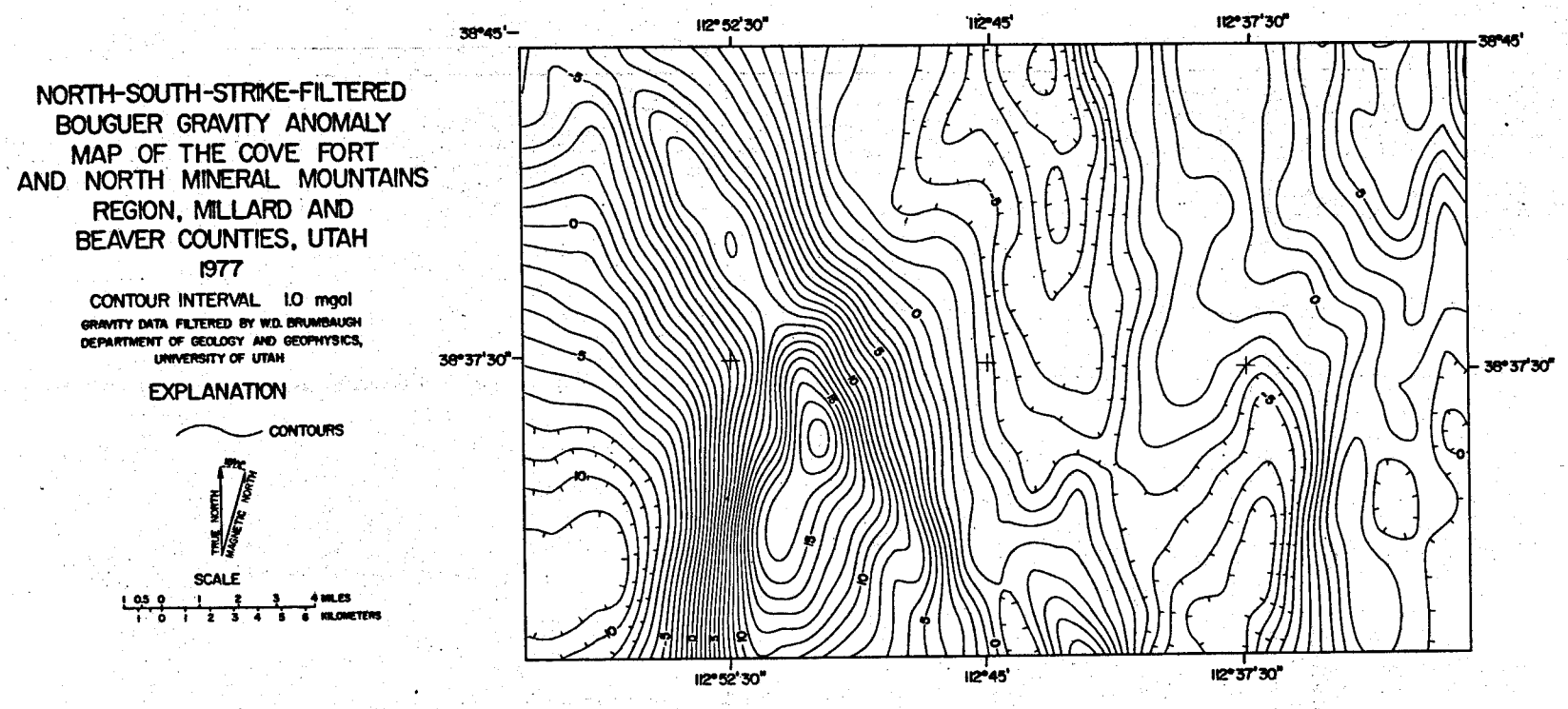

Figure 11 North-south strike-filtered Bouguer gravity anomaly map of the north Mineral Mountains and Cove Fort region, Beaver and Millard counties, Utah; contour interval = 1 mgal

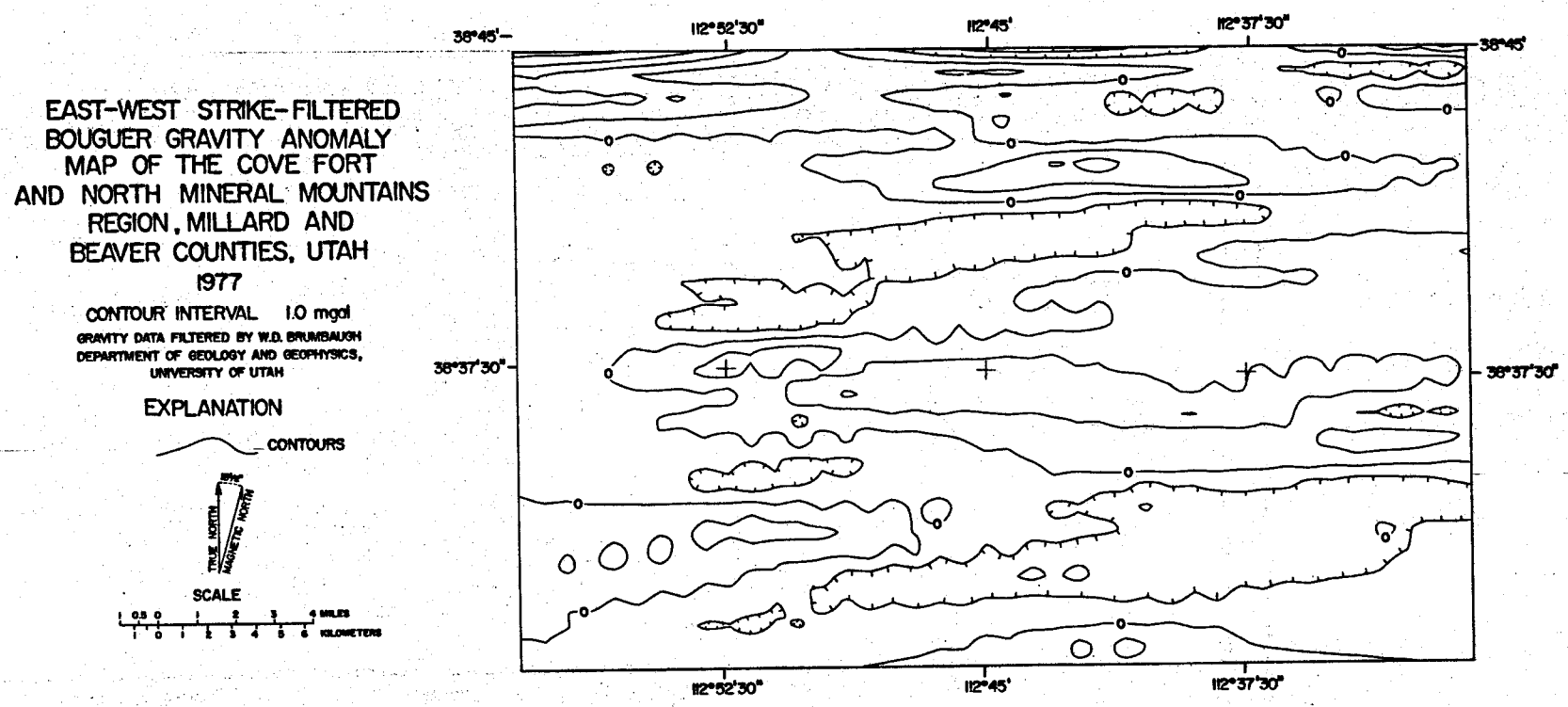

Figure 12 East-west strike-filtered Bouguer gravity anomaly map of the north Mineral Mountains and Cove Fort region, Beaver and Millard Counties, Utah; Contour interval = 1 mgal

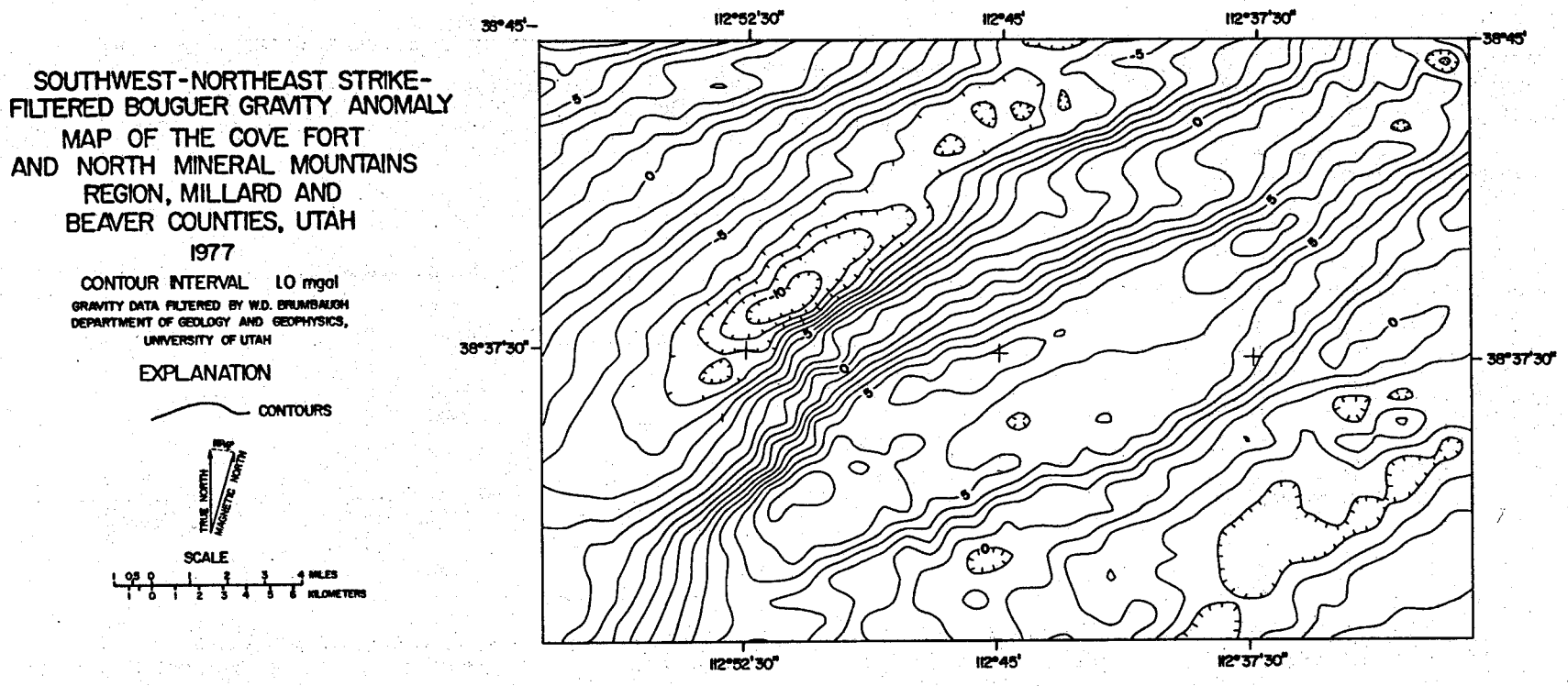

Figure 13 Northeast-southwest strike-filtered Bouguer gravity anomaly map of the north Mineral Mountains and Cove Fort region, Beaver and Millard counties, Utah; contour interval = 1 mgal

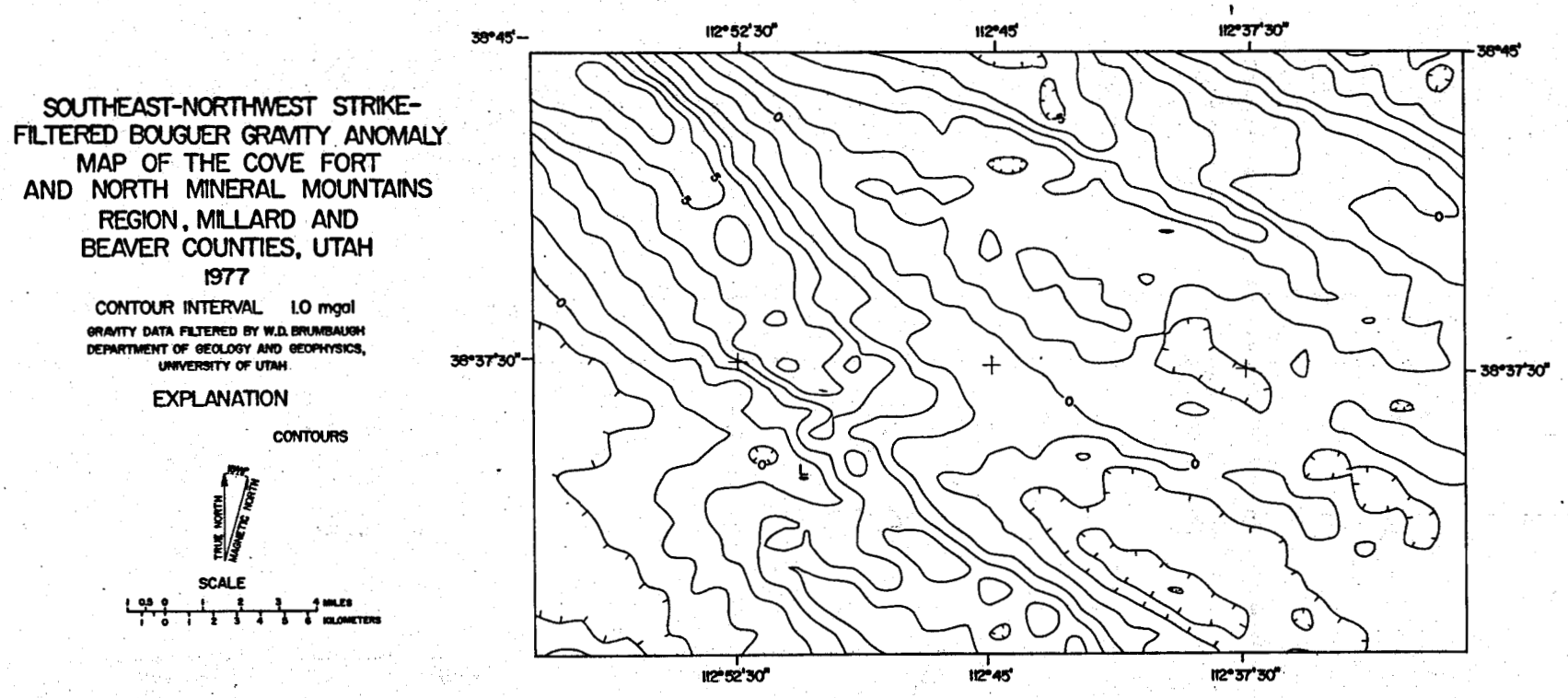

Figure 14 Northwest-southeast strike-filtered Bouguer gravity anomaly map of the north Mineral Mountains and Cove Fort region, Beaver and Millard counties, Utah; contour interval = 1 mgal

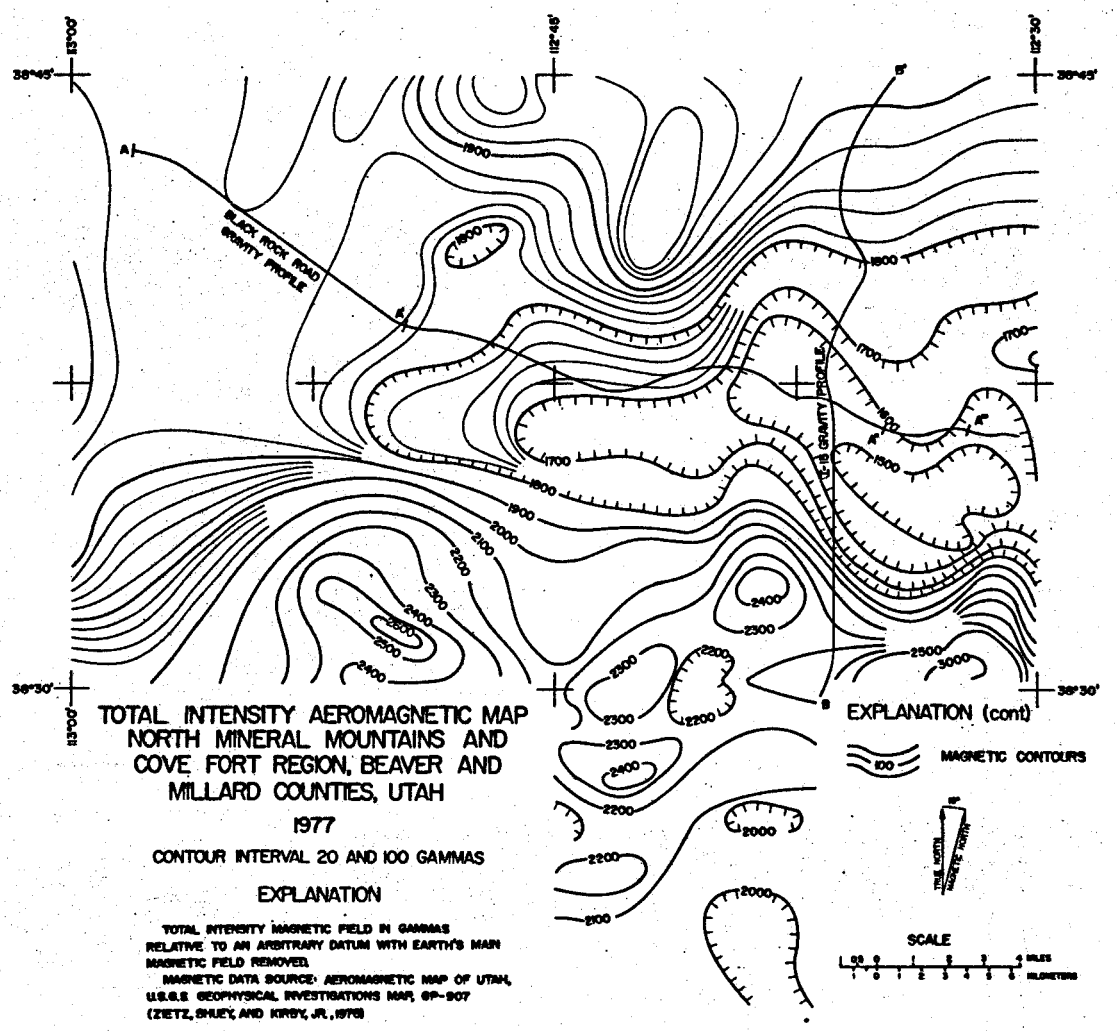

Figure 15 Regional aeromagnetic anomaly map of the north Mineral Mountains and Cove Fort region, Beaver and Millard counties, Utah; contour interval = 20 and 100 gammas

The four following strike-filtered maps show these anomalous trends together with features not clearly evidenced in the previous residual gravity maps:

1) The north-south strike-filtered gravity anomaly map (Fig. 11) shows an unexpected continuation of the Black Rock Desert gravity low south to the Beaver Valley gravity low. There is also an apparent left-lateral offset to the west of the Black Rock Desert gravity low at about the same latitude as the Pinnacle Pass Contact zone found at the north end of the Mineral Mountains granitic pluton.

2) Surprisingly, the east-west strike-filtered Bouguer gravity anomaly map (Fig. 12) shows no strong east-west lineations. This suggests little vertical movement in east-west fault zones that would create north-south lateral density contrasts. Of those east-west trends present, the most significant are two gravity highs, one extending east and the other west that terminate over the Pinnacle Pass Contact zone in the north Mineral Mountains.

3) The northeast-southwest strike-filtered Bouguer gravity anomaly map (Fig. 13) emphasizes a residual gravity low with 4-mgal closure centered over the Black Rock - north Mineral Mountains gravity saddle that extends between the Milford Valley and Black Rock Desert gravity lows. A steep gravity gradient exists across the strike-filter direction across the map connecting all of the Paleozoic rocks that crop out in the survey area (except the outliers in Cunningham Wash). This gravity gradient appears to be left-laterally offset in the northern Cove Creek area. The gravity saddle associated with Sulphurdale shows up in this map as an elongated gravity low of 1-mgal closure extending from the northern Beaver Valley gravity low to Clear Creek Canyon. It incorporates the low to the east of Sulphurdale and lies transverse to the suspected range-front fault zone separating north Beaver Valley from the Tushar Mountains. The Sulphur Cove area shows a residual gravity low of 1-mgal closure with another slightly larger residual gravity low about 2 km to the west. This second gravity low lies along the range-front fault zone, mentioned above, to the north and east of Cove Fort. It was noted that here, too, were found sulphurous deposits, some mining prospects, and hydrothermal alteration. A gravity high centered in Clear Creek Canyon of 2-mgal

closure separates the set of gravity lows associated with Cove Fort from the gravity low associated with Sulphurdale,

4) The most significant feature portrayed in the northwest-southeast strike-filtered Bouguer gravity anomaly map (Fig. 14) is a 4-km, right-lateral offset in the gravity contours. This offset occurs between the Black Rock and the north Mineral Mountains gravity highs in the region of the Pinnacle Pass Contact zone. It was also noticed that quartz latite dikes found in the Pinnacle Pass Contact zone trended almost exclusively in a north-northwest-south-southeast direction. Additional anomalies are right-laterally offset in an east-west direction across much of the survey area. The aeromagnetic intensity gradient (Fig. 15) discussed earlier also falls within the offset zone. It is probably most important, though, to note the coincidence of the upwarped edge of the buried Laramide overthrust sheet (see section on the I-15 gravity profile) and the aeromagnetic intensity gradient with this left-lateral offset in the gravity contours as indications of a deep-seated east-west-trending structural feature.

GRAVITY PROFILES AND INTERPRETIVE MODELS

Interpretation Techniques

The following two interpretive gravity profiles comprise the detailed gravity conducted during the survey. They are roughly orthogonal, the Black Road profile extending east and west, and the Interstate Highway 15 (I-15) profile extending north and south. The station spacing along the east-west Black Rock Road traverse was approximately 1 km while the station spacing along the I-15 traverse was approximately 1/10 mi. Once a regional gravity gradient was chosen and removed from the observed gravity data (Appendix 4), the gravity profiles were modeled as if the data were taken over a flat surface; therefore the depths to "bedrock" cited in Figures 16 and 17 are with respect to the surface elevation.

Grant and West (1965) and Nettleton (1976) supplied the characteristic curves for preliminary analysis of the profile data. Only one fault was modeled for each major inflection in the residual gravity data. The major inferred faults determined from both gravity profiles have been plotted on the General Geology Map (Fig. 3) perpendicular to the associated traverse unless they confirm previously mapped or inferred faults of a definite strike.

A two-dimensional modeling technique (Appendix 5) was used to refine the initial model. Only two-layer models were considered. Bedrock was assumed to be a uniform density of 2.67 gm/cc and the

overlying material was assumed to be a variable mix of alluvium and/or volcanics ranging in density from 2.00 to 2.40 gm/cc.

The Beaver Valley Oil Co.'s dry oil well (see Data Control Section) west of Black Rock and the surface exposures of bedrock were the only depth controls available on both gravity profiles. Error bars have not been included on the interpretive gravity profiles because at the scale of Figures 16 and 17, error bars of less than 1 mgal would be illegible, and the magnitude of the anomalies modeled are generally an order of magnitude greater than the estimated error, which is estimated to be 0.5 mgal in the valley areas (see Data Error Analysis Section).

Black Rock Road Gravity Profile

The Black Rock Road gravity profile intersects most of the major north-south-trending contours observed in the terrain-corrected Bouguer gravity anomaly data. This profile extends 44 km east from Black Rock to 5 km east of Cove Fort entirely over alluvium. As mentioned previously, only one drill hole exists for depth control. The computed two-dimensional model along this profile assumes a strike length long compared to the anomaly width being modeled. In several cases pointed out later, this is not true.

The interpretive model is composed of 4 segments with assumed density contrasts, west to east, of -0.5, -0.45, -0.5, -0.35 gm/cc. This infers differing densities (in a horizontal direction) of the volcanics believed to be covering the bedrock over various portions of the profile along with the alluvium (Fig. 16).

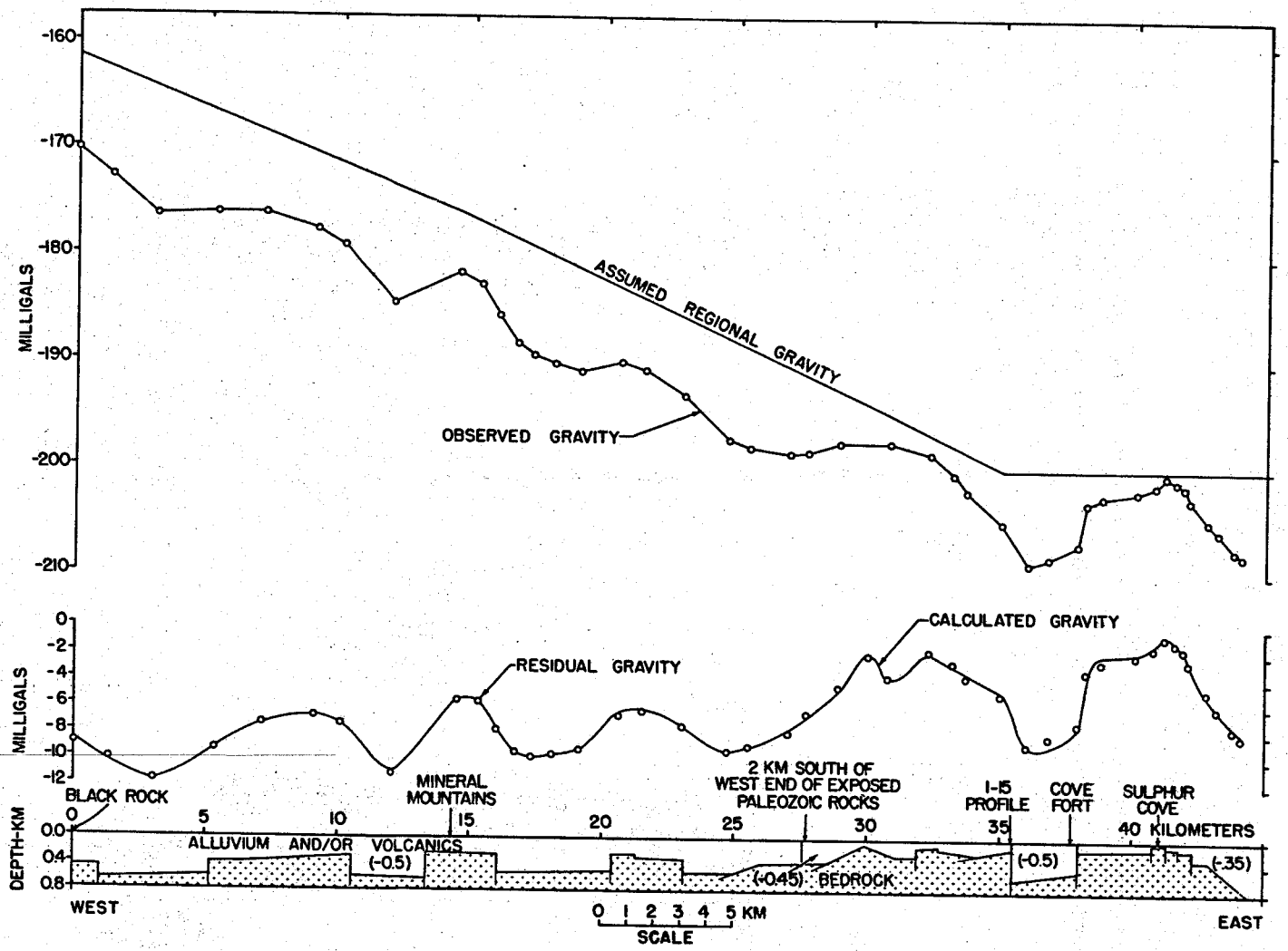

Figure 16 Interpretive two-dimensional model for the Black Rock Road gravity profile; numbers in cross-section indicates assumed density contrasts in gm/cc between valley fill and bedrock.

The westernmost segment of the calculated model contains 3 grabens and 3 horsts. The first graben is a gravity reentrant from the north Milford Valley gravity low, evident on the second vertical derivative Bouguer gravity anomaly map (Fig. 10) as a gravity low with 4 mgal closure. The balance of this segment of the inferred subsurface model is of dubious geologic validity. The gravity gradients modeled close or change direction close to the traverse and thus violate the "infinite" strike-length assumption. As modeled, however, the north Mineral Mountains are represented by an upthrown fault block with high angle faulting on the east and west with throws of 550 m and 630 m respectively. The graben modeled to the west of the fault block noted above is a representation of the gravity saddle separating the Black Rock gravity high and the north Mineral Mountains gravity high. To the east of the Mineral Mountains fault block, a topographic low area flanking the range, is a modeled graben coincident with the topographic low land drainage area east of the mountains range with an average depth to bedrock of 500 m. Several high-angle faults occur in the Cove Creek area about 4-6 km east of the north Mineral Mountains. These faults bound a fault block upthrown about 500 m on the west and 300 meters on the east. The inferred faults bounding this horst align with faults mapped by Hintze (1963) in the volcanics to the north. East of this fault block the basement displays a series of low angle rises as the Paleozoic rocks are approached from the west.

Here lies the second segment of the subsurface which was modeled at a density contrast of -.045 gm/cc. Although basement relief is

apparent, structural control is probably not Basin and Range. Surface exposures in this area show upturned bedding planes overlain by andesitic and basaltic volcanics. The eastern edge of this segment forms a high angle Basin and Range-type fault, but again, the model is only approximate due to the lack of an "infinite" strike-length.

The third calculated model segment represents the small valley west of Cove Fort. This valley is bounded on the east by a range front fault modeled with a density contrast of -0.5 gm/cc and displays a buried throw of 500 m. The west boundary is a three-dimensional structure with an apparent buried throw of 750 m. The valley fill, which was assumed to be alluvium, may in places consist of thin, vesicular basalts (of about the same density as the alluvium, as such basalts are exposed in near-by road cuts.

East of this small valley an upthrown fault block of basement material overlain by volcanics and a thin veneer of alluvium was modeled. The average density contrast was assumed to be -0.35 gm/cc giving a minimum depth of burial of about 15 m. Sulphur Cove lies due north of the highest part of this fault block. It is noted that the bedrock deepens near the east end of the profile. The surface rocks here are principally Dry Hollow latites.

Interstate Highway 15 Gravity Profile

The Interstate Highway 15 (I-15) gravity profile extends in a north-south direction for about 38 km from latitudes $38^{o}30'$ to $38^{o}45'$ N. Along this profile, an interpretive two-dimensional model was calculated in an attempt to detect basement structure orthogonal to

the Basin and Range grain. The profile lies over alluvium on the south but has 3 bedrock exposures in its northern half.

The two-layer model calculated for this gravity profile is shown in Figure 17. It is comprised of uniform density (2.67 gm/cc) bedrock overlain by alluvium and volcanics of variable density. The calculated model was segregated into three segments of densities, south to north, -0.5, -0.45, -0.40 gm/cc, indicating a higher concentration of surface volcanics to the north.

The residual gravity anomaly observed over the central part of the I-15 profile comprises a steep gravity gradient (with a total relief of 16 mgal) with a series of step-like features. Along the southern part of the profile, the residual gravity anomaly values (Appendix 4) fluctuate between -12 and -16 mgal. This section of the profile was modeled at a density contrast of -0.5 gm/cc and basement relief is indicated in Figure 17 alternately as upthrown and down-thrown fault blocks of bedrock. The calculated model for the central segment of the profile shows a "sawtooth" pattern that may be a manifestation of near-surface density contrasts that cannot be adequately represented by a two-later model. However, the probable cause of this gravity gradient (with 16 mgal of relief) is a relation to the overthrust sheet found to the north involving the upwarped edge of the Paleozoic over Mesozoic sedimentary strata modeled as having a minimum thickness of about 3500 ft (1.2 km). Evidence of this explanation is in the bedding planes seen in road cuts in Dog Valley Pass along I-15 which have a dip of about 65^{o} NNW. This central part of the I-15 profile was modeled at a density contrast

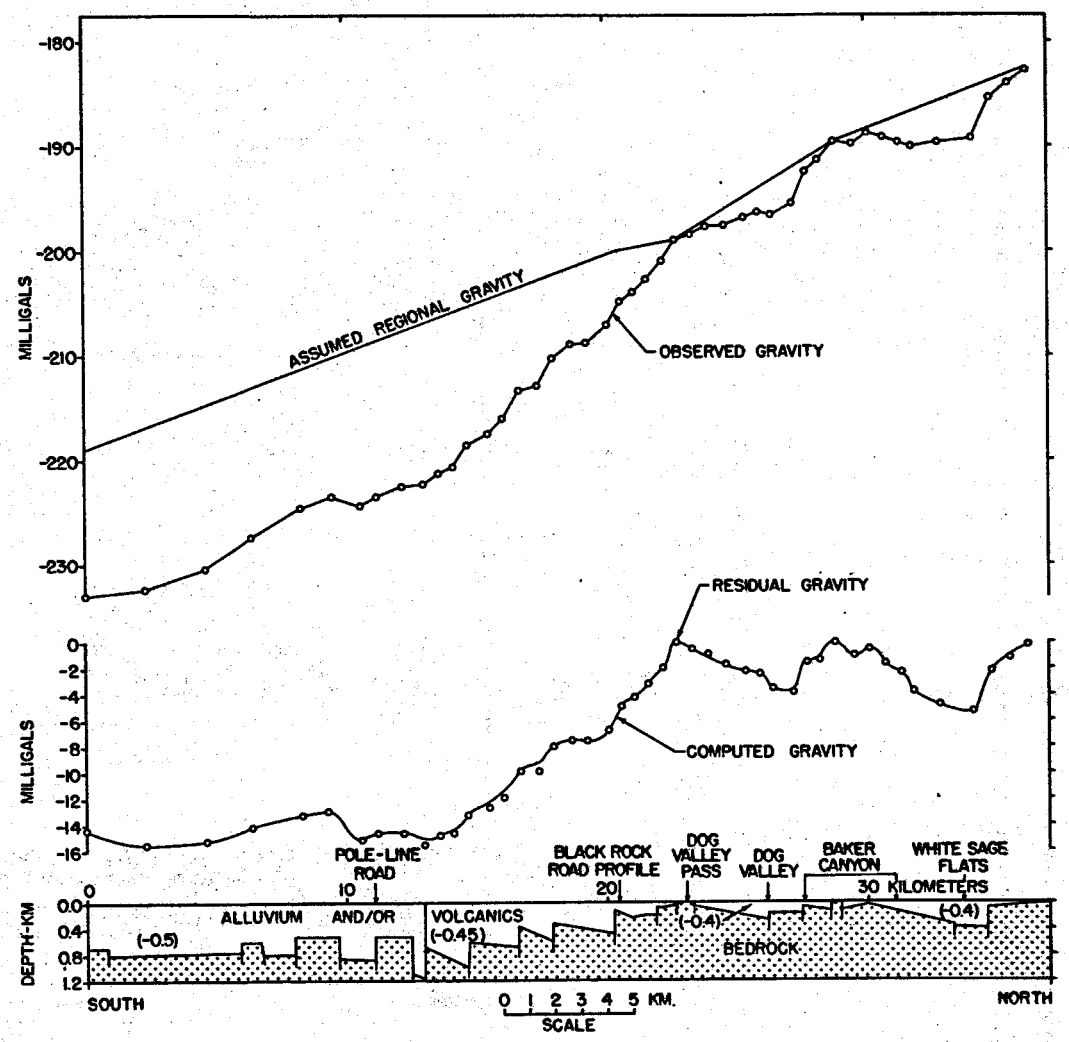

Figure 17 Interpretive two-dimensional model for the Interstate Highway 15 gravity profile; numbers in cross section indicates assumed density contrasts in gm/cc between valley fill and bedrock

of -0.45 gm/cc due to the volcanics observed, and the relative surface densities measured, in the area (Table 1, Appendix 2). A recess in the bedrock is noted at the intersection of the first and second profile sections where the density contrast changes from -0.5 gm/cc to -0.45 gm/cc. Although the model shows a downfaulted block of alluvium and/or volcanics, with a total depth of 1.2 km, it may also be interpreted to be a narrow zone of low-density material in the bedrock itself. It is also noted that this low-density zone is on an east-west line joining Negro Mag Wash in the Mineral Mountains with the Pine Creek Canyon-Sulphurdale area in the Tushar Mountains. Another observation is that the majority of gravity contours forming the Clear Creek Canyon gravity gradient extend parallel to the assumed strike of the central section of the calculated model for this gravity profile throughout the region between Pine Creek Canyon on the south and Dog Valley Pass on the north.

Along the northern part of the profile, the two anomalies specifically modeled were the gravity lows over Dog Valley and White Sage Flats. At a density contrast of -0.4 gm/cc the calculated model seen in Figure 17 shows a depth to bedrock in Dog Valley of about 1150 ft and a depth to bedrock in White Sage Flats of about 1400 ft.

SUMMARY AND CONCLUSIONS

General.--During the summers of 1975 and 1976, a gravity survey was conducted in the Cove Fort - Sulphurdale KGRA and north Mineral Mountains area, Millard and Beaver counties, Utah. The survey consisted of 671 gravity stations covering an area of about 1300 km^2, and included two orthogonal gravity profiles traversing the area. The purpose of the study was to aid in evaluating the geothermal potential of this region by delineating, as nearly as possible, the near-surface structural setting as evidenced by the earth's gravity field.

Interpretation Techniques.--The data are presented as a regional terrain-corrected Bouguer gravity anomaly map of 1-mgal contour interval of the entire survey area, an isometric, three-dimensional gravity anomaly surface, and as an area terrain-corrected Bouguer gravity anomaly map (also of 1-mgal contour interval) of the Cove Fort - Sulphurdale KGRA. Hand-digitized (at 1-km interval on the Universal Transverse Mercator grid) gravity data from the regional contour map were filtered in the frequency and space domains using the anomaly separation techniques of Fourier decomposition, second vertical derivative, strike-filter, and polynomial fitting analysis, respectively. These anomaly separation maps were compared with the original terrain-corrected Bouguer gravity anomaly, aeromagnetic

anomaly (derived from the Aeromagnetic State Map of Utah), and general geology maps of the region to arrive at a reasonable subsurface structural setting consistent with the known surface geology and inferred geologic trends.

Gravity Patterns and Interpretation.--The principal gravity highs and lows are a function of depth to bedrock. Bedrock as used in this study means any material of density 2.67 gm/cc or higher. Density contrasts used assume a single layer of bedrock overburden composed of alluvium and volcanics of density 2.0 to 2.3 gm/cc.

It was found that of the approximately 68-mgal gravity relief over the survey area, 20 mgal should be assigned to density contrasts in the deep crust due to their large areal extent (long wave length) and the remaining 38 mgal of relief was assumed to be due to near-surface density contrasts. No prominent gravity feature was observed that would indicate either a molten or a solidified magma chamber at depth or near-surface. East-west anomalous trends in the gravity data, however, were observed that correspond with density contrasts along recognized geomorphic and structural lineations.

Residual gravity gradients of 0.5 to 8.0 mgal/km across north-trending gravity contours observed through the Cove Fort area, the Sulphurdale area, and the areas east of the East Mineral Mountains, along the west flanks of the Tushar Mountains, and on both the east and west flanks of the north Mineral Mountains, were attributed to north-trending Basin and Range high-angle faults. The density contrast causing the observed gravity gradients is thought to be created by basement rocks in contact with volcanics and/or alluvial valley fill.

Major gravity highs exist over the community of Black Rock area, the north Mineral Mountains, the Paleozoic outcrops in the east Cove Creek-Dog Valley-White Sage Flats areas, the Laramide overthrust zone of the southern Pavant Range, and the Paleozoic sediments and Tertiary intrusives of the East Mineral Mountains. The principal gravity lows, which occurred over northern Milford and Beaver valleys, the southern Black Rock Desert (where no noticeable topographic relief suggesting a valley exists), and Cunningham Wash are separated from the above gravity highs by steep gravity gradients. A gravity low with a closure of 2 mgal corresponds with Sulphur Cove, a circular-shaped topographic feature containing sulphur deposits. The gravity gradients surrounding the southern Black Rock Desert (within the survey area) and the northern end of Milford Valley are attributed to both crustal downwarping of the sedimentary rocks and associated faulting, whereas the gradient found around the north end of Beaver Valley is attributed principally to the upwarped edge of the Laramide overthrust sheet.

Several significant gravity saddles with various alignments were observed in the survey area. The Pinnacle Pass Contact zone corresponds with a small gravity saddle that separates the gravity highs associated with the Mineral Mountains pluton on the south from those observed over the mapped overthrust sheet of Paleozoic rocks to the north. In the area of this contact zone, the gravity highs are apparently right-laterally offset about 2.5 km along a possible east-west strike-slip fault zone; but the evidence of a right-lateral offset in the surface geology of the igneous-sedimentary contact zone

is lacking.

Several north-south anomalies consisting of contour offsets, gravity closures, and interruptions of smooth gravity contours were observed in both the terrain-corrected Bouguer gravity anomaly map and the residual gravity anomaly maps from the Mineral Mountains to the Tushar Mountains. These east-west gravity features correlated well with geomorphic and structural features extending from Pinnacle Pass to Clear Creek Canyon on the north, and from Negro Mag Wash east to Pine Creek Canyon on the south. This east-west band contains both the Roosevelt Hot Springs and the Cove Fort-Sulphurdale KGRAs.

Structural features within the Cove Fort-Sulphurdale KGRA were shown to indicate both north-northeast and north-south-trending high-angle faults near Sulphurdale and Sulphur Cove. Sulphur Cove lies in a gravity low of at least 2-mgal closure that is probably due to hydrothermal alteration of the underlying material. Sulphurdale was shown to lie on a small gravity nose extending west from a gravity high in the Tushar Mountains area (possibly due to a rift in the range-front fault along the western flanks of the Tushar Mountains) overlying the junction of Basin and Range high-angle faults trending north-south and the above-mentioned zone trending north-northeast.

The aeromagnetic data show a strong gradient with east-west-striking contours in the Pinnacle Pass igneous-sedimentary contact zone (high magnetic intensity to the south and low to the north) and indicate some closure over the Mineral Mountains pluton. This pronounced magnetic gradient extends through the survey area from

Milford Valley on the west to Clear Creek Canyon on the east, and supports gravity data that indicates a possible major east-west structural feature.

An extension of the Laramide overthrust sheet observed in the southern Pavant Range is indicated as extending under alluvial cover by: 1) a west-southwestward-trending gravity nose that lies over the Paleozoic exposures in east Cove Creek area, and 2) the east-northeastward-trending gravity nose originating over the Paleozoic rocks exposed north of the Pinnacle Pass Contact zone. The junction of these two gravity noses forms a saddle that separates the Black Rock Desert gravity low on the north-northeast from the north Beaver Valley gravity low on the south-southeast. A possible buried, upwarped edge of the above overthrust is suggested by the 16-mgal relief found on the north-south trending I-15 gravith profile between Sulphurdale on the south and Dog Valley Pass on the north.

Data obtained from the east-west Black Rock Road gravity profile resulted in a calculated model of the bedrock that shows simplified Basin and Range faulting to the west. The small valley adjacent to Cove Fort was modeled as a downthrown fault block (with a density contrast of -0.5 gm/cc) bounded by high-angle faults with throws of 500 m on the east and 750 m on the west. A gravity high with 4 mgal closure, lying due south of the Sulphur Cove gravity low, is attributed to an upthrown fault block of sedimentary rocks underlying the exposed volcanics in this area.

Data obtained from the north-south Interstate Highway 15 gravity profile resulted in a calculated model showing a steep gravity

gradient of 16-mgal relief and with step-like anomalies. The gradient is preferably interpreted as the gravity response of near-surface Paleozoic bedrock, associated with a buried, upwarped edge of the Laramide overthrust sheet exposed to the north, interfacing with lower-density volcanics and alluvial valley fill overlying the deeper bedrock to the south. The location of this postulated overthrust margin lies along an eastward extension of the Pinnacle Pass Contact zone.

Inferred Structural Setting.--The reduced gravity data correlate well with the known geology and other geophysical data of the region and indicate evidence for newly interpreted geologic features, tectonic trends, and structural continuities. Tectonic activity in this region has been both varied and great, and the observed gravity anomaly patterns represent as assemblage of density contrasts that are the product of several diastrophic events. Observed gravity features indicate that the Basin and Range-Colorado plateau transition zone within the survey area is complicated by at least five-fold regional intervals of deformation: 1) Laramide overthrust faulting followed by local folding of stratified and overthrust rocks, 2) Basin and Range faulting, principally high-angle faults trending north-south, 3) large-scale warping and faulting of the basement and overlying rocks by the Colorado plateau uplift (probably contemporaneous with Basin and Range faulting), 4) extrusion and intrusion of large volumes of igneous material, and 5) principally right-lateral strike-slip faulting. These combined events developed the density contrasts observed over the entire survey region,

resulting in four basic fracture patterns being superimposed: 1) low-angle thrust faults, 2) high-angle, north-south-trending (Basin and Range) faults, 3) high-angle dip-slip north-northeast-trending faults, and 4) high-angle strike-slip, east-west-trending faults.

The principal occurrences of hydrothermal alteration, hot spring deposits, and flowing hot springs and hot-water wells apparently coincide with inferred intersections of east-west and north-south and/or north-northeast trending fault zones.

APPENDIX 1

APPLICATION OF GRAVITY SURVEYS IN GEOTHERMAL EXPLORATIONS

Gravity surveys have been applied in almost every geothermal prospect published to date. However, because gravity does not give a unique signature over each geothermal prospect, some confusion has arisen as to what information the gravity anomaly map gives at each prospect. Some examples of the application of gravity surveys obtained at other well-known geothermal areas will be discussed so as to show the correlation of the gravity field with geologic structure as discussed by Banwell (1970).

Gravity Highs

At the Imperial Valley KGRA in California south of the Salton Sea, a residual gravity high of about 4-mgal closure is observed encompassing an area of high heat flow, as described by Rex (1972). Biehler and Combs (1972) postulate that this feature may reflect either an emplacement of higher density rhyolite domes or a densification process in which the loosely consolidated sediments increase in density owing to cementation and/or thermal metamorphism by circulating hot brines. McNitt (1965) states that this gravity high could also be due to a local structural high, possibly a horst.

The gravity surveys at Wairakei, New Zealand also show a positive anomaly which may possibly be caused by a horst block within an area of

regional subsidance as discussed by McNitt (1965). Grose (1971) states that the gravity high at Wairaikei and other fields in New Zealand are probably caused by densification.

The Glass Mountain KGRA in Siskiyou County, California is centered over a concealed Miocene cladera as described by Anderson and Axtell (1972). A positive gravity anomaly of almost 4-mgal closure is noted over this feature. This ancient depression is almost totally filled by lavas. It may be important to note that the above examples of these pronounced gravity highs occur in areas of regional subsidence (McNitt, 1965).

Gravity Lows

Peters (1974) shows that a pronounced gravity low with 15-20 mgal of total closure is obtained over the Geysers geothermal field, which lies 75 miles north of San Francisco. The anomaly is indicative of a magma chamber at a relatively shallow depth in the earth's crust beneath the Clear Lake volcanic field. Anderson and Axtell (1972) suggest that perhaps a molten or near-molten body underlies portions of the region at depth of 3 or more miles.

A similar feature is described by McNitt (1965) over the Larderello field, in northern Italy. This negative anomaly has closure of about 10-25 mgal. It is thought to be caused by a cooling intrusion at great depth as described by Grose (1971).

Again, it may be important to note that both the Geysers and the Larderello fields occur in areas of regional uplift (McNitt, 1965).

Gravity Gradients

Strong gravity gradients will usually denote steeply dipping

faults or faulting. The gravity method is very powerful in delineating such structure. Faults may be important in a geothermal area as they may act as conduits which bring thermal fluid from great depths or else they may merely act to increase reservoir permeability.

The gravity anomaly at the Lake City KGRA in Modoc County, California is an example of this type of feature. Anderson and Axtell (1972) show a gravity gradient of up to 25 mgal in 2 miles occurring here. This important structural feature is the Surprise Valley fault which has a displacement of over 5,000 feet. It should also be noted that a mud volcano and hot spring are centered in this large gravity gradient.

In summary, significant gravity anomalies may be obtained in geothermal areas that will assist in the geologic interpretation. It should be emphasized, however, that the relationship between the gravity anomalies (highs, low, or gradients) to the geology in the geothermal area may be complex; and, according to Combs (1972), the gravity method is open to gross misinterpretation if not used in conjunction with other exploration techniques.

APPENDIX 2

Location and wet bulk density of rock samples collected from the survey area

Rock Types	Location: Latitude N. Deg. Min.	Location: Longitude W. Deg. Min.#	Gravity Station No.	West Bulk Density (gm/cc)
Granite	38 33.17	112 46.67[d]	WB-406	2.60
Granite[1]	38 32.48	112 48.92[d]	WB-741	2.56
Granite[1]	38 30.56	112 52.18[c]	WB-715	2.57
Granite	38 34.97	112 40.13[g]	WB-273	2.62
Granite	38 29.36	112 42.20[i]	WB-356	2.61
Granite	38 29.36	112 42.20[i]	WB-356	2.67
Granite	38 29.36	112 42.20[i]	WB-356	2.57
Granite	38 35.19	112 48.31[d]	WB-526	2.55
Granite	38 35.19	112 48.31[d]	WB-526	2.58
Granite	38 33.10	112 47.46[d]	WB-507	2.69
Rhyolite	38 31.28	112 39.24[g]	WB-076	2.45
Rhyolite	38 30.29	112 39.79[g]	WB-077	2.08
Rhyolite	38 37.97	112 36.42[f]	WB-206	2.45
Rhyolite	38 37.54	112 36.55[f]	WB-213	2.45
Rhyolite	38 38.58	112 36.22[f]	WB-199	2.35
Rhyolite	38 38.65	112 36.18[f]	WB-198	2.62
Rhyolite	38 39.19	112 35.82[f]	WB-191	2.24
Rhyolite	38 38.67	112 44.58[e]	WB-316	2.41
Rhyolite	38 38.86	112 43.77[e]	WB-306	2.39
Rhyolite	38 38.70	112 33.79[f]	WB-385	2.53
Rhyolite	38 27.04	112 40.84[i]	WB-374	2.48
Rhyolite	38 38.30	112 34.09[f]	WB-384	2.23
Rhyolite	38 26.60	112 40.44[i]	WB-369	2.32
Rhyolite	38 38.13	112 33.56[f]	WB-483	2.31
Rhyolite	38 38.13	112 33.56[f]	WB-483	2.38
Rhyolite	38 38.13	112 33.56[f]	WB-483	2.40
Rhyolite	38 32.10	112 33.97[h]	WB-434	2.34

Rock Types	Location: Latitude N. Deg. Min.	Location: Longitude W. Deg. Min.#	Gravity Station No.	Wet Bulk Density (gm/cc)
Rhyolite	38 33.69	112 34.12[h]	WB-430	2.62
Rhyolite	38 30.64	112 33.16[h]	WB-437	2.37
Rhyolite	38 36.20	112 33.28[h]	WB-396	2.48
Rhyolite	38 42.99	112 51.64[b]	WB-575	2.40
Rhyolite	38 34.08	112 48.04[d]	WB-509	2.78
Rhyolite	38 34.08	112 48.04[d]	WB-509	2.58
Rhyolite	38 33.61	112 46.90[d]	WB-508	2.56
Rhyolite	38 31.92	112 33.68[h]	WB-485	1.92
Rhyolite	38 41.56	112 31.14[f]	WB-487	1.98
Rhyolite	38 43.56	112 49.33[b]	WB-598	2.24
Rhyolite	38 28.96	112 39.35[i]	WB-360	2.19
Lamprophyre Dike	38 33.10	112 47.46[d]	WB-507	3.44
Latite	38 27.48	112 39.50[i]	WB-371	1.92
Latite	38 35.41	112 48.87[d]	WB-593	2.55
Latite	38 35.35	112 49.85[d]	WB-658	1.98
Basalt	38 34.03	112 40.51[g]	WB-014	2.40
Basalt	38 35.59	112 40.02[g]	WB-013	2.30
Basalt	38 35.97	112 39.26[g]	WB-012	2.20
Basalt	38 35.74	112 41.19[g]	WB-107	2.68
Basalt	38 35.98	112 35.92[h]	WB-423	2.52
Basalt	38 40.90	112 50.66[b]	WB-600	2.53
Limestone	38 40.50	112 35.40[f]	WB-025	2.73
Limestone	38 39.99	112 33.65[f]	WB-028	2.69
Limestone	38 39.99	112 33.65[f]	WB-028	2.62
Limestone	38 29.62	112 41.65[i]	WB-355	2.74
Limestone	38 42.48	112 44.51[e]	WB-295	2.29
Limestone	38 42.44	112 43.42[e]	WB-292	2.56
Limestone	38 26.43	112 41.21[i]	WB-370	2.70
Limestone	38 42.47	112 32.79[f]	WB-482	2.79

Rock Types	Location: Latitude No. Deg. Min.	Location: Longitude W. Deg. Min.#	Gravity Station No.	Wet Bulk Density (gm/cc)
Limestone	38 37.10	112 49.62[d]	WB-587	2.63
Limestone	38 35.19	112 48.31[d]	WB-526	2.55
Limestone	38 42.71	112 31.73[f]	WB-488	2.66
Limestone	38 35.71	112 50.13[d]	WB-657	2.70
Limestone	38 36.07	112 50.13[d]	WB-656	2.72
Sandstone	38 39.39	112 33.28[e]	WB-452	2.57
Quartzite	38 39.38	112 38.48[e]	WB-037	2.60
Quartzite	38 29.62	112 41.65[e]	WB-355	2.60
Quartzite	38 34.97	112 40.13[g]	WB-273	2.62
Quartzite	38 34.97	112 40.13[g]	WB-273	2.53
Quartzite	38 41.01	112 35.19[f]	WB-244	2.60
Quartzite	38 38.05	112 32.48[f]	WB-484	2.41
Quartzite	38.37.10	112 49.62[d]	WB-587	2.63
Quartzite	38 37.15	112 50.36[d]	WB-655	2.61

[1] Wet Bulk density obtained from Crebs (1976).

Letter superscript after longitude value denotes the U.S. Geological Survey 7 1/2 - minute topographic quadrangle map (preliminary sheet) from which the sample location was obtained, where the following designations are used.

a -- Black Rock 3 NW
b -- Black Rock 3 NE
c -- Black Rock 3 SW
d -- Black Rock 3 SE
e -- Cove Fort NW
f -- Cove Fort NE
g -- Cove Fort NW
h -- Cove Fort SE
i -- Beaver NW

APPENDIX 3

DESCRIPTION OF GRAVITY FIELD BASE STATIONS AND HIGHWAY RIGHT-OF-WAY MARKERS USED IN THE GRAVITY SURVEY

F.B.-1 (same as WB-1) field base station (See Figs. 1 and 2)

U.S. Geological Survey 7 1/2-minute topographic quadrangle map:

Cove Fort SE (preliminary sheet)

Latitude - 38°35.11' N.

Longitude - 112°35.11' W.

Elevation - 5998 ft.

Nature - U.S. Highway 91 right-of-way marker

Gravity Value - 979482.04 mgal

The F.B.-1 gravity field base is located on the concrete pad of old U.S. Highway 91 right-of-way marker about 10 ft east of the east side of the highway near a telephone pole located about 1 1/4 miles south of Cove Fort and at the point where the 6,000 ft. contour crosses the road. The marker is located at the base of a fence post (1 1/4 inch steel angle-iron) in the eastern highway stock exclusion fence.

F.B.-2 field base station (See Figs. land 2)

U.S. Geological Survey 7 1/2-minute topographic quadrangle map:

Black Rock 3 NE 1/4 (preliminary sheet)

Latitude- 38°38.24' N

Longitude - 112°50.70' W

Elevation- 5260 ft.

Nature- road intersection

Gravity Value- 979564.91 mgal

The F.B.-2 gravity field base is located at the junction of the Black Rock and Antelope Springs roads at the north end of the Mineral Mountains. An aluminum stake about 3/4 inch in diameter pounded flush with the ground marks the exact spot, which is located in the crotch of the "Y" forming the road intersection. At the time of last occupation by the author (August 1976), a piece of quartzite about 10 inches in diameter was placed over the stake for each location at a later date.

Highway right-of-way markers

Nature- 2-inch galvanized iron pipe with a brass cap on top and embedded in concrete - similar to U.S.G.S. section corners found in the area.

Location- found along fences bordering U.S. Interstate Highway 15, Interstate Highway 70, and U.S. Highway 91. They are usually but not always marked by a pointed stake or several 1-inch-wide lathes woven into the fence itself over the spot. Rarely are they more than 20 ft from either side of the roadway.

Frequency- generally they are placed every 1/10 mile, but are found at all discontinuous changes in direction of the right-of-way and register distance in tenths of a mile plus so many

feet (if placed at other than even tenths of miles).

Elevation Accuracy- the elevation in feet (to 0.01 ft) and the year of the survey are stamped into the top of each brass cap.

APPENDIX 4

METHODS USED TO OBTAIN ASSUMED REGIONAL GRAVITY TRENDS AND RESIDUAL MAPS

Least-mean-square Polynomial Fitting -- Maps

Polynomial fitting was used to remove gravity anomalies of long wave length from the gravity data. It was accomplished by inputting the gridded gravity values into existing computer software of Dr. J. R Montgomery.

Least-mean-square polynomial surfaces.--These routines calculated least-mean-square polynomial surfaces from the gridded gravity data through order 10. The difference,

$$d_i = g_{io} - g_{ic}$$

where:

d_i = difference at the i^{th} point

g_{io} = gravity value observed at the i^{th} point

g_{ic} = gravity calculated at the i^{th} point

was calculated at each grid point, i, for each polynomial order. A root-mean-square (RMS) value was then calculated for each polynomial as,

$$RMS = \sqrt{\frac{\left(\sum_{i=1}^{n} d_i^2\right)}{n}}$$

where n = 1107 (the total number of grid points involved in the

64 x 128 array). A plot of the gridded data RMS values versus polynomial order is shown in Figure 19.

A similar calculation,

$$d_s = g_{so} - g_{sc}$$

where:

d_s = difference at the $s^{\underline{th}}$ station

g_{so} = gravity value observed at the $s^{\underline{th}}$ station

g_{sc} = gravity value calculated at the $s^{\underline{th}}$ station

gave the difference at each random data point, s (geographic point of observation), for each polynomial order. A random data RMS value was then calculated for each polynomial (Fig. 18).

The largest decrease in the RMS-error occurs between the first and second order polynomial surfaces (Fig. 18), while a similar decrease occurs between polynomial surfaces of order 2 and 3 in Figure 19. This is attributed to unavoidable aliasing introduced by the digitization process. In general this aliasing distributed the magnitude of anomalies smaller than 2 km contained in the random data set throughout the balance of the anomaly field. In the frequency domain this has the effect of folding the "power" of anomalies represented by frequencies higher than the Nyquist frequency (0.5 cycles/km) back into the balance of the power spectrum of those anomalies represented as frequencies lower than the Nyquist frequency.

Least-mean-square polynomial residual map.--The distinct change in slope between the second- and third-order polynomials and the form of higher-order polynomials on both the random data and the gridded

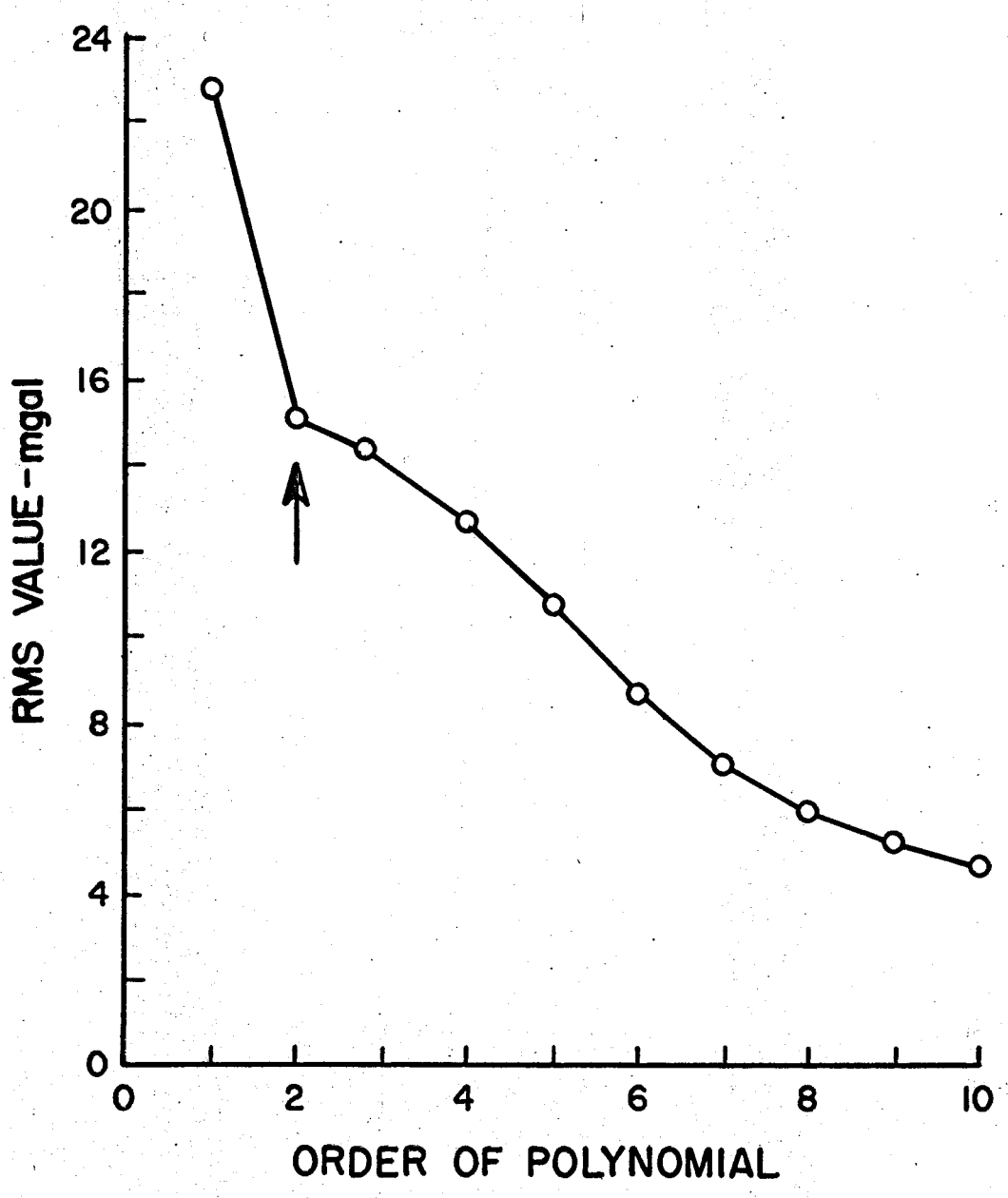

Figure 18 Graph of the RMS value of the difference between observed and calculated gravity values versus polynomial order for the random data

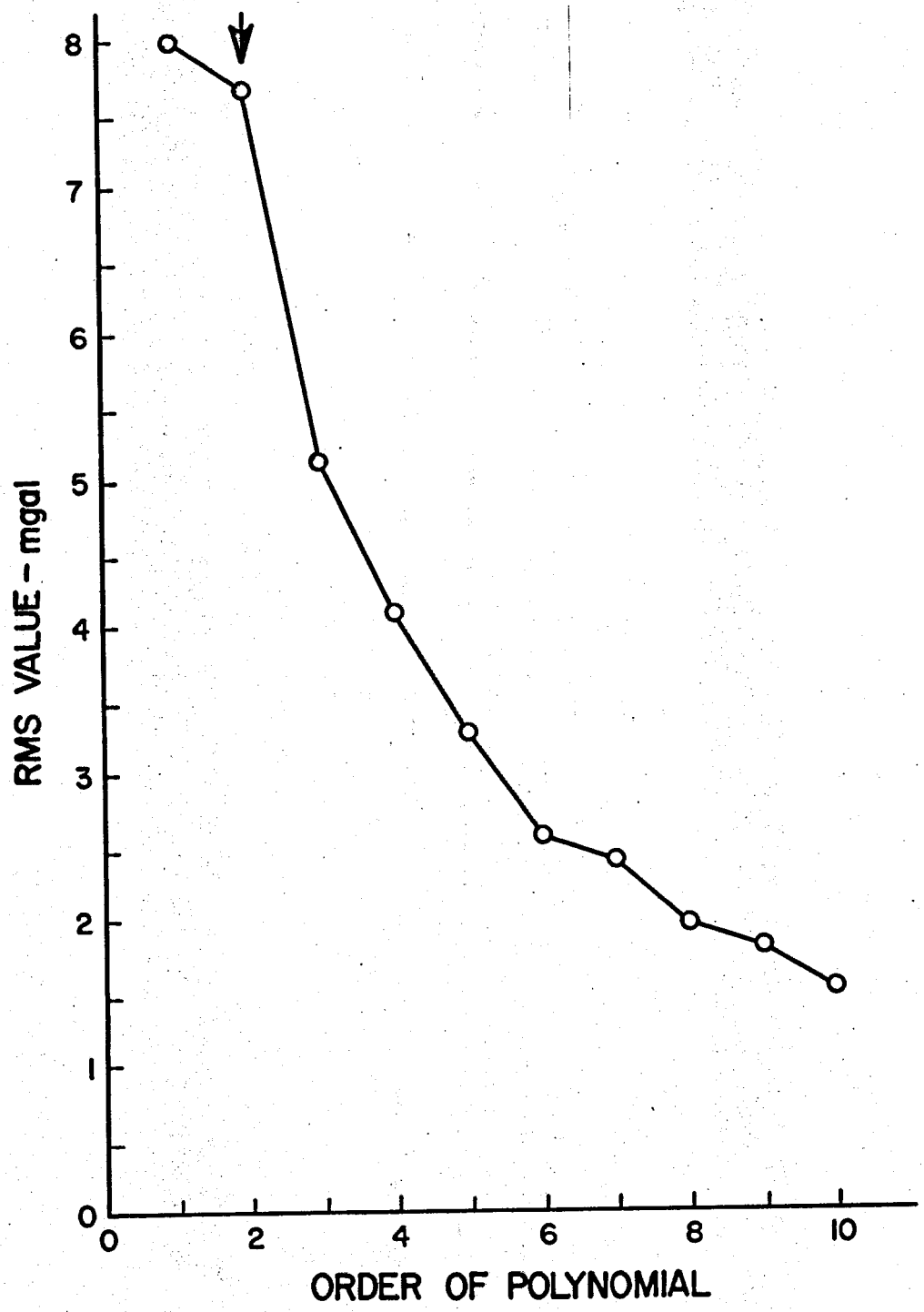

Figure 19 Graph of the RMS value of the difference between observed and calculated gravity values versus polnomial order for the gridded data.

data plots helped form the opinion of Drs. K. L. Cook, J. R Montgomery, and the author that the second-order polynomial surface best represented the "average" gravity surface in the survey area. The second-order polynomial surface calculated from the gridded data is shown in Figure 20 (since it was the gridded data that was used for the computer processed aids to help interpretation--Appendix 5). As a check, a second-order polynomial residual Bouguer gravity anomaly contour map was compiled and compared with a high-pass filtered Bouguer gravity anomaly contour map containing only frequencies whose wave lengths completely fit within the survey area's smallest dimension.

Gravity Profiles

For computational ease, the assumed regional gravity trend was approximated by piece-wise linear segments over the length of the gravity profiles. The points of discontinuity were chosen at or near outcrops of Paleozoic or Mesozoic sediments, the tie point between the roughly orthogonal profiles, and in the case of the east end of the Black Rock Road profile, to give a few tens of meters of alluvium cover over an observed gravity high with Paleozoic and Mesozoic outcrops at the surface within about 1 km north of the gravity profile at this location.

Black Rock Road profile.--The Black Rock Road profile has four regional match points. The west end of the assumed regional was tied to the average terrain-corrected gravity anomaly values of -165 mgal recorded by R. W. Case (1977) in the Cricket Mountains 4 km west of

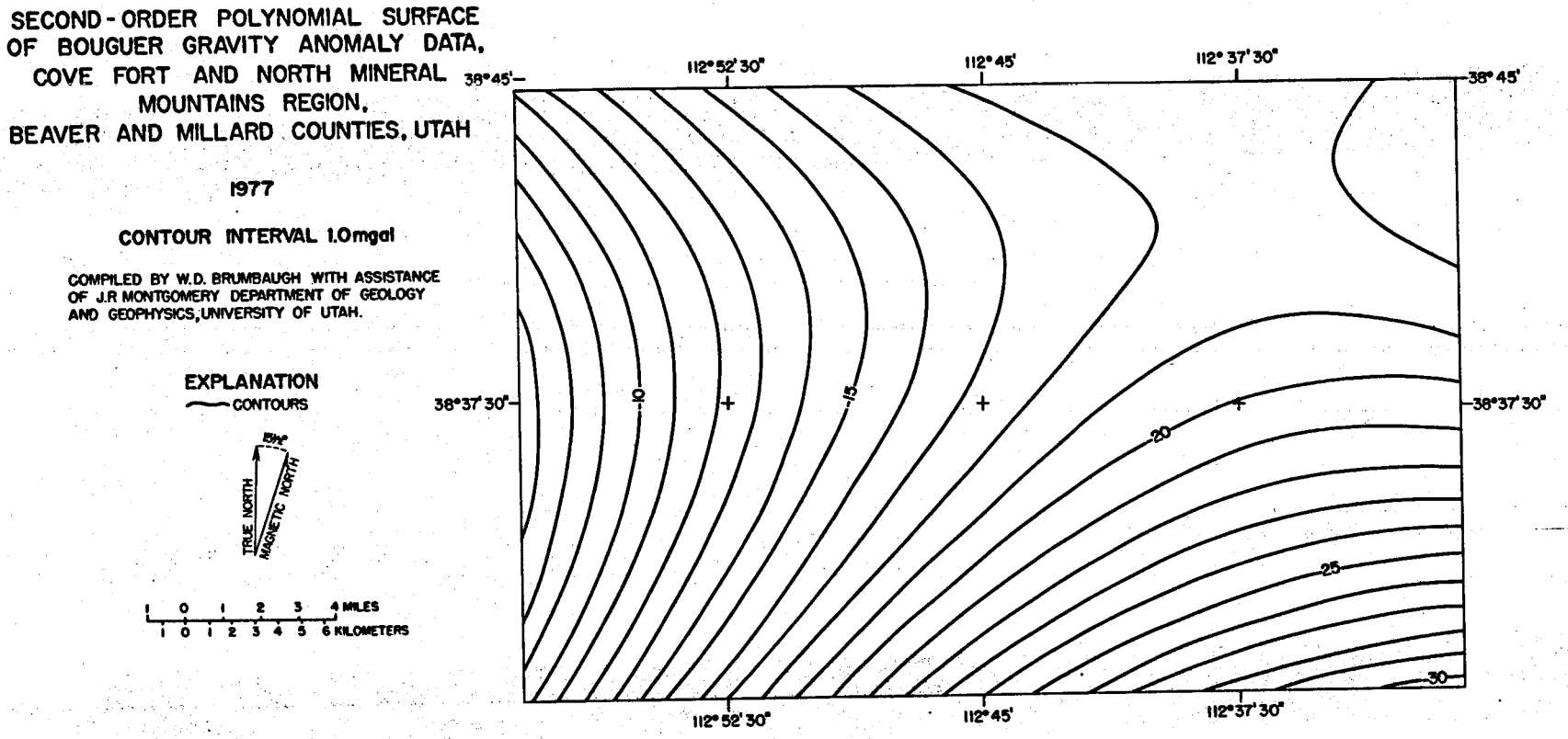

Figure 20 Second-order polynomial surface of Bouguer gravity anomaly data Cove Fort and north Mineral Mountains region, Beaver and Millard counties, Utah; contour interval = 1 mgal

the community of Black Rock. The westernmost Paleozoic outcrop within the survey area lies at the north end of the Mineral Range and has an average terrain-corrected Bouguer gravity anomaly value of -176 mgal. To the east, the next Paleozoic outcrop occurs north of the Cove Fort Cinder Cone, about 1/2 km north of the profile; and the average gravity value over these Paleozoic sediments was -195 mgal. Two linear line segments connecting these three values along the profile, crossing the western border of the survey area at -165.35 mgal, form essentially a straight line. The east-west flexure in the second-order polynomial surface best fitting the gravity data occurs just west of Cove Fort, where Black Rock Road intersects U.S. Interstate Highway 15. From this point the polynomial surface increases in amplitude to the west, but assumes almost a constant value to the east-southeast (along the Black Rock Road extending into Clear Creek Canyon towards Monroe, Utah). A discontinuity was therefore introduced at this intersection point by making the remaining assumed regional gravity along the Black Rock Road profile a constant value of -200 mgal. This value was chosen to give a few tens of meters of alluvium cover over the gravity anomaly in Clear Creek Canyon, is previously noted.

Interstate Highway 15 profile.--Along the Interstate Highway 15 profile the second-order polynomial surface has a fairly constant gradient from the survey area's southern boundary north to Cove Fort. Further north, however, the surface shows a positive flexure which is expressed in the assumed regional gravity of the profile by straight-line segments joining those terrain-corrected Bouguer gravity

anomaly values observed at or near Paleozoic outcrops along the profile.

Along the south end of the Interstate Highway 15 profile, the assumed regional gravity was determined by using the same north-south regional gradient that was observed 4 km west of the profile between the Cove Fort cinder cone-Paleozoic match point (-195 mgal) on the Black Rock Road profile and Limestone Point (-214 mgal), east of the Tom Harris Mine in Cunningham Wash (a total relief of -19 mgal). By applying this assumed gradient to the -200 mgal value at the tie point between the Black Rock Road and the Interstate Highway 15 profiles, the southern end of the Interstate Highway 15 assumed regional was set at -219 mgal.

To the north of the interprofile tie point (occurring at gravity station number WB-155), stations WB-204 (-199 mgal), WB-462 (-190 mgal) and a point 1/2 km north of station WB-249 (-182 mgal) on the profile's northern border supplied the respective bedrock match point readings for the remaining assumed regional gravity values.

APPENDIX 5

COMPUTER PROCESSING OF DATA

Extensive computer processing in both the frequency and space domains was employed in this study to enhance geologic interpretation of the gravity data. Most software used in this study originated with Dr. R. T. Shuey and Mr. T. J. Crebs in the frequency domain, 2) dimensional forward gravity modeling algorithm, and 3) Dr. J. R Montgomery who supplied polynomial-fitting routines and assistance in their use. To facilitate using this existing software on the University of Utah UNIVAC 1108, the terrain-corrected, Bouguer gravity data set was digitized in a rectangular array. The digitized values were then Fourier transformed and filtered to gibe desired residual maps. The detailed profile data were modeled in the space domain only. The following discussion details these steps.

The reduced gravity values were first plotted at their appropriate map locations by latitude and longitude, using a polyconic projection, on a Calcomp plotter at a scale of 1:62,500. Due to the non-randomness observed in the data distribution (high density in the valleys and low density in the mountains) contouring and subsequent digitizing was done by hand instead of using a computational random-to-grid algorithm. This had the additional advantage of acting as a low-pass filter reducing any sharp "kinks" introduced by unreasonable data points or extreme decrease

in data spacing. An array of 41 by 27 data points was picked on the Universal Transverse Mercator grid corners (a 1-km digitization interval) from the hand contours.

The next step was to determine and subtract out an assumed regional gravity surface containing both the mean and the trend. This was accomplished using polynominal fitting techniques (Appendix 4). Before transformation into the frequency domain, the data points on the perimeter of the residual, rectangular array were extended in a border 5 grid units wide as constants, and then tapered to the residual data's mean zero plane using a half-cosine bell.

The two-dimensional, Fast Fourier Transformation algorithm employed then required the bordered, tapered residual data be padded with zeroes to a 64 by 128 data set. Final Fourier transformed data were placed on a Fastran file for multiplication by the appropriate filter factors.

To produce the second vertical derivative residuals, the data set was first low-passed at a cut-off frequency of 0.33 cycles/km to suppress excessive amplification of high frequency components. The Fourier transformed, low-passed data were then multiplied by the filter factor function $RS = 4\pi^2 (f_x^2 + f_y^2)$ were f_x and f_y are the retained frequencies in the north (y) and east (x) directions.

The high-pass filtered Bouguer gravity anomaly map was compiled by subtracting a low-pass filtered data set (with a cut-off frequency of 0.05 cyckes/km, - equivalent to a wave length of 20 km which is the minimum dimension of the gravity survey area) from the original transformed values. The filter factor function used for this operation was:

$$RR \quad 1, \sqrt{f_x^2 + f_y^2} < fc$$

$$0, \sqrt{f_x^2 + f_y^2} > fc$$

where RR is the filter factor to be applied to the transformed data and f_c is the cut-off frequency of 0.05 cycles/km. This ideal response was tapered with a Hanning window between zero and one to minimize the "Gibbs effect".

The strike-filtered maps, which emphasize anomalies trending in the four azimuthal directions: north-south, east-west, northeast-southwest, and northwest-southeast, were produced by band-pass filtering the transformed data with respect to direction instead of with respect to frequency.

Since a vector in the space domain is orthogonal to its counterpart in the frequency domain, the strike-filter windows were defined as follows:

East-West Strike-Filter Azimuths 225° to 315°

North-South Strike-Filter Azimuths 135° to 225°

Northeast-Southwest Strike-Filter Azimuths 90° to 180°

Northwest-Southeast Strike-Filter Azimuths 0° to 90°

The taper width in all cases was set at 30°. To accomplish this directional band-pass filtering, a filter factor RR, was calculated that would multiply the transformed gravity data found within a directional "pie slice" by one and transformed gravity data found anywhere else by zero. Data found near the edge of any given "pie slice" window were multiplied by a cosine tapered "RR" filter factor value between zero and one, again to minimize the Gibbs effect upon transformation back from the frequency

domain to the space domain.

The Black Rock Road and Interstate Highway 15 profile data were modeled with software modified by J. H. Snow from the Talwani 2-D software employed by the Department of Geology and Geophysics, University of Utah for several years. After resolving a forward model for an initial guess, Snow's routine conducts a one-dimensional direct linear optimization of user specified vertex location and/or polygon density to minimize the sum of the squares of the differences between the observed anomalies and those computed from the assumed model. Step size, tolerance, movement sequence, direction of vertex movement, and polygon density limits are input by the user along with the initial model. Further refinement of the model's vertices' positions was accomplished with Snow's linear inversion routine which utilizes the output from the forward problem optimization routine, described above, as its input. This inversion routine expresses the forward problem as a Taylor series expansion that generates N equations in M unknowns; N is the number of observations (stations) and M is the number of parameters to be resolved. By inverting this M by N matrix, these N equations are solved. This is only a general description since both of the above routines will be detailed by Snow (1977, personal communication) in a paper now in preparation.

APPENDIX 6

Table of the Gravity Data

NOTES: 1) Units are as follows:

	UNITS
Latitude	degrees, minutes
Longitude	degrees, minutes
Elevation	feet
Free-air anomaly value	mgal
Simple Bouguer anomaly value[1]	mgal
Terrain-correction value[1]	mgal
Terrain-corrected Bouguer anomaly value[1]	mgal

2) Coding is as follows:

MLFRD--Milford gravity base station

WB069--number designation of gravity station taken by author

1 A density contrast of 2.67 gm/cc was assumed for both the Bouguer and terrain corrections. Terrain corrections were made 1) from zones B through E using U.S.C. & G.S. zone charts and 2) from zone E through 0.4 of zone L (20 km total) using M. Kane's computer algorithm.

STATION NUMBER	LATITUDE DEG	LATITUDE MIN	LONGITUDE DEG	LONGITUDE MIN	ELEVATION IN FEET	FREE-AIR ANOMALY	SIMPLE BOUGUER	TERRAIN CORRECTION	TERR-CORR BOUGUER
FB001	38.	35.01	112.	35.11	5998.	-9.05	-213.34	1.48	-211.86
WB002	38.	34.38	112.	35.39	6047.	-9.91	-215.87	1.51	-214.36
WB003	38.	37.33	112.	38.20	5875.	.90	-199.20	.47	-198.73
WB004	38.	37.01	112.	37.77	5885.	-.59	-201.03	.64	-200.39
WB005	38.	35.77	112.	34.86	5997.	-4.80	-209.06	1.29	-207.77
WB006	38.	35.76	112.	35.40	5953.	-8.92	-211.68	1.21	-210.47
WB007	38.	36.43	112.	35.40	5942.	-6.96	-209.35	1.11	-208.24
WB008	38.	36.65	112.	35.97	5939.	-6.43	-208.71	.84	-207.87
WB009	38.	36.98	112.	36.38	5970.	-2.40	-205.74	.72	-205.02
WB010	38.	36.88	112.	37.42	5891.	-2.00	-202.65	.64	-202.01
WB011	38.	36.79	112.	38.72	5865.	1.89	-197.87	.51	-197.36
WB012	38.	35.97	112.	39.26	5981.	.89	-202.82	.49	-202.33
WB013	38.	35.59	112.	40.02	6047.	1.96	-204.00	1.10	-202.90
WB014	38.	34.03	112.	40.51	6172.	-1.07	-211.29	.71	-210.58
WB015	38.	32.64	112.	39.76	6417.	-3.16	-221.72	2.52	-219.20
WB016	38.	31.68	112.	39.40	6091.	12.43	-219.89	.91	-218.98
WB017	38.	31.80	112.	38.40	6105.	16.58	-224.51	1.23	-223.28
W2018	38.	32.33	112.	37.14	6060.	17.87	-224.28	1.42	-222.86
WB019	38.	32.84	112.	36.04	6068.	16.24	-222.91	1.61	-221.30
WB020	38.	33.19	112.	35.89	6085.	13.89	-221.14	1.89	-219.25
WB021	38.	33.81	112.	35.62	6092.	-9.90	-217.39	1.60	-215.79
WB022	38.	39.58	112.	34.50	5762.	-1.05	-197.30	1.43	-195.87
WB023	38.	40.30	112.	34.49	5710.	-1.42	-195.90	1.43	-194.47
WB024	38.	40.30	112.	34.78	5688.	-2.70	-196.43	1.27	-195.16
WB025	38.	40.50	112.	35.40	5689.	-1.71	-195.47	1.79	-193.68
WB026	38.	40.30	112.	33.62	5806.	1.82	-195.93	1.90	-194.03
WB027	38.	40.28	112.	33.88	5773.	.99	-195.64	1.86	-193.78
WB028	38.	39.99	112.	33.65	6064.	10.24	-196.30	2.68	-193.62
WB029	38.	38.34	112.	33.92	6270.	10.86	-202.70	1.97	-200.73
WB030	38.	36.84	112.	34.82	6033.	-.06	-205.54	1.32	-204.22

STATION NUMBER	LATITUDE DEG	MIN	LONGITUDE DEG	MIN	ELEVATION IN FEET	FREE-AIR ANOMALY	SIMPLE BOUGUER	TERRAIN CORRECTION	TERR-CORR BOUGUER
WB031	38.	36.08	112.	34.60	6024.	.67	-204.51	1.41	-203.10
WB032	38.	37.63	112.	38.31	5905.	2.96	-198.16	.42	-197.74
WB033	38.	38.16	112.	38.37	5912.	3.57	-197.80	.40	-197.40
WB034	38.	38.53	112.	38.45	5912.	4.60	-196.76	.39	-196.37
WB035	38.	38.79	112.	38.48	5895.	4.30	-196.48	.42	-196.06
WB036	38.	39.12	112.	38.46	5929.	7.81	-194.14	.46	-193.68
WB037	38.	39.38	112.	38.48	5945.	9.34	-193.14	.76	-192.38
WB038	38.	39.67	112.	38.66	5966.	11.01	-192.20	.39	-191.81
WB039	38.	39.78	112.	38.82	5992.	11.43	-192.66	.52	-192.14
WB040	38.	40.09	112.	39.22	6089.	14.04	-193.36	.50	-192.86
WB041	38.	40.26	112.	39.42	6043.	11.16	-194.66	.45	-194.21
WB042	38.	40.50	112.	39.66	6023.	10.16	-194.98	.43	-194.55
WB043	38.	40.74	112.	39.82	5993.	8.08	-196.04	.63	-195.41
WB044	38.	41.48	112.	40.00	5838.	1.46	-197.38	.44	-196.94
WB045	38.	42.05	112.	39.22	5760.	.67	-195.52	.87	-194.65
WB046	38.	41.53	112.	40.93	5674.	-7.83	-201.09	.42	-200.67
WB047	38.	41.46	112.	41.52	5700.	-6.97	-201.11	.36	-200.75
WB048	38.	41.72	112.	42.26	5781.	-4.46	-201.36	.44	-200.92
WB049	38.	42.45	112.	42.62	5806.	5.95	-191.80	.52	-191.28
WB050	38.	42.60	112.	42.54	5621.	10.06	-201.51	.38	-201.13
WB051	38.	42.81	112.	42.12	5590.	10.39	-200.79	.39	-200.40
WB052	38.	42.85	112.	41.89	5533.	11.53	-199.98	.40	-199.58
WB053	38.	42.91	112.	41.53	5493.	13.46	-200.55	.54	-200.01
WB054	38.	42.75	112.	41.08	5406.	14.77	-198.90	.80	-198.10
WB055	38.	42.80	112.	41.32	5357.	22.28	-204.74	.82	-203.92
WB056	38.	43.33	112.	40.78	5326.	18.60	-200.00	.76	-199.24
WB057	38.	43.97	112.	40.88	5204.	24.09	-201.34	.55	-200.79
WB058	38.	43.70	112.	41.25	5268.	23.95	-203.38	.50	-202.88
WB059	38.	43.86	112.	40.63	5201.	23.86	-201.01	.58	-200.43
WB060	38.	44.15	112.	39.62	5195.	22.51	-199.45	.49	-198.96

STATION NUMBER	LATITUDE DEG	LATITUDE MIN	LONGITUDE DEG	LONGITUDE MIN	ELEVATION IN FEET	FREE-AIR ANOMALY	SIMPLE BOUGUER	TERRAIN CORRECTION	TERR-CORR BOUGUER
WB061	38.	44.39	112.	38.90	5256.	16.61	-195.63	.45	-195.18
WB062	38.	44.48	112.	38.30	5225.	21.14	-199.10	.43	-198.67
WB063	38.	44.45	112.	37.80	5275.	14.20	-193.87	.39	-193.48
WB064	38.	39.56	112.	34.38	5796.	-.96	-198.37	1.41	-196.96
WB065	38.	39.74	112.	33.75	5809.	.90	-196.95	1.85	-195.10
WB066	38.	39.97	112.	34.11	5787.	5.37	-191.73	1.45	-190.28
WB067	38.	41.13	112.	39.75	5914.	5.67	-195.76	.77	-194.99
WB068	38.	42.12	112.	42.32	5734.	-5.80	-201.10	.37	-200.73
WB069	38.	39.50	112.	36.76	6122.	12.89	-195.63	.88	-194.75
WB070	38.	39.45	112.	35.90	5830.	.68	-197.89	1.23	-196.66
WB071	38.	44.28	112.	36.08	5177.	13.26	-189.59	.60	-188.99
WB072	38.	44.63	112.	35.46	5088.	13.48	-186.77	.73	-186.04
WB073	38.	32.42	112.	36.20	6072.	16.78	-223.59	1.81	-221.78
WB074	38.	31.04	112.	36.30	6149.	16.32	-225.76	2.27	-223.49
WB075	38.	31.62	112.	38.22	6110.	17.79	-225.89	1.39	-224.50
WB076	38.	31.28	112.	39.24	6223.	-9.31	-221.26	1.16	-220.10
WB077	38.	30.29	112.	39.79	6607.	-2.86	-227.89	2.20	-225.69
WB078	38.	30.88	112.	40.10	6454.	-.69	-220.52	2.46	-218.06
WB079	38.	31.03	112.	40.44	6144.	-7.32	-216.59	.98	-215.61
WB080	38.	31.41	112.	40.59	6096.	-7.76	-215.39	.83	-214.56
WB081	38.	31.72	112.	41.50	6026.	-7.32	-212.57	.91	-211.66
WB082	38.	31.15	112.	41.40	6132.	-2.33	-211.19	.91	-210.28
WB083	38.	30.75	112.	41.51	6242.	3.39	-209.21	.94	-208.27
WB084	38.	31.18	112.	43.81	6209.	-1.30	-212.78	1.11	-211.67
WB085	38.	31.49	112.	44.37	5996.	-5.47	-209.69	1.29	-208.40
WB086	38.	32.31	112.	43.56	5830.	10.26	-208.83	.94	-207.89
WB087	38.	32.26	112.	42.74	5851.	-9.43	-208.71	.91	-207.80
WB088	38.	43.58	112.	37.18	5377.	-9.06	-192.20	.56	-191.64
WB089	38.	43.24	112.	38.22	5472.	-6.42	-192.80	.49	-192.31
WB090	38.	43.05	112.	38.89	5497.	-6.25	-193.48	.58	-192.90

STATION NUMBER	LATITUDE DEG	MIN	LONGITUDE DEG	MIN	ELEVATION IN FEET	FREE-AIR ANOMALY	SIMPLE BOUGUER	TERRAIN CORRECTION	TERR-CORR BOUGUER
WB091	38.	41.18	112.	41.52	5701.	-6.36	-200.53	.38	-200.15
WB092	38.	40.89	112.	41.52	5705.	-5.56	-199.87	.45	-199.42
WB093	38.	40.30	112.	41.52	5724.	-3.64	-198.60	.52	-198.08
WB094	38.	40.46	112.	41.52	5718.	-4.47	-199.22	.54	-198.68
WB095	38.	39.36	112.	41.82	5774.	-.87	-197.53	.31	-197.22
WB096	38.	40.47	112.	42.62	6026.	4.13	-201.11	.46	-200.65
WB097	38.	38.10	112.	42.20	5698.	-3.71	-197.78	.33	-197.45
WB098	38.	37.70	112.	41.54	5783.	-2.31	-199.28	.31	-198.97
WB099	38.	37.57	112.	41.27	5749.	-2.51	-198.32	.42	-197.90
WB100	38.	37.70	112.	39.26	5855.	1.32	-198.10	.39	-197.71
WB101	38.	36.63	112.	39.54	5862.	.63	-199.03	.44	-198.59
WB102	38.	36.01	112.	39.81	5915.	.03	-201.44	.63	-200.81
WB103	38.	36.24	112.	40.12	5875.	-.46	-200.56	.62	-199.94
WB104	38.	36.96	112.	38.38	5889.	1.20	-199.38	.46	-198.92
WB105	38.	35.96	112.	40.38	5893.	-.95	-201.67	.50	-201.17
WB106	38.	35.98	112.	40.68	5847.	-2.19	-201.34	.50	-200.84
WB107	38.	35.74	112.	41.19	5824.	-3.90	-202.26	.46	-201.80
WB108	38.	35.31	112.	41.40	5804.	-6.69	-204.37	.57	-203.80
WB109	38.	35.20	112.	41.50	5804.	-6.53	-204.21	.62	-203.59
WB110	38.	35.04	112.	42.12	5800.	-6.08	-203.62	.56	-203.06
WB111	38.	34.79	112.	42.22	5809.	-5.86	-203.71	.52	-203.19
WB112	38.	34.33	112.	41.70	5807.	-9.10	-206.88	.57	-206.31
WB113	38.	34.23	112.	41.50	5888.	-7.75	-208.29	.69	-207.60
WB114	38.	33.68	112.	42.05	5826.	10.58	-209.02	.62	-208.40
WB115	38.	33.82	112.	41.98	5826.	10.05	-208.49	.56	-207.93
WB116	38.	32.10	112.	41.58	5958.	-9.21	-212.14	.84	-211.30
WB117	38.	32.51	112.	41.38	5990.	-8.68	-212.70	.76	-211.94
WB118	38.	32.85	112.	41.30	5985.	-8.95	-212.80	.67	-212.13
WB119	38.	33.19	112.	41.09	5979.	-8.26	-211.90	.69	-211.21
WB120	38.	33.25	112.	41.36	5940.	11.64	-213.96	.72	-213.24

STATION NUMBER	LATITUDE DEG	LATITUDE MIN	LONGITUDE DEG	LONGITUDE MIN	ELEVATION IN FEET	FREE-AIR ANOMALY	SIMPLE BOUGUER	TERRAIN CORRECTION	TERR-CORR BOUGUER
WB121	38.	33.45	112.	42.07	5836.	10.65	-209.43	.63	-208.80
WB122	38.	34.65	112.	43.07	5681.	13.98	-207.48	.64	-206.84
WB123	38.	35.32	112.	43.60	5588.	11.08	-201.41	.63	-200.78
WB124	38.	37.11	112.	43.25	5621.	-6.14	-197.59	.31	-197.28
WB125	38.	37.18	112.	42.67	5628.	-6.67	-198.36	.36	-198.00
WB126	38.	37.41	112.	41.80	5742.	-3.31	-198.89	.36	-198.53
WB127	38.	34.65	112.	36.10	6011.	12.31	-217.04	1.04	-216.00
WB128	38.	34.57	112.	36.11	6013.	12.62	-217.42	1.07	-216.35
WB129	38.	34.51	112.	36.12	6015.	13.06	-217.93	1.06	-216.87
WB130	38.	34.32	112.	36.13	6020.	13.50	-218.54	1.21	-217.33
WB131	38.	34.23	112.	36.14	6024.	13.88	-219.06	1.21	-217.85
WB132	38.	34.13	112.	36.16	6029.	14.18	-219.53	1.23	-218.30
WB133	38.	34.05	112.	36.15	6044.	13.46	-219.32	1.20	-218.12
WB134	38.	33.97	112.	36.16	6053.	13.55	-219.72	1.18	-218.54
WB135	38.	33.80	112.	36.19	6060.	14.83	-221.24	1.30	-219.94
WB136	38.	33.88	112.	36.18	6020.	18.06	-223.10	1.32	-221.78
WB137	38.	33.72	112.	36.21	6060.	15.16	-221.56	1.33	-220.23
WB138	38.	33.63	112.	36.22	6066.	15.08	-221.69	1.32	-220.37
WB139	38.	33.56	112.	36.23	6069.	15.24	-221.95	1.32	-220.63
WB140	38.	33.49	112.	36.26	6057.	15.66	-221.96	1.38	-220.58
WB141	38.	33.40	112.	36.28	6044.	16.46	-222.32	1.42	-220.90
WB142	38.	33.31	112.	36.30	6043.	16.92	-222.74	1.47	-221.27
WB143	38.	33.23	112.	36.31	6040.	17.05	-222.77	1.59	-221.18
WB144	38.	33.05	112.	36.34	6042.	17.53	-223.32	1.64	-221.68
WB145	38.	33.13	112.	36.32	6042.	17.17	-222.96	1.59	-221.37
WB146	38.	32.97	112.	36.36	6042.	18.02	-223.81	1.62	-222.19
WB147	38.	32.88	112.	36.38	6042.	18.33	-224.12	1.59	-222.53
WB148	38.	32.79	112.	36.39	6046.	17.13	-223.05	1.59	-221.46
WB149	38.	32.71	112.	36.42	6047.	18.28	-224.24	1.73	-222.51
WB150	38.	32.63	112.	36.43	6048.	18.16	-224.15	1.70	-222.45

STATION NUMBER	LATITUDE DEG	MIN	LONGITUDE DEG	MIN	ELEVATION IN FEET	FREE-AIR ANOMALY	SIMPLE BOUGUER	TERRAIN CORRECTION	TERR-CORR BOUGUER
WB151	38.	32.54	112.	36.44	6050.	18.05	-224.11	1.71	-222.40
WB152	38.	32.46	112.	36.45	6050.	20.48	-226.54	1.72	-224.82
WB153	38.	32.08	112.	36.52	6079.	17.91	-224.96	1.79	-223.17
WB154	38.	32.00	112.	36.53	6085.	17.93	-225.18	1.80	-223.38
WB155	38.	36.95	112.	36.45	5968.	-2.50	-205.77	.75	-205.02
WB156	38.	36.85	112.	36.49	5940.	-4.90	-207.22	.76	-206.46
WB157	38.	36.77	112.	36.49	5917.	-6.25	-207.78	.74	-207.04
WB158	38.	36.61	112.	36.49	5923.	-6.93	-208.67	.71	-207.96
WB159	38.	36.53	112.	36.48	5917.	-7.32	-208.86	.78	-208.08
WB160	38.	36.45	112.	36.48	5920.	-6.88	-208.52	.77	-207.75
WB161	38.	36.36	112.	36.48	5909.	-8.01	-209.27	.82	-208.45
WB162	38.	36.28	112.	36.48	5910.	-8.29	-209.59	.82	-208.77
WB163	38.	36.19	112.	36.48	5913.	-8.46	-209.86	.79	-209.07
WB164	38.	36.10	112.	36.47	5916.	-8.54	-210.04	.79	-209.25
WB165	38.	36.01	112.	36.46	5922.	-7.91	-209.61	.81	-208.80
WB166	38.	35.93	112.	36.44	5926.	-7.83	-209.67	.87	-208.80
WB167	38.	35.85	112.	36.42	5929.	-8.33	-210.27	.88	-209.39
WB168	38.	35.76	112.	36.40	5928.	-9.20	-211.11	.88	-210.23
WB169	38.	35.60	112.	36.32	6015.	-8.07	-212.94	.88	-212.06
WB170	38.	35.51	112.	36.30	6013.	-8.43	-213.24	.82	-212.42
WB171	38.	35.43	112.	36.28	6008.	-8.85	-213.48	1.06	-212.42
WB172	38.	35.35	112.	36.27	6053.	-7.41	-213.58	.86	-212.72
WB173	38.	35.26	112.	36.25	6045.	-7.91	-213.80	.92	-212.88
WB174	38.	35.17	112.	36.25	6042.	-8.39	-214.18	.85	-213.33
WB175	38.	35.08	112.	36.24	6031.	-8.75	-214.16	.87	-213.29
WB176	38.	35.00	112.	36.20	6040.	-8.60	-214.32	.89	-213.43
WB177	38.	34.91	112.	36.19	6020.	10.77	-215.82	1.03	-214.79
WB178	38.	34.83	112.	36.16	6031.	10.85	-216.27	1.02	-215.25
WB179	38.	34.75	112.	36.13	6020.	11.32	-216.36	1.04	-215.32
WB180	38.	35.67	112.	36.34	5936.	-9.01	-211.19	.91	-210.28

STATION NUMBER	LATITUDE DEG	MIN	LONGITUDE DEG	MIN	ELEVATION IN FEET	FREE-AIR ANOMALY	SIMPLE BOUGUER	TERRAIN CORRECTION	TERR-CORR BOUGUER
WB181	38.	34.40	112.	36.12	6014.	13.40	-218.24	1.09	-217.15
WB182	38.	37.03	112.	36.41	5973.	-2.01	-205.45	.68	-204.77
WB183	38.	37.11	112.	36.46	5960.	-2.97	-205.97	.76	-205.21
WB184	38.	37.19	112.	36.48	5966.	-1.88	-205.09	.73	-204.36
WB185	38.	37.26	112.	36.51	5972.	-1.33	-204.73	.67	-204.06
WB186	38.	39.52	112.	35.56	5757.	-1.78	-197.86	1.23	-196.63
WB187	38.	39.44	112.	35.62	5777.	-1.13	-197.90	1.15	-196.75
WB188	38.	39.40	112.	35.66	5786.	-.53	-197.60	1.19	-196.41
WB189	38.	39.32	112.	35.73	5804.	-.38	-198.06	1.14	-196.92
WB190	38.	39.26	112.	35.77	5812.	-.18	-198.14	1.06	-197.08
WB191	38.	39.19	112.	35.82	5841.	.92	-198.02	1.12	-196.90
WB192	38.	39.11	112.	35.88	5846.	.55	-198.57	1.06	-197.51
WB193	38.	39.03	112.	35.92	5855.	.71	-198.71	1.17	-197.54
WB194	38.	38.95	112.	35.97	5864.	1.01	-198.72	1.31	-197.41
WB195	38.	38.88	112.	36.02	5888.	1.55	-198.99	1.20	-197.79
WB196	38.	38.80	112.	36.07	5918.	2.73	-198.83	1.23	-197.60
WB197	38.	38.72	112.	36.12	5960.	5.18	-197.82	1.03	-196.79
WB198	38.	38.65	112.	36.18	5971.	4.33	-199.04	1.06	-197.98
WB199	38.	38.58	112.	36.22	6021.	6.06	-199.01	.78	-198.23
WB200	38.	38.50	112.	36.29	6068.	7.67	-199.01	.68	-198.33
WB201	38.	38.42	112.	36.37	6052.	7.22	-198.91	.66	-198.25
WB202	38.	38.35	112.	36.39	6080.	7.97	-199.11	.67	-198.44
WB203	38.	38.24	112.	36.46	6092.	8.08	-199.41	.74	-198.67
WB204	38.	38.19	112.	36.47	6115.	8.58	-199.69	.81	-198.88
WB205	38.	38.10	112.	36.48	6181.	9.98	-200.55	.79	-199.76
WB206	38.	37.97	112.	36.42	6166.	8.89	-201.13	.90	-200.23
WB207	38.	37.91	112.	36.39	6135.	7.64	-201.31	.76	-200.55
WB208	38.	37.85	112.	36.37	6116.	6.59	-201.72	.74	-200.98
WB209	38.	37.80	112.	36.36	6099.	5.75	-201.98	.78	-201.20
WB210	38.	37.71	112.	36.40	6070.	3.73	-203.01	.74	-202.27

STATION NUMBER	LATITUDE DEG	MIN	LONGITUDE DEG	MIN	ELEVATION IN FEET	FREE-AIR ANOMALY	SIMPLE BOUGUER	TERRAIN CORRECTION	TERR-CORR BOUGUER
WB211	38.	37.66	112.	36.42	6050.	2.93	-203.13	.70	-202.43
WB212	38.	37.58	112.	36.46	6044.	2.58	-203.28	.65	-202.63
WB213	38.	37.54	112.	36.55	6044.	2.86	-203.00	.67	-202.33
WB214	38.	37.45	112.	36.51	6013.	.81	-203.99	.77	-203.22
WB215	38.	37.37	112.	36.51	5981.	-.80	-204.52	.68	-203.84
WB216	38.	37.32	112.	36.50	5973.	-1.13	-204.57	.71	-203.86
WB217	38.	39.58	112.	35.48	5742.	-2.10	-197.68	1.32	-196.36
WB218	38.	39.63	112.	35.44	5734.	-2.40	-197.70	1.33	-196.37
WB219	38.	39.68	112.	35.42	5726.	-2.58	-197.60	1.34	-196.26
WB220	38.	39.78	112.	35.36	5711.	-3.07	-197.59	1.41	-196.18
WB221	38.	39.85	112.	35.30	5702.	-3.59	-197.80	1.39	-196.41
WB222	38.	39.90	112.	35.27	5698.	-3.88	-197.96	1.45	-196.51
WB223	38.	39.96	112.	35.24	5694.	-4.09	-198.02	1.45	-196.57
WB224	38.	40.09	112.	35.18	5687.	-4.13	-197.83	1.59	-196.24
WB225	38.	40.22	112.	35.18	5685.	-3.64	-197.27	1.51	-195.76
WB226	38.	40.38	112.	35.24	5684.	-3.21	-196.81	1.38	-195.43
WB227	38.	40.44	112.	35.28	5685.	-2.63	-196.26	1.43	-194.83
WB228	38.	40.49	112.	35.32	5686.	-2.17	-195.84	1.55	-194.29
WB229	38.	34.86	112.	37.28	6151.	-4.37	-213.88	1.07	-212.81
WB230	38.	34.35	112.	38.30	6498.	6.46	-214.86	1.61	-213.25
WB231	38.	32.58	112.	43.47	5796.	11.29	-208.70	.87	-207.83
WB232	38.	32.73	112.	44.18	5744.	12.33	-207.97	.95	-207.02
WB233	38.	33.49	112.	44.82	5668.	13.72	-206.77	.93	-205.84
WB234	38.	31.93	112.	43.94	5829.	13.00	-211.53	1.50	-210.03
WB235	38.	35.66	112.	43.85	5580.	10.68	-200.74	.55	-200.19
WB236	38.	36.07	112.	43.92	5605.	-9.09	-200.00	.38	-199.62
WB237	38.	36.67	112.	43.86	5638.	-5.78	-197.81	.30	-197.51
WB238	38.	36.28	112.	44.78	5554.	-7.35	-196.52	.39	-196.13
WB239	38.	37.00	112.	44.92	5555.	-4.30	-193.50	.29	-193.21
WB240	38.	37.30	112.	44.93	5563.	-3.15	-192.63	.29	-192.34

STATION NUMBER	LATITUDE DEG	MIN	LONGITUDE DEG	MIN	ELEVATION IN FEET	FREE-AIR ANOMALY	SIMPLE BOUGUER	TERRAIN CORRECTION	TERR-CORR BOUGUER
WB241	38.	37.66	112.	44.95	5573.	-2.26	-192.07	.27	-191.80
WB242	38.	37.42	112.	44.32	5589.	-3.53	-193.89	.52	-193.37
WB243	38.	37.71	112.	40.38	5858.	1.31	-198.22	.65	-197.57
WB244	38.	41.01	112.	35.19	5786.	5.17	-191.90	1.36	-190.54
WB245	38.	41.21	112.	35.24	5735.	4.72	-190.62	1.10	-189.52
WB246	38.	42.15	112.	35.55	5496.	-.91	-188.10	1.00	-187.10
WB247	38.	43.76	112.	35.34	5136.	13.49	-188.42	.84	-187.58
WB248	38.	44.46	112.	34.77	5032.	13.44	-184.83	.88	-183.95
WB249	38.	44.73	112.	34.46	5029.	12.06	-183.35	.80	-182.55
WB250	38.	43.78	112.	36.70	5282.	12.40	-192.31	1.08	-191.23
WB251	38.	42.57	112.	37.60	5750.	1.72	-194.12	1.63	-192.49
WB252	38.	41.63	112.	37.82	6000.	6.34	-198.02	.77	-197.25
WB253	38.	40.80	112.	37.74	6064.	14.03	-192.51	.60	-191.91
WB254	38.	40.83	112.	37.38	6080.	14.23	-192.86	1.04	-191.82
WB255	38.	40.78	112.	36.78	6040.	14.38	-191.34	1.21	-190.13
WB256	38.	40.53	112.	36.42	6062.	13.84	-192.63	.73	-191.90
WB257	38.	40.36	112.	38.24	6049.	14.03	-192.00	.67	-191.33
WB258	38.	40.14	112.	38.51	6012.	11.98	-192.79	.40	-192.39
WB259	38.	44.11	112.	38.38	5320.	14.04	-195.24	.52	-194.72
WB260	38.	42.00	112.	41.42	5596.	-9.83	-200.43	1.56	-198.87
WB261	38.	40.39	112.	40.84	6217.	22.79	-188.96	.91	-188.05
WB262	38.	39.91	112.	40.30	5952.	8.63	-194.09	.37	-193.72
WB264	38.	38.74	112.	41.94	5740.	-2.24	-197.74	.30	-197.44
WB265	38.	38.28	112.	42.66	5696.	-2.78	-196.79	.30	-196.49
WB266	38.	38.15	112.	39.93	5893.	3.97	-196.75	.38	-196.37
WB267	38.	38.58	112.	39.26	5942.	7.03	-195.36	.42	-194.94
WB268	38.	33.31	112.	39.52	6290.	-2.00	-216.24	.61	-215.63
WB269	38.	33.62	112.	39.80	6253.	-2.09	-215.06	.62	-214.44
WB270	38.	34.35	112.	40.22	6100.	-2.27	-210.03	.63	-209.40
WB271	38.	34.47	112.	40.04	6115.	-2.28	-210.56	.69	-209.87

STATION NUMBER	LATITUDE DEG	LATITUDE MIN	LONGITUDE DEG	LONGITUDE MIN	ELEVATION IN FEET	FREE-AIR ANOMALY	SIMPLE BOUGUER	TERRAIN CORRECTION	TERR-CORR BOUGUER
WB272	38.	34.75	112.	39.82	6101.	-1.66	-209.46	.64	-208.82
WB273	38.	34.97	112.	40.13	5921.	11.10	-212.77	.64	-212.13
WB274	38.	35.26	112.	40.06	5973.	-1.62	-205.06	.60	-204.46
WB275	38.	35.75	112.	39.80	5951.	.40	-202.29	.70	-201.59
WB276	38.	41.88	112.	39.54	5809.	1.08	-196.77	.58	-196.19
WB277	38.	37.98	112.	39.12	5848.	1.97	-197.21	.42	-196.79
WB278	38.	41.18	112.	40.67	5750.	-3.16	-199.00	.74	-198.26
WB279	38.	42.86	112.	38.92	5517.	-5.35	-193.26	.64	-192.62
WB280	38.	42.60	112.	39.22	5600.	-2.97	-193.70	.77	-192.93
WB281	38.	44.65	112.	36.98	5214.	15.22	-192.81	.52	-192.29
WB282	38.	44.65	112.	36.46	5170.	15.27	-191.36	.51	-190.85
WB283	38.	44.66	112.	35.88	5148.	13.90	-189.24	.64	-188.60
WB284	38.	44.83	112.	36.79	5172.	15.77	-191.93	.47	-191.46
WB285	38.	44.28	112.	37.05	5250.	13.99	-192.80	.43	-192.37
WB286	38.	44.24	112.	40.66	5190.	23.93	-200.70	.39	-200.31
WB287	38.	44.66	112.	40.33	5149.	25.54	-200.91	.35	-200.56
WB288	38.	44.25	112.	41.14	5200.	24.66	-201.77	.38	-201.39
WB289	38.	44.66	112.	41.54	5165.	26.56	-202.48	.38	-202.10
WB290	38.	44.88	112.	40.93	5248.	22.24	-200.99	.65	-200.34
WB291	38.	43.20	112.	41.61	5440.	20.71	-206.00	.60	-205.40
WB292	38.	42.44	112.	43.42	5720.	-4.51	-199.33	.52	-198.81
WB293	38.	42.78	112.	43.93	5771.	-6.13	-202.69	.51	-202.18
WB294	38.	43.31	112.	44.40	5696.	-7.76	-201.76	.50	-201.26
WB295	38.	42.48	112.	44.51	5857.	-.30	-199.79	.58	-199.21
WB296	38.	41.97	112.	44.42	5950.	3.81	-198.84	.63	-198.21
WB297	38.	41.49	112.	43.75	5949.	2.36	-200.26	.53	-199.73
WB298	38.	41.63	112.	43.15	5914.	-.34	-201.77	.48	-201.29
WB299	38.	42.18	112.	42.80	5714.	-7.21	-201.83	.40	-201.43
WB300	38.	40.88	112.	42.38	5930.	-1.90	-203.87	.44	-203.43
WB301	38.	39.43	112.	42.18	5840.	2.13	-196.78	.38	-196.40

STATION NUMBER	LATITUDE DEG	LATITUDE MIN	LONGITUDE DEG	LONGITUDE MIN	ELEVATION IN FEET	FREE-AIR ANOMALY	SIMPLE BOUGUER	TERRAIN CORRECTION	TERR-CORR BOUGUER
WB302	38.	39.71	112.	42.55	5867.	1.23	-198.60	.45	-198.15
WB303	38.	39.96	112.	43.05	5966.	3.58	-199.63	.39	-199.24
WB304	38.	39.88	112.	43.54	5960.	4.55	-198.45	.40	-198.05
WB305	38.	39.26	112.	43.62	5833.	-.28	-198.95	.67	-198.28
WB306	38.	38.86	112.	43.77	5773.	-.64	-197.27	.50	-196.77
WB307	38.	38.60	112.	43.92	5756.	.25	-195.80	.41	-195.39
WB308	38.	38.30	112.	43.94	5723.	.06	-194.86	.44	-194.42
WB309	38.	37.97	112.	43.90	5677.	-.77	-194.13	.40	-193.73
WB310	38.	37.60	112.	43.95	5615.	-2.85	-194.10	.52	-193.58
WB311	38.	39.50	112.	44.11	5926.	2.40	-199.44	.44	-199.00
WB312	38.	38.41	112.	43.47	5717.	-1.86	-196.58	.31	-196.27
WB313	38.	38.39	112.	43.10	5694.	-3.02	-196.95	.30	-196.65
WB314	38.	39.00	112.	43.08	5783.	-1.81	-198.78	.48	-198.30
WB315	38.	38.00	112.	43.19	5660.	-3.37	-196.15	.34	-195.81
WB316	38.	38.67	112.	44.58	5705.	-.97	-195.28	.31	-194.97
WB317	38.	39.10	112.	44.89	5715.	-1.30	-195.95	.38	-195.57
WB318	38.	38.33	112.	44.96	5617.	-1.61	-192.93	.32	-192.61
WB319	38.	40.31	112.	35.18	5685.	-3.65	-197.28	1.52	-195.76
WB320	38.	42.34	112.	33.92	5537.	1.81	-186.78	2.26	-184.52
WB321	38.	43.40	112.	32.47	5503.	1.53	-185.91	2.76	-183.15
WB322	38.	44.64	112.	31.52	5423.	6.63	-178.08	1.54	-176.54
WB323	38.	43.59	112.	33.48	5195.	-8.23	-185.17	1.69	-183.48
WB324	38.	44.51	112.	32.55	5241.	-2.88	-181.38	1.34	-180.04
WB325	38.	23.10	112.	42.86	6313.	-2.91	-217.93	.82	-217.11
WB326	38.	24.10	112.	43.42	6322.	-1.64	-216.97	.97	-216.00
WB327	38.	24.88	112.	43.96	6444.	4.30	-215.18	1.28	-213.90
WB328	38.	25.16	112.	44.08	6518.	7.53	-214.47	1.19	-213.28
WB329	38.	26.67	112.	44.28	6822.	16.91	-215.45	1.17	-214.28
WB330	38.	27.28	112.	44.32	6902.	19.90	-215.18	1.32	-213.86
WB331	38.	28.72	112.	44.72	7226.	34.33	-211.78	1.19	-210.59

STATION NUMBER	LATITUDE DEG	MIN	LONGITUDE DEG	MIN	ELEVATION IN FEET	FREE-AIR ANOMALY	SIMPLE BOUGUER	TERRAIN CORRECTION	TERR-CORR BOUGUER
WB332	38.	28.82	112.	42.92	7024.	25.54	-213.69	.94	-212.75
WB333	38.	28.32	112.	41.88	7148.	28.80	-214.66	.92	-213.74
WB334	38.	28.60	112.	41.66	7235.	30.86	-215.56	1.08	-214.48
WB335	38.	23.13	112.	43.88	6084.	-6.82	-214.05	1.21	-212.84
WB336	38.	22.50	112.	41.98	6159.	10.64	-220.41	4.09	-216.32
WB337	38.	24.58	112.	42.62	6680.	9.44	-218.08	1.27	-216.81
WB338	38.	25.14	112.	42.80	6805.	15.69	-216.09	2.30	-213.79
WB339	38.	26.32	112.	43.07	7010.	21.52	-217.24	2.46	-214.78
WB340	38.	25.86	112.	43.00	6951.	19.96	-216.79	2.29	-214.50
WB341	38.	23.26	112.	42.17	6383.	-.63	-218.04	.92	-217.12
WB342	38.	25.09	112.	42.05	7170.	25.24	-218.97	2.52	-216.45
WB343	38.	23.98	112.	42.17	6711.	9.10	-219.47	1.71	-217.76
WB344	38.	25.82	112.	42.29	7344.	31.60	-218.53	2.72	-215.81
WB345	38.	25.65	112.	41.48	7153.	22.30	-221.34	2.25	-219.09
WB346	38.	23.82	112.	44.56	6320.	5.97	-209.28	1.89	-207.39
WB347	38.	25.42	112.	44.76	*****	11.88	-213.83	1.41	-212.42
WB348	38.	25.79	112.	44.38	6649.	11.73	-214.74	1.35	-213.39
WB349	38.	29.10	112.	43.92	7099.	27.94	-213.86	1.34	-212.52
WB350	38.	24.54	112.	41.75	7061.	18.38	-222.11	2.72	-219.39
WB351	38.	26.34	112.	42.15	7240.	27.98	-218.62	1.68	-216.94
WB352	38.	27.09	112.	42.44	7320.	31.80	-217.52	1.72	-215.80
WB353	38.	29.81	112.	42.13	7384.	30.60	-220.90	3.44	-217.46
WB354	38.	27.23	112.	41.70	7292.	28.77	-219.60	1.42	-218.18
WB355	38.	29.62	112.	41.65	6784.	17.11	-213.95	1.76	-212.19
WB356	38.	29.36	112.	42.20	7304.	31.40	-217.38	5.23	-212.15
WB357	38.	29.34	112.	43.01	7074.	27.47	-213.47	1.80	-211.67
WB358	38.	27.64	112.	41.18	6956.	22.31	-214.61	.97	-213.64
WB359	38.	28.27	112.	40.12	7418.	29.93	-222.72	2.11	-220.61
WB360	38.	28.96	112.	39.35	7478.	23.00	-231.70	4.43	-227.27
WB361	38.	28.07	112.	39.62	7396.	26.13	-225.78	1.87	-223.91

STATION NUMBER	LATITUDE DEG	MIN	LONGITUDE DEG	MIN	ELEVATION IN FEET	FREE-AIR ANOMALY	SIMPLE BOUGUER	TERRAIN CORRECTION	TERR-CORR BOUGUER
WB362	38.	22.18	112.	40.98	*****	19.18	-223.30	4.83	-218.47
WB363	38.	23.05	112.	40.35	6077.	14.40	-221.38	.88	-220.50
WB364	38.	23.83	112.	40.00	6136.	12.04	-221.04	1.01	-220.03
WB365	38.	24.46	112.	40.12	6258.	-5.90	-219.04	.97	-218.07
WB366	38.	24.86	112.	40.14	6358.	-2.69	-219.24	1.08	-218.16
WB367	38.	25.50	112.	39.35	6235.	10.69	-223.06	1.14	-221.92
WB368	38.	25.91	112.	40.14	6412.	.89	-217.50	1.52	-215.98
WB369	38.	26.60	112.	40.44	6808.	14.29	-217.59	1.51	-216.08
WB370	38.	26.43	112.	41.21	7238.	28.49	-218.03	3.64	-214.39
WB371	38.	27.48	112.	39.50	7888.	30.59	-238.08	9.95	-228.13
WB372	38.	27.04	112.	39.52	7394.	22.96	-228.88	4.79	-224.09
WB373	38.	28.88	112.	41.18	7665.	38.43	-222.64	8.64	-214.00
WB374	38.	27.04	112.	40.84	7003.	22.28	-216.24	1.60	-214.64
WB375	38.	36.08	112.	34.87	5998.	-4.09	-208.38	1.12	-207.26
WB376	38.	36.23	112.	34.64	6007.	-1.05	-205.65	1.47	-204.18
MILFR	38.	23.70	113.	.60	4957.	32.58	-201.42	.00	-201.42
WB377	38.	36.49	112.	34.72	6016.	-1.46	-206.37	1.48	-204.89
WB378	38.	36.68	112.	34.78	6025.	-.94	-206.16	1.28	-204.88
WB379	38.	37.26	112.	34.80	6014.	1.65	-203.18	1.56	-201.62
WB380	38.	37.51	112.	34.68	6080.	4.42	-202.66	1.76	-200.90
WB381	38.	37.88	112.	34.36	6154.	6.54	-203.06	1.92	-201.14
WB382	38.	38.03	112.	34.03	6248.	10.74	-202.07	1.92	-200.15
WB383	38.	38.13	112.	33.56	6379.	16.50	-200.77	3.44	-197.33
WB384	38.	38.30	112.	34.09	6318.	11.35	-203.84	1.77	-202.07
WB385	38.	38.70	112.	33.79	6163.	7.94	-201.97	1.94	-200.03
WB386	38.	35.95	112.	34.12	6088.	3.27	-204.09	1.55	-202.54
WB387	38.	36.51	112.	33.27	6250.	8.79	-204.09	1.58	-202.51
WB388	38.	36.88	112.	33.42	6367.	14.36	-202.50	1.51	-200.99
WB389	38.	37.09	112.	33.56	6411.	15.58	-202.78	1.73	-201.05
WB390	38.	37.27	112.	32.48	6560.	20.25	-203.18	2.13	-201.05

STATION NUMBER	LATITUDE DEG	MIN	LONGITUDE DEG	MIN	ELEVATION IN FEET	FREE-AIR ANOMALY	SIMPLE BOUGUER	TERRAIN CORRECTION	TERR-CORR BOUGUER
WB391	38.	37.05	112.	32.66	6433.	15.33	-203.78	1.77	-202.01
WB392	38.	36.76	112.	32.87	6353.	10.95	-205.43	1.59	-203.84
WB393	38.	36.65	112.	33.08	6299.	10.80	-203.74	1.53	-202.21
WB394	38.	36.80	112.	32.60	6404.	12.36	-205.76	1.69	-204.07
WB395	38.	37.12	112.	32.40	6522.	18.48	-203.66	2.04	-201.62
WB396	38.	36.20	112.	33.28	6275.	9.24	-204.48	2.47	-202.01
WB397	38.	36.18	112.	31.05	6592.	16.30	-208.22	2.25	-205.97
WB398	38.	36.16	112.	31.14	6571.	15.80	-208.01	2.27	-205.74
WB399	38.	36.13	112.	31.30	6535.	15.34	-207.24	2.32	-204.92
WB400	38.	36.10	112.	31.41	6510.	14.49	-207.24	2.50	-204.74
WB401	38.	36.13	112.	31.78	6465.	15.10	-205.10	2.45	-202.65
WB402	38.	36.16	112.	31.88	6453.	15.16	-204.62	2.15	-202.47
WB403	38.	36.20	112.	32.00	6426.	15.23	-203.64	2.12	-201.52
WB404	38.	36.23	112.	32.27	6387.	14.43	-203.11	2.07	-201.04
WB405	38.	36.23	112.	32.33	6360.	12.89	-203.74	2.12	-201.62
WB406	38.	36.24	112.	32.52	6350.	13.76	-202.52	1.94	-200.58
WB407	38.	36.25	112.	32.80	6286.	10.78	-203.32	1.89	-201.43
WB408	38.	34.13	112.	34.92	6186.	-3.14	-213.84	1.86	-211.98
WB409	38.	33.92	112.	34.57	6338.	4.10	-211.77	2.07	-209.70
WB410	38.	34.17	112.	34.30	6409.	6.77	-211.52	2.55	-208.97
WB411	38.	34.55	112.	34.25	6326.	4.73	-210.74	2.11	-208.63
WB412	38.	34.74	112.	34.06	6334.	5.99	-209.75	2.80	-206.95
WB413	38.	35.15	112.	34.04	6269.	4.94	-208.59	2.04	-206.55
WB414	38.	35.55	112.	33.89	6191.	4.36	-206.51	2.22	-204.29
WB415	38.	35.83	112.	33.62	6249.	7.08	-205.76	2.56	-203.20
WB416	38.	33.75	112.	35.20	6136.	-7.07	-216.07	1.95	-214.12
WB417	38.	31.74	112.	36.27	6114.	18.02	-226.26	1.88	-224.38
WB418	38.	30.08	112.	36.60	6258.	15.77	-228.92	2.02	-226.90
WB419	38.	30.00	112.	36.99	6230.	16.59	-228.79	1.84	-226.95
WB420	38.	30.44	112.	37.30	6224.	16.66	-228.65	1.66	-226.99

STATION NUMBER	LATITUDE DEG	LATITUDE MIN	LONGITUDE DEG	LONGITUDE MIN	ELEVATION IN FEET	FREE-AIR ANOMALY	SIMPLE BOUGUER	TERRAIN CORRECTION	TERR-CORR BOUGUER
WB421	38.	30.97	112.	37.40	6138.	18.66	-227.72	1.38	-226.34
WB422	38.	31.62	112.	37.11	6089.	19.05	-226.44	1.45	-224.99
WB423	38.	35.98	112.	35.92	6063.	-5.80	-212.31	1.41	-210.90
WB424	38.	36.20	112.	30.65	6717.	19.17	-209.61	2.14	-207.47
WB425	38.	36.01	112.	30.50	6816.	21.23	-210.92	2.80	-208.12
WB426	38.	35.88	112.	30.53	6856.	21.65	-211.87	3.00	-208.87
WB427	38.	35.67	112.	31.68	6633.	17.88	-208.04	3.02	-205.02
WB428	38.	35.26	112.	31.85	6843.	20.71	-212.37	3.90	-208.47
WB429	38.	33.65	112.	34.78	6190.	-4.18	-215.01	2.43	-212.58
WB430	38.	33.69	112.	34.12	6500.	7.67	-213.72	2.61	-211.11
WB431	38.	33.50	112.	33.83	6646.	11.94	-214.43	3.37	-211.06
WB432	38.	32.99	112.	33.92	6735.	12.94	-216.45	3.63	-212.82
WB433	38.	32.64	112.	34.00	6838.	15.93	-216.97	3.74	-213.23
WB434	38.	32.10	112.	33.97	7321.	29.49	-219.87	5.63	-214.24
WB435	38.	31.61	112.	33.93	7232.	23.97	-222.35	4.59	-217.76
WB436	38.	31.16	112.	34.04	7219.	24.82	-221.06	3.02	-218.04
WB437	38.	30.64	112.	34.16	7670.	32.70	-228.54	9.41	-219.13
WB438	38.	30.16	112.	34.29	6838.	10.53	-222.37	5.26	-217.11
WB439	38.	30.22	112.	34.95	6638.	1.64	-224.45	3.89	-220.56
WB440	38.	30.46	112.	35.93	6358.	-7.42	-223.97	3.36	-220.61
WB441	38.	30.55	112.	36.40	6233.	14.43	-226.73	2.11	-224.62
WB442	38.	34.85	112.	35.99	6005.	11.53	-216.06	1.26	-214.80
WB443	38.	35.08	112.	35.48	5990.	10.84	-214.86	1.16	-213.70
WB444	38.	35.17	112.	35.26	5983.	10.15	-213.93	1.41	-212.52
WB445	38.	35.30	112.	34.92	5981.	-8.64	-212.35	1.58	-210.77
WB446	38.	35.41	112.	34.72	6004.	-5.89	-210.39	1.65	-208.74
WB447	38.	35.49	112.	34.56	6058.	-.68	-207.01	1.65	-205.36
WB448	38.	35.57	112.	34.36	6080.	.84	-206.25	1.59	-204.66
WB449	38.	35.66	112.	34.18	6103.	1.88	-205.99	1.63	-204.36
WB450	38.	35.77	112.	33.94	6121.	3.19	-205.29	1.83	-203.46

STATION NUMBER	LATITUDE DEG	LATITUDE MIN	LONGITUDE DEG	LONGITUDE MIN	ELEVATION IN FEET	FREE-AIR ANOMALY	SIMPLE BOUGUER	TERRAIN CORRECTION	TERR-CORR BOUGUER
WB451	38.	35.88	112.	33.71	6143.	4.72	-204.51	1.97	-202.54
WB452	38.	39.39	112.	33.28	6089.	8.69	-198.70	2.67	-196.03
WB453	38.	40.50	112.	32.99	5918.	6.70	-194.87	2.62	-192.25
WB454	38.	40.68	112.	32.16	6040.	11.12	-194.60	3.84	-190.76
WB455	38.	40.39	112.	31.32	6200.	12.88	-198.30	4.66	-193.64
WB456	38.	41.67	112.	34.40	5749.	7.26	-188.55	1.75	-186.80
WB457	38.	42.23	112.	34.70	5520.	-.40	-188.41	1.63	-186.78
WB458	38.	40.61	112.	35.48	5703.	-.05	-194.30	1.89	-192.41
WB459	38.	40.67	112.	35.52	5709.	.39	-194.05	1.43	-192.62
WB460	38.	40.85	112.	35.68	5727.	2.44	-192.62	1.09	-191.53
WB461	38.	41.00	112.	35.82	5728.	3.49	-191.61	1.62	-189.99
WB462	38.	41.08	112.	35.94	5731.	4.02	-191.18	1.64	-189.54
WB463	38.	41.25	112.	36.01	5689.	2.35	-191.42	2.11	-189.31
WB464	38.	41.41	112.	35.97	5656.	1.17	-191.48	1.69	-189.79
WB465	38.	41.60	112.	35.97	5619.	.01	-191.38	2.16	-189.22
WB466	38.	41.75	112.	36.01	5592.	-.36	-190.82	2.15	-188.67
WB467	38.	41.94	112.	36.06	5518.	-4.93	-192.87	2.47	-190.40
WB468	38.	42.10	112.	35.98	5509.	-3.09	-190.73	1.73	-189.00
WB469	38.	42.27	112.	35.98	5437.	-7.66	-192.84	1.53	-191.31
WB470	38.	42.45	112.	35.92	5449.	-4.90	-190.49	1.41	-189.08
WB471	38.	42.61	112.	35.92	5360.	10.85	-193.41	1.40	-192.01
WB472	38.	42.79	112.	35.88	5385.	-7.35	-190.77	1.15	-189.62
WB473	38.	42.96	112.	35.86	5357.	-8.57	-191.03	1.11	-189.92
WB474	38.	43.21	112.	35.77	5320.	-9.73	-190.93	.90	-190.03
WB475	38.	43.38	112.	35.70	5236.	15.46	-193.80	.97	-192.83
WB476	38.	43.52	112.	35.60	5271.	10.97	-190.50	.80	-189.70
WB477	38.	43.68	112.	35.50	5241.	11.90	-190.41	.79	-189.62
WB478	38.	43.84	112.	35.42	5200.	12.93	-190.05	.78	-189.27
WB479	38.	44.00	112.	35.30	5151.	13.87	-189.32	.82	-188.50
WB480	38.	44.18	112.	35.07	5075.	13.29	-186.15	.78	-185.37

STATION NUMBER	LATITUDE DEG	LATITUDE MIN	LONGITUDE DEG	LONGITUDE MIN	ELEVATION IN FEET	FREE-AIR ANOMALY	SIMPLE BOUGUER	TERRAIN CORRECTION	TERR-CORR BOUGUER
WB481	38.	44.35	112.	34.84	5112.	13.99	-188.10	.78	-187.32
WB482	38.	42.47	112.	32.79	6401.	26.45	-191.57	8.64	-182.93
WB483	38.	36.83	112.	31.76	7015.	31.03	-207.90	4.70	-203.20
WB484	38.	38.05	112.	32.48	7487.	48.49	-206.51	8.92	-197.59
WB485	38.	31.92	112.	33.68	7189.	25.30	-219.56	4.80	-214.76
WB486	38.	35.13	112.	32.58	7679.	38.06	-223.49	11.43	-212.06
WB487	38.	41.56	112.	31.14	6710.	32.44	-196.10	4.21	-191.89
WB488	38.	42.71	112.	31.73	6288.	25.41	-188.76	4.76	-184.00
WB489	38.	30.40	112.	46.00	6855.	28.35	-205.13	2.10	-203.03
WB490	38.	30.23	112.	46.05	6813.	26.51	-205.54	1.51	-204.03
WB491	38.	31.12	112.	45.31	6242.	6.51	-206.10	1.80	-204.30
WB492	38.	31.40	112.	45.40	6282.	8.10	-205.87	1.57	-204.30
WB493	38.	31.86	112.	45.47	6153.	5.93	-203.64	1.54	-202.10
WB494	38.	32.24	112.	45.52	6028.	.13	-205.19	1.52	-203.67
WB495	38.	33.58	112.	46.31	5785.	-.07	-197.11	1.49	-195.62
WB496	38.	33.28	112.	46.12	5865.	.86	-198.90	1.41	-197.49
WB497	38.	32.57	112.	45.76	5970.	.44	-202.89	1.59	-201.30
WB498	38.	32.60	112.	45.31	5873.	-5.97	-206.00	1.26	-204.74
WB499	38.	34.10	112.	46.69	5738.	2.18	-193.26	1.37	-191.89
WB500	38.	34.43	112.	46.74	5677.	.57	-192.79	1.18	-191.61
WB501	38.	34.69	112.	46.78	5630.	-.80	-192.56	1.11	-191.45
WB502	38.	34.71	112.	46.40	5605.	-3.61	-194.51	.89	-193.62
WB503	38.	35.12	112.	45.92	5610.	-6.61	-197.69	.59	-197.10
WB504	38.	35.18	112.	45.18	5773.	-2.58	-199.21	.74	-198.47
WB505	38.	34.25	112.	45.20	5675.	-8.48	-201.77	.73	-201.04
WB506	38.	34.35	112.	46.15	5627.	-4.35	-196.01	.91	-195.10
WB507	38.	33.10	112.	47.46	6825.	36.97	-195.49	.68	-194.81
WB508	38.	33.61	112.	46.90	5995.	13.16	-191.03	2.76	-188.27
WB509	38.	34.08	112.	48.04	6610.	34.91	-190.23	6.34	-183.89
WB510	38.	34.46	112.	47.60	5912.	14.75	-186.61	2.09	-184.52

STATION NUMBER	LATITUDE DEG MIN	LONGITUDE DEG MIN	ELEVATION IN FEET	FREE-AIR ANOMALY	SIMPLE BOUGUER	TERRAIN CORRECTION	TERR-CORR BOUGUER
WB511	38. 35.74	112. 45.25	5569.	-8.02	-197.70	.49	-197.21
WB512	38. 35.52	112. 45.48	5590.	-7.41	-197.80	.49	-197.31
WB513	38. 37.78	112. 45.20	5555.	-1.89	-191.09	.32	-190.77
WB514	38. 38.00	112. 45.78	5515.	-2.53	-190.37	.37	-190.00
WB515	38. 38.18	112. 46.35	5486.	-3.99	-190.84	.32	-190.52
WB516	38. 38.50	112. 47.41	5409.	-6.20	-190.43	.35	-190.08
WB517	38. 38.30	112. 46.80	5458.	-5.22	-191.12	.32	-190.80
WB518	38. 38.64	112. 47.92	5398.	-5.73	-189.59	.29	-189.30
WB519	38. 38.68	112. 48.31	5382.	-5.25	-188.56	.32	-188.24
WB520	38. 38.24	112. 48.30	5390.	-3.09	-186.68	.47	-186.21
WB521	38. 37.80	112. 48.30	5409.	.58	-183.66	.70	-182.96
WB522	38. 37.06	112. 48.08	5447.	3.41	-182.12	1.00	-181.12
WB523	38. 36.49	112. 47.82	5468.	1.37	-184.87	1.05	-183.82
WB524	38. 35.81	112. 47.40	5511.	-.95	-188.65	1.05	-187.60
WB525	38. 35.20	112. 47.15	5585.	.18	-190.04	1.08	-188.96
WB526	38. 35.19	112. 48.31	6125.	20.71	-187.91	5.06	-182.85
WB527	38. 38.65	112. 49.81	5383.	1.22	-182.12	.52	-181.60
WB528	38. 38.16	112. 49.64	5632.	12.89	-178.93	2.10	-176.83
WB529	38. 38.58	112. 49.29	5385.	.11	-183.30	.50	-182.80
WB530	38. 38.60	112. 48.78	5368.	-3.27	-186.10	.41	-185.69
WB531	38. 39.01	112. 47.34	5429.	-6.02	-190.93	.28	-190.65
WB532	38. 39.38	112. 47.22	5421.	-7.48	-192.12	.28	-191.84
WB533	38. 39.83	112. 47.12	5430.	-9.23	-194.18	.30	-193.88
WB534	38. 41.70	112. 47.12	5402.	14.83	-198.83	.62	-198.21
WB535	38. 41.98	112. 47.32	5322.	15.86	-197.13	.25	-196.88
WB536	38. 41.38	112. 47.36	5331.	17.26	-198.84	.31	-198.53
WB537	38. 41.00	112. 47.50	5350.	16.54	-198.76	.30	-198.46
WB538	38. 40.44	112. 47.37	5389.	14.06	-197.61	.31	-197.30
WB539	38. 41.91	112. 47.81	5274.	17.51	-197.15	.23	-196.92
WB540	38. 41.92	112. 48.50	5251.	17.35	-196.20	.19	-196.01

STATION NUMBER	LATITUDE DEG	MIN	LONGITUDE DEG	MIN	ELEVATION IN FEET	FREE-AIR ANOMALY	SIMPLE BOUGUER	TERRAIN CORRECTION	TERR-CORR BOUGUER
WB541	38.	41.95	112.	49.08	5248.	14.80	-193.55	.21	-193.34
WB542	38.	41.68	112.	49.38	5243.	14.34	-192.91	.19	-192.72
WB543	38.	41.28	112.	50.10	5221.	11.83	-189.65	.17	-189.48
WB544	38.	40.70	112.	49.23	5277.	14.64	-194.37	.18	-194.19
WB545	38.	40.18	112.	49.10	5326.	11.73	-193.14	.18	-192.96
WB546	38.	39.56	112.	49.14	5342.	-8.36	-190.31	.24	-190.07
WB547	38.	39.10	112.	49.10	5364.	-5.10	-187.80	.28	-187.52
WB548	38.	40.05	112.	49.42	5335.	-9.50	-191.21	.19	-191.02
WB549	38.	42.30	112.	48.68	5253.	15.31	-194.23	.19	-194.04
WB550	38.	42.77	112.	48.25	5227.	14.35	-192.38	.23	-192.15
WB551	38.	43.38	112.	47.88	5168.	16.93	-192.95	.27	-192.68
WB552	38.	44.00	112.	47.50	5149.	19.49	-194.86	.25	-194.61
WB553	38.	44.45	112.	47.22	5218.	17.17	-194.90	.36	-194.54
WB554	38.	44.76	112.	47.01	5144.	19.97	-195.17	.67	-194.50
WB555	38.	44.10	112.	46.70	5309.	16.76	-197.59	1.68	-195.91
WB556	38.	44.06	112.	45.78	5380.	16.97	-200.21	.79	-199.42
WB557	38.	44.34	112.	45.06	5622.	12.59	-204.07	1.78	-202.29
WB558	38.	42.08	112.	49.62	5325.	-9.94	-191.30	.22	-191.08
WB559	38.	42.29	112.	50.38	5397.	-3.19	-187.02	.26	-186.76
WB560	38.	42.44	112.	50.94	5402.	.03	-183.97	.32	-183.65
WB561	38.	42.48	112.	51.65	5303.	1.06	-179.56	.25	-179.31
WB562	38.	42.04	112.	51.08	5342.	-1.42	-183.37	.28	-183.09
WB563	38.	41.66	112.	52.00	5176.	-1.08	-177.37	.17	-177.20
WB564	38.	40.56	112.	51.00	5158.	-7.81	-183.49	.22	-183.27
WB565	38.	39.60	112.	51.52	5128.	-7.39	-182.05	.22	-181.83
WB566	38.	39.13	112.	51.39	5110.	10.67	-184.72	.30	-184.42
WB567	38.	38.65	112.	51.32	5144.	-9.61	-184.81	.41	-184.40
WB568	38.	39.28	112.	52.18	5063.	10.31	-182.76	.29	-182.47
WB569	38.	39.49	112.	52.28	5078.	-8.84	-181.80	.22	-181.58
WB570	38.	40.02	112.	52.25	5090.	-5.90	-179.26	.20	-179.06

STATION NUMBER	LATITUDE DEG	LATITUDE MIN	LONGITUDE DEG	LONGITUDE MIN	ELEVATION IN FEET	FREE-AIR ANOMALY	SIMPLE BOUGUER	TERRAIN CORRECTION	TERR-CORR BOUGUER
WB571	38.	40.41	112.	52.08	5107.	-3.84	-177.78	.20	-177.58
WB572	38.	40.84	112.	52.18	5121.	-3.03	-177.45	.16	-177.29
WB573	38.	41.34	112.	52.12	5140.	-1.71	-176.78	.15	-176.63
WB574	38.	42.08	112.	52.13	5225.	.87	-177.09	.22	-176.87
WB575	38.	42.99	112.	51.64	5435.	5.65	-179.46	.54	-178.92
WB576	38.	43.28	112.	52.09	5306.	2.79	-177.93	.36	-177.57
WB577	38.	43.54	112.	52.12	5325.	4.10	-177.27	.42	-176.85
WB578	38.	43.75	112.	52.32	5299.	4.20	-176.29	.37	-175.92
WB579	38.	43.36	112.	46.38	5227.	22.16	-200.19	.40	-199.79
WB580	38.	42.55	112.	46.49	5408.	15.41	-199.61	.62	-198.99
WB581	38.	42.03	112.	45.26	5873.	.65	-199.39	1.55	-197.84
WB582	38.	40.34	112.	45.41	5993.	6.81	-197.31	1.04	-196.27
WB583	38.	39.95	112.	45.36	6102.	8.39	-199.44	3.50	-195.94
WB584	38.	40.65	112.	45.51	6048.	8.04	-197.96	1.12	-196.84
WB585	38.	39.41	112.	45.34	5741.	.61	-194.93	.67	-194.26
WB586	38.	38.71	112.	45.87	5572.	-2.74	-192.52	.26	-192.26
WB587	38.	37.10	112.	49.62	7110.	49.40	-192.77	17.92	-174.85
WB588	38.	36.94	112.	49.59	7123.	50.63	-191.98	19.81	-172.17
WB589	38.	36.45	112.	49.25	7230.	51.29	-194.97	20.62	-174.35
WB590	38.	36.28	112.	49.20	7100.	49.01	-192.82	16.30	-176.52
WB591	38.	36.00	112.	49.18	6990.	48.84	-189.24	14.17	-175.07
WB592	38.	35.60	112.	48.92	6550.	41.69	-181.40	4.16	-177.24
WB593	38.	35.41	112.	48.87	6655.	42.09	-184.58	5.20	-179.38
WB594	38.	34.88	112.	48.72	7175.	49.26	-195.12	17.58	-177.54
WB595	38.	44.60	112.	49.49	5283.	-8.06	-188.00	.38	-187.62
WB596	38.	44.84	112.	48.89	5203.	12.22	-189.44	.20	-189.24
WB597	38.	44.01	112.	49.46	5593.	-1.25	-191.75	2.36	-189.39
WB598	38.	43.56	112.	49.33	5472.	-4.92	-191.30	1.12	-190.18
WB599	38.	43.06	112.	48.80	5212.	17.99	-195.51	.36	-195.15
WB600	38.	40.90	112.	50.66	5261.	-6.97	-186.16	.40	-185.76

STATION NUMBER	LATITUDE DEG MIN	LONGITUDE DEG MIN	ELEVATION IN FEET	FREE-AIR ANOMALY	SIMPLE BOUGUER	TERRAIN CORRECTION	TERR-CORR BOUGUER
WB601	38. 37.44	112. 51.00	5325.	3.48	-177.89	1.56	-176.33
WB602	38. 37.44	112. 50.70	5495.	10.70	-176.46	2.53	-173.93
WB603	38. 36.90	112. 50.78	5511.	10.46	-177.25	2.09	-175.16
WB604	38. 37.85	112. 51.58	5116.	-9.74	-183.99	.71	-183.28
WB605	38. 36.56	112. 51.28	5305.	-.72	-181.41	1.15	-180.26
WB606	38. 36.10	112. 51.06	5403.	3.32	-180.71	1.17	-179.54
WB607	38. 35.53	112. 51.05	5492.	6.12	-180.94	1.15	-179.79
WB608	38. 35.24	112. 51.12	5505.	7.21	-180.29	1.10	-179.19
WB609	38. 34.88	112. 51.25	5540.	10.39	-178.30	1.13	-177.17
WB610	38. 33.75	112. 51.32	5650.	16.53	-175.91	1.32	-174.59
WB611	38. 36.10	112. 51.50	5315.	-3.81	-184.83	.91	-183.92
WB612	38. 36.98	112. 51.58	5180.	-8.36	-184.79	.93	-183.86
WB613	38. 40.45	112. 52.71	5087.	-4.53	-177.80	.16	-177.64
WB614	38. 42.32	112. 52.69	5104.	-2.77	-176.61	.14	-176.47
WB615	38. 41.08	112. 53.82	5020.	-5.36	-176.34	.13	-176.21
WB616	38. 42.22	112. 53.87	5047.	.80	-171.10	.13	-170.97
WB617	38. 42.66	112. 53.84	5048.	1.56	-170.37	.14	-170.23
WB618	38. 42.37	112. 56.14	4952.	-7.74	-176.40	.10	-176.30
WB619	38. 42.53	112. 55.14	4968.	-4.24	-173.45	.11	-173.34
WB620	38. 42.60	112. 54.72	5012.	-.59	-171.30	.11	-171.19
WB621	38. 42.98	112. 54.35	5034.	2.12	-169.34	.12	-169.22
WB622	38. 43.37	112. 54.11	5040.	3.47	-168.19	.13	-168.06
WB623	38. 43.92	112. 53.83	5065.	2.16	-170.35	.15	-170.20
WB624	38. 44.40	112. 53.88	5055.	.75	-171.43	.15	-171.28
WB625	38. 44.72	112. 53.50	5110.	1.23	-172.81	.18	-172.63
WB626	38. 43.94	112. 52.60	5246.	4.74	-173.94	.31	-173.63
WB627	38. 44.40	112. 52.82	5202.	3.35	-173.83	.22	-173.61
WB628	38. 43.02	112. 58.01	4850.	-5.20	-170.39	.14	-170.25
WB629	38. 42.84	112. 57.15	4922.	-5.39	-173.03	.13	-172.90
WB630	38. 43.09	112. 56.68	4937.	-4.61	-172.76	.11	-172.65

STATION NUMBER	LATITUDE DEG	MIN	LONGITUDE DEG	MIN	ELEVATION IN FEET	FREE-AIR ANOMALY	SIMPLE BOUGUER	TERRAIN CORRECTION	TERR-CORR BOUGUER
WB631	38.	43.40	112.	56.54	4942.	-3.34	-171.67	.12	-171.55
WB632	38.	43.66	112.	56.40	4951.	-1.76	-170.39	.11	-170.28
WB633	38.	44.12	112.	56.25	4976.	1.64	-167.85	.12	-167.73
WB634	38.	44.59	112.	56.05	4998.	5.74	-164.50	.15	-164.35
WB635	38.	45.09	112.	56.05	4887.	.46	-165.99	.39	-165.60
WB636	38.	44.87	112.	55.36	5020.	3.43	-167.55	.14	-167.41
WB637	38.	41.69	112.	56.96	4932.	-9.52	-177.50	.09	-177.41
WB638	38.	41.01	112.	56.49	4957.	11.64	-180.47	.09	-180.38
WB639	38.	40.26	112.	56.38	4956.	13.99	-182.79	.09	-182.70
WB640	38.	44.10	112.	57.82	4847.	-.11	-165.20	.23	-164.97
WB641	38.	42.17	112.	58.25	4858.	-7.75	-173.22	.11	-173.11
WB642	38.	41.33	112.	58.50	4873.	10.07	-176.04	.10	-175.94
WB643	38.	40.12	112.	58.78	4900.	13.35	-180.24	.09	-180.15
WB644	38.	39.18	112.	58.87	4898.	17.20	-184.03	.09	-183.94
WB645	38.	38.32	112.	58.95	4875.	20.75	-186.80	.12	-186.68
WB646	38.	37.92	112.	58.98	4877.	22.27	-188.38	.12	-188.26
WB647	38.	39.17	112.	57.14	4944.	17.57	-185.96	.10	-185.86
WB648	38.	37.40	112.	57.16	4910.	25.67	-192.91	.14	-192.77
WB649	38.	41.58	112.	54.87	4975.	-6.87	-176.32	.11	-176.21
WB650	38.	37.01	112.	59.07	4872.	24.78	-190.72	.14	-190.58
WB651	38.	35.24	112.	59.07	4886.	28.69	-195.11	.17	-194.94
WB652	38.	34.84	112.	59.04	4882.	30.02	-196.30	.18	-196.12
WB653	38.	38.45	112.	50.29	5351.	3.58	-178.67	2.26	-176.41
WB654	38.	37.85	112.	39.62	5835.	1.83	-196.91	.45	-196.46
WB655	38.	37.15	112.	50.36	5910.	23.89	-177.41	4.26	-173.15
WB656	38.	36.07	112.	50.13	6185.	31.20	-179.46	7.70	-171.76
WB657	38.	35.71	112.	50.13	6170.	27.59	-182.56	5.58	-176.98
WB658	38.	35.35	112.	49.85	6067.	28.88	-177.76	2.95	-174.81
WB659	38.	35.29	112.	50.42	5725.	18.42	-176.57	1.48	-175.09
WB660	38.	34.33	112.	50.39	6110.	29.94	-178.17	4.21	-173.96

STATION NUMBER	LATITUDE DEG	LATITUDE MIN	LONGITUDE DEG	LONGITUDE MIN	ELEVATION IN FEET	FREE-AIR ANOMALY	SIMPLE BOUGUER	TERRAIN CORRECTION	TERR-CORR BOUGUER
WB661	38.	33.48	112.	50.33	6531.	36.67	-185.77	8.26	-177.51
WB662	38.	34.16	112.	51.36	5590.	15.23	-175.16	1.75	-173.41
WB663	38.	35.33	112.	50.07	5800.	20.58	-176.97	1.72	-175.25
WB664	38.	35.10	112.	49.70	6040.	27.05	-178.67	2.60	-176.07
WB665	38.	34.78	112.	49.30	6200.	29.37	-181.80	3.92	-177.88
WB666	38.	34.60	112.	49.42	6905.	45.00	-190.18	11.16	-179.02
WB667	38.	34.27	112.	49.28	7060.	51.02	-189.45	8.41	-181.04
WB668	38.	35.98	112.	48.46	6050.	21.78	-184.28	3.35	-180.93
WB669	38.	34.52	112.	48.53	6985.	43.80	-194.11	12.09	-182.02
WB670	38.	34.02	112.	48.76	7719.	58.57	-204.34	22.51	-181.83
WB671	38.	33.95	112.	49.73	7290.	53.40	-194.90	16.62	-178.28
FB002	38.	38.24	112.	53.70	5260.	-.25	-179.41	.00	-179.41

REFERENCES

Anderson, P. N., and Axtell, L. H., 1972, Geothermal resources in California: Geothermal overviews of the western United States. Published by Geothermal Resources Council, Davis, California.

Armstrong, R. L., 1970, Geochronology of Tertiary ingneous rocks, eastern Basin and Range province, western Utah, eastern Nevada, and vicinity, U.S.A.: Geochim. et Cosmochim. Acta, v. 34, p. 203-232.

Banwell, C. J., 1970, Geophysical techniques in geothermal exploration. Geothermics, special issue, 2, v. 1, p. 32-56.

Biehler, S., 1971, Gravity studies in the Imperial Valley. In cooperative geological-geophysical-geochemical investigation of geothermal resources in the Imperial Valley area of California. University of California, Riverside, Education Research Service, p. 29-41.

_____, and Combs, J., 1972, Correlations of gravity and geothermal anomalies in the Imperial Valley, Southern California (abs). Geol. Soc. America Abstracts with Programs, v. 4, no. 3, p. 128.

Bowers, D., 1977, M. S. thesis in preparation, Univ. of Utah.

Butler, B. S., and Gale, H. S., 1912, Alunite near Marysvale, Utah: Mine and Sci. Press, p. 104, 210-211.

Butler, B. S., Loughlin, G. F., Heikes, V. C., and others, 1920, The Ore Deposits of Utah: U. S. Geol. Survey Prof. Paper 111, 672 p.

California Division of Mines, Gravity map of Geysers area Mineral Information Service, September 1966, v. 19, no. 9, p. 148-149.

Callaghan, Eugene, 1938, Preliminary report on the alunite deposits of the Marysvale region, Utah: U. S. Geol. Survey Bull. 886-D, p. 91-134.

_____, 1939, Volcanic sequence in the Marysvale region in southwest-central Utah: Am. Geophys. Union Trans., pt. III, p. 438-452.

Callaghan, Eugene, 1973, Mineral resource potential of Piute County, Utah and adjoining area: Utah Geol. and Mineralog. Survey Bull. 102 p.

Callaghan, E., and Parker, R. L., 1961a, Geologic map of part of the Beaver quadrangle, Utah: U. S. Geol. Survey Mineral Inv. Field Studies Map MF-202.

_____, 1961b, Geology of the Monroe quadrangle, Utah: U. S. Geol. Survey Geol. Quad. Map GQ-155.

_____, 1962a, Geology of the Delano Peak quadrangle, Utah: U. S. Geol. Survey Geol. Quad. Map GQ-153.

_____, 1962b, Geology of the Sevier quadrangle, Utah: U. S. Geol. Survey Geol. Quad. Map GQ-156.

Carter, J. A., 1977, M. S. thesis in preparation, Univ. of Utah.

Caskey, C. F., and Shuey, R. T., 1975, Mid-tertiary volcanic stratigraphy, Servier-Cove Fort Area, Central Utah; Utah Geology, v. 2, no. 1, p. 17-25.

Chapman, R. H., 1975, Geophysical Study of the Clear Lake Region: California Special Report 116, California Div. of Mines and Geology.

Combs, J., 1972, Review and discussion of geothermal exploration techniques. Compendium of first day papers presented at the first conference of the Geothermal Resources, Council, El Centro, California Feb., 1972, p. 49-68.

Combs, J., and Muffler, L. P., 1973, Exploration for geothermal resources: Geothermal Energy, Resources, Production, Stimulation, Edited by Kruger, P., and Otte, C., Stanford University Press, Stanford, Calif., 1972, p. 107.

Condie, K. C., 1960, Petrogenesis of the Mineral Range pluton, Southwestern Utah; unpublished M. S. Thesis, Univ. of Utah, 49 p.

Condie, K. C., and Barsky, C. K., 1972, Origin of Quarternary basalts from the Black Rock Desert region, Utah: Geol. Soc. America Bull., v. 83, p. 333-352.

Cook, K. L., Halverson, M. O., Stepp, J. C., Berg, J. W., Jr., 1964, Regional gravity survey of the northern Great Salt Lake Desert and adjacent areas in Utah, Nevada, and Idaho; Geol. Soc. America Bull., v. 75, p. 715-740.

Cook, K. L., Nilsen, T. H., and Lambert, J. F., 1971, Gravity base station network in Utah - 1967: Utah Geol. and Mineralogical Survey Bull. 92.

Cook, K. L., Montgomery, J. R., Smith, J. T., and Gray, E. F., 1975, Simple Bouguer gravity anomaly map of Utah: Utah Geol. and Mineralogical Survey, Map 37.

Coplex, T. B., et al., 1973, Preliminary findings of an investigation of the Dunes thermal anomaly, Emperial Valley, California, Dept. of Water Resources.

Crawford, A. L., and Buranek, A. M., 1945, Tungsten deposits of the Mineral Range, Beaver County, Utah; Utah Eng. Exp. Sta. Bull, 25, p. 6-48.

Crebs, T. J., 1976, Gravity and ground magnetic surveys of the central Mineral Mountains, Utah, unpublished M. S. thesis, Univ. of Utah, 129 p.

Crosby, G. W., 1959, Geology of the South Pavant Range, Millard and Sevier Counties, Utah: Geol. Soc. of America Spec. Paper 160.

_____, 1972, Dual origin of Basin and Range faults, in Plateau-Basin and Range transition zone central Utah; Utah Geol. Assoc. Publication no. 2.

_____, 1973, Regional structure in south-western Utah; Geology of the Milford area, Hintze, L. F., and Whelan, J. A., Editors, Utah Geol. Assoc. Publication no. 3, 94 p.

Dobrin, M. B., 1960, Introduction to geophysical Prospecting: 2nd ed., New York, McGraw Hill, 446 p.

Dutton, C. E., 1880, Report on the geology of the high plateaus of Utah: U. S. Geo. and Geol. Survey Rocky Mountain Region, 307 p.

Eardley, A. J., 1948, Paleozoic Cordilleran geosyncline, and related orogeny, Geol. Soc. America Bull. 57, p. 1189.

Eardley, A. J., and Beutner, E. L., 1934, Geomorphology of Marysvale Canyon and vicinity, Utah: Utah Acad. Sci. Proc., v. 11, p. 149-159.

Earll, F. N., 1957, Geology of the central Mineral Range, Beaver County, Utah: unpublished Ph. D. thesis, University of Utah.

Elkins, T. A., 1951, The second vertical derivative method of gravity interpretation: Geophysics, v. 16, no. 1, p. 29-50.

Evans, S. H., Jr., 1977, Ph. D., thesis in preparation; University of Utah.

Grindley, G. W., and Williams, G. J., 1965, Geothermal waters. Eight Commonwealth Mining and Metallurgical Congress, Australia and New Zealand, 1965, v. 4.

Grose, L. T., 1971, Geothermal energy, geology, exploration, and developments, Colorado School of Mines and Mineral Industries Bull., part 1, v. 14, no. 6, p. 1-14.

Hardman, Elwood, 1964, Regional survey of central Iron and Washington Counties, Utah; unpublished M. S. thesis, University of Utah, 107 p.

Heylmun, E. B., 1963, Oil and gas possibilities of Utah, re-evaluated: Utah Geol. and Mineral Survey Bull., 54, no. 26, p. 287-301.

Hintze, L. F., 1960, Preliminary geology map of the Richfield, Utah 2° quadrangle: Brigham Young University.

_____, 1963, (compiler), Geologic map of southwestern Utah: Utah Geol. and Mineralog. Survey.

Hosckstein, M. P., Hunt, T. M., 1970, Seismic, gravity and magnetic studies, Broadlands, geothermal field, New Zealand. Geothermics, special issue, 2,v. 2, pt. 1, p. 333-46.

Hoover, J. D., 1973, Late Cenozoic basalts and realted rocks in the Black Rock Desert, Utah; unpublished M. S. thesis, Brigham Young University.

Isherwood, W. F., 1975, Gravity and magnetic studies of the Geysers Clear Lake Geothermal region, California, Department of the Interior, Geol. Survey. Open-file report 75-368, 1975.

Kane, M. F., 1962, A comprehensive system of terrain corrections using a digital computer: Geophysics, v. 27, no. 4, p. 455-462.

Kresl, M., and Novak, V., 1970, Terrestrial heat flow in the territory of Czechoslovakia and the measurement of thermal conductivity with fully automatic apparatus. Geothermics, special issue, 2, v. 2, pt. 1, in press.

Lee, W. L., 1908, Water resources of Beaver County, Utah: U. S. Geol. Survey Water-Supply Paper 217, 57 p.

Leise, H. C., 1957, Geology of the northern Mineral Range, Millard and Beaver Counties, Utah; unpublished M. S. thesis, University of Utah, 88 p.

Lipman, P. W., Rowley, P. D., and Pallister, J. S., Pleistocene rhyolite of the Mineral Range, Utah-geothermal and archeological significance (abs.): Program with Abstracts, Geol Soc. America Annual Meeting, Salt Lake City, Utah, Oct. 20-22, 1975, v. 7, no. 7, p 1173.

Loughlin, G. F., 1915, Recent alunite developments near Marysvale and Beaver, Utah: U. S. Geol. Survey Bull., 620-K, p. 237-270.

Maxey, G. B., 1946, Geology of part of the Pavant Range, Millard County, Utah: Am. Jour. Sci., v. 244, p. 324-356.

McNitt, J. R., 1965, Reveiw of geothermal resources: in W. H. K. Lee ed., Terrestial heat flow, Amer. Geophys. Union Mon., sec. 8, p. 240-266.

Mudgett, P. M., 1963, Regional gravity survey of parts of Beaver and Millard Counties, Utah: Unpublished M. S. thesis, University of Utah, 19 p.

Mundorff, J. C., 1970, Major thermal springs of Utah: Utah Geol. and Mineral Survey Water Resources Bull. 13.

Nettleton, L. L., 1949, Geophysical prospecting for oil: McGraw-Hill Book Company, New York.

_____, 1976, Gravity and magnetics on oil prospecting: McGraw-Hill, New York.

Olson, T. L., 1976, Seismicity of the Roosevelt Hot Springs and Cove Fort areas, Beaver and Millard Counties, Utah; unpublished M. S. thesis, University of Utah.

Peters, S., 1974, Civil engineering features of a geothermal power plant, Presented at ASCE National Meeting on Water Resources Engineering at Los Angeles, California.

Petersen, C. A., 1975, Geology of the Roosevelt area, Beaver County, Utah; unpublished M. S. thesis, University of Utah, 49 p.

Peterson, D. L., 1972, Complete Bouguer anomaly map of parts of Beaver, Iron and Millard Counties, southwestern Utah; U. S. Geol. Survey open file map.

Rex, R. W., 1972, Cooperative geological-geophysical-geochemical investigations of geothermal resources in the Imperial Valley: First Conference of the Geothermal Resources Council, El Centro, Calif.

Rinehart, J. S., 1975, Faulting in geothermal areas. Geothermal Energy, v. 3, no. 12, p. 7-24, Dec. 1975.

Rodrigues, E. L., 1960, Economic geology of the sulphur deposits at Sulphurdale, Utah; unpublished M. S. thesis, University of Utah.

Shuey, R. T., 1974, Aeromagnetic map of Utah: Utah Geol. and Mineral Survey and Dept. of Geol. and Geophy., University of Utah.

Slemmons, D. B., 1967, Pliocene and Quaternary crustal movements of the Basin and Range Province, U. S. A.; J. of Geosciences, Osaka City University, v. 10, p. 91-103.

Smith, R. B., and M. L. Sbar, 1974, Contemporary tectonics and seismicity of the western United States with emphasis on the Intermountain seismic belt, Bull. Geol. Soc. America, v. 85, p. 1205-1218.

Sontag, R. J., 1965, Regional gravity survey of parts of Beaver, Millard, Piute, and Sevier Counties, Utah; unpublished M. S. thesis, University of Utah, 32 p.

Stanley, W. D. et al, 1973, Preliminary results of geoelectrical investigation near Clear Lake, Calif.: U. S. Geol. Survey, 20 p.

Stewart, S. W., 1958, Gravity survey of Ogden Valley in the Wasatch Mountains, north central Utah: Am. Geophys. Union Trans., v. 39, p. 1151-1157.

Studt, F. E., 1958, Geophysical reconnaissance at Kawreau, New Zealand, N. Z. Jour. of Geol. and Geoph. v. 1, no. 2, p. 219-246.

Swick, C. H., 1942, Pendulum gravity measurements and isostatic reductions: U. S. Coast and Geodetic Survey Spec. Pub. 232.

Talwani, M., Worsel, J. L., and Landisman, M., 1959, Rapid gravity computations for two-dimensional bodies with application to the Mendocino submarine fracture zone: Jour. Geophys. Research, v. 64, p. 49-59.

Thangsuphanich, I., 1976, Regional gravity survey over the southern Mineral Mountains, Beaver County, Utah; unpublished M. S. thesis, Univ. of Utah, 49 p.

Water Resources of the Milford Area, Utah, Technical Pub. No. 43, State of Utah, Dept. of Natural Resources, 1974.

Willard, M. E., and E. Callaghan, 1962, Geology of the Marysvale quadrangle, Utah: U. S. Geol. Survey Geol. Quad. Map GQ-154.

Zietz, I., Shuey, R. T., Kirby, J. R. Jr., 1976, Aeromagnetic map of Utah; U. S. Geol. Survey Geophys. Invest. Map GP-907.

Zimmerman, J. T., 1960, Geology of the Cove Creek area Millard and Beaver Counties, Utah; unpublished M. S. thesis, University of Utah.

VITA

Name	William Donald Brumbaugh
Birthplace	Lansing, Michigan
Birthdate	[redacted]
High Schools	St. Joseph's - Addis Ababa, Ethiopia Highland High School - Salt Lake City, Utah
Military Service 1968-1974	U.S. Army, Idaho National Guard, honorable discharge
University	University of Utah Salt Lake City, Utah
Degree 1975	B. S. in Physics University of Utah Salt Lake City, Utah
Graduate Student 1975-1977	Department of Geology and Geophysics University of Utah Salt Lake City, Utah
Teaching Assistant Autumn Quarter 1975-1976	Department of Geology and Geophysics University of Utah Salt Lake City, Utah
Research Assistant Winter and Spring Quarters 1975-1976	Department of Geology and Geophysics University of Utah Salt Lake City, Utah